

Fakultät für Medizin der Technischen Universität München

Function and substrates of the Alzheimer's disease protease BACE1

Jasenka Rudan Njavro

Vollständiger Abdruck der von der

Fakultät für Medizin

der Technischen Universität München zur Erlangung des akademischen Grades

eines Doktors der Naturwissenschaften (Dr. rer. nat.)

genehmigten Dissertation.

Vorsitzender: Prof. Dr. Thomas Misgeld

Prüfende/-r der Dissertation:

1. Prof. Dr. Stefan Lichtenthaler
2. Prof. Dr. Wolfgang Wurst

Die Dissertation wurde am 12.04.2019 bei der Technischen Universität München
eingereicht und durch die

Fakultät für Medizin am 08.10.2019 angenommen.

TABLE OF CONTENT

ABSTRACT	3
ZUSAMMENFASSUNG	4
LIST OF ABBREVIATIONS	5
1. INTRODUCTION	7
1.1. History of Alzheimer’s disease.....	7
1.2. Epidemiology of Alzheimer’s disease	7
1.3. Pathology of the disease	7
1.4. Familial and sporadic Alzheimer’s disease.....	8
1.5. The amyloid hypothesis of Alzheimer’s disease	9
1.6. Amyloid precursor protein (APP) and its processing	11
1.7. The β -site amyloid precursor protein cleaving enzyme 1 (BACE1).....	12
1.8. BACE1 cellular localization and trafficking.....	14
1.9. BACE1 deficient mice.....	14
1.10. BACE1 substrates and functions	14
1.11. BACE1 as a drug target in Alzheimer’s disease	16
1.12. The Seizure protein family	19
1.13. Seizure protein family as the main BACE1 substrates	20
2. AIM OF THE WORK	22
3. MATERIAL AND METHODS	23
3.1. Material.....	23
3.1.1. General reagents and chemicals.....	23
3.1.2. Primers	25
3.1.3. Buffers	26
3.1.4. Kits.....	27
3.1.5. Equipment.....	27
3.2. DNA methods	28
3.2.1. Polymerase Chain Reaction (PCR).....	28
3.2.2. Cloning of DNA constructs	28
3.2.3. Gibson assembly	30
3.2.4. Transformation of competent E. coli bacteria.....	30
3.2.5. Mini preps – preparation of DNA for construct screening.....	30
3.2.6. Midi preps – preparation of DNA for transfection.....	30
3.2.7. Sequencing of cloned DNA constructs	31
3.2.8. DNA isolation	31
3.2.9. Genotyping	31
3.3. Cell culture methods.....	33
3.3.1. Cell culture.....	33
3.3.2. Cell lines	33
3.3.3. Cryopreservation.....	33
3.3.4. Transient transfection.....	33
3.3.5. Lentivirus production.....	33
3.3.6. Stable cell line production	34
3.3.7. Primary cortical neurons isolation and culture.....	35
3.3.8. Compound treatment.....	35
3.4. Protein analysis methods	35
3.4.1. Cell lysis	35
3.4.2. Protein quantification.....	36
3.4.3. Concanavalin A enrichment.....	36
3.4.4. Co-immunoprecipitation	36

3.4.5.	Mouse brain fractionation: membrane and soluble fraction.....	37
3.4.6.	Crude membrane preparation.....	37
3.4.7.	Surface Spanning Protein Enrichment with Click Sugars – SUSPECS.....	37
3.4.8.	Western blot analysis.....	38
3.4.9.	Quantification and statistical analysis.....	40
3.4.10.	Brain slice preparation.....	40
3.4.11.	Immunostaining of brain sections.....	40
3.4.12.	Sample preparation for mass spectrometric measurement.....	40
3.4.13.	LC-MS/MS analysis.....	41
3.4.14.	LC-MS/MS data analysis and statistical evaluation.....	42
3.5.	Animal work.....	42
3.5.1.	Mouse lines.....	42
3.5.2.	Behavioural testing.....	43
3.5.3.	DigiGait analysis.....	44
3.5.4.	Ledge beam analysis.....	44
3.5.5.	Forelimb grip strength analysis.....	44
3.5.6.	Rotarod analysis.....	44
4.	RESULTS.....	46
4.1.	BACE1 substrates in secretome and surfaceome.....	46
4.1.1.	BACE1 substrate shedding in the overexpressing system of HEK293T cells.....	46
4.1.2.	SUSPECS method as a valuable tool to study cell surfaceomes.....	49
4.1.3.	Accumulation of BACE1 substrates on the neuronal surface.....	50
4.1.4.	Validation of BACE1 substrates in BACE1 ^{-/-} brains.....	53
4.2.	Seizure 6-like protein (as one of the main BACE1 substrates).....	54
4.2.1.	Expression pattern of SEZ6L.....	54
4.2.2.	Behavioural analyses of SEZ6L ^{-/-} mice.....	56
4.2.3.	Proteomic analysis of the cerebellar membranes of adult SEZ6L ^{-/-} mice.....	60
4.2.4.	Proteomic analysis of the cerebellar membranes of young SEZ6L ^{-/-} mice.....	63
4.2.5.	Whole proteome analysis of the young SEZ6L ^{-/-} cerebellum.....	68
4.2.6.	Comparison of the adult and young SEZ6L proteome.....	72
4.2.7.	SEZ6L interaction partners.....	73
5.	DISCUSSION.....	78
5.1.	BACE1 substrates from SPECS and SUSPECS.....	78
5.1.1.	Validation of SPECS candidates reveals new BACE1 substrates.....	78
5.1.2.	SUSPECS shows altered neuronal surfaceome upon BACE1 inhibition.....	79
5.2.	Seizure 6-like protein.....	81
5.2.1.	SEZ6L ^{-/-} mice have a motor phenotype.....	82
5.2.2.	SEZ6L ^{-/-} cerebellum has an altered proteome.....	84
5.2.3.	SEZ6L interaction partners reveal potential role in immunity.....	86
6.	CONCLUSION.....	88
7.	LITERATURE.....	90
8.	ACKNOWLEDGMENT.....	105
	List of publications.....	106

ABSTRACT

Alzheimer's disease (AD) is a progressive neurodegenerative disorder and the most common cause of dementia of elderly. To date there are no disease-modifying therapies available despite extensive efforts to understand the underlying molecular and pathophysiological pathways. An early event in the pathology of the disease is the cleavage of amyloid precursor protein (APP) by β -site amyloid precursor protein (APP)-cleaving enzyme 1 (BACE1) and initiation of amyloid- β (A β) production. BACE1 is currently a major target for drug development and there are ongoing clinical trials that inhibit this enzyme. BACE1 was thought to be a safe target, but several studies using BACE1-deficient (BACE1^{-/-}) mice revealed that BACE1 has a broad range of physiological substrates and functions, including axon guidance, neurogenesis and neuronal network functions. Therapeutic development should therefore be taken with precautions, as the inhibitors may lead to adverse effects arising from the functional inhibition of BACE1 and its substrates. Thus, it is crucial to better understand BACE1 biology and proteolytic functions through investigating additional substrates and the effect of loss of cleavage of BACE1 substrates.

To address this issue, here I first validated the novel BACE1 substrate candidates CACHD1, GLG1, and LRRN1, thereby providing the evidences of additional confirmed substrates with unknown function and possible BACE1 inhibition-related consequences. Additionally, I established a new proteomic method called **Surface-Spanning Protein Enrichment with Click Sugars (SUSPECS)** for surface glycoprotein enrichment and used it to monitor changes of the cell surface proteome of primary murine neurons upon BACE1 inhibition. Pharmacological BACE1 inhibition resulted in altered surface proteins, increasing the abundance of BACE1 substrates, but also apparent nonsubstrates, indicating possible secondary effects of BACE1 inhibition. Finally, this thesis focusses on the biological role of a substrate which is mainly processed by BACE1, Seizure 6-like protein (SEZ6L), applying behavioural and proteomic studies. SEZ6L-deficient (SEZ6L^{-/-}) mice were found to exhibit a motor discoordination phenotype on rotarod and have as well altered gait patterns assessed with DigiGait. Although there were no apparent BACE1 related phenotypes, proteomic analysis of SEZ6L-deficient cerebellum revealed downregulation of proteins, including CaMKIV, KHDRBS1, Syngap1 and OLFM1, that are involved in neurodegeneration, cerebellar development and synaptic plasticity. Moreover, by studying interaction partners of SEZ6L, we identified two novel candidates, complement C3 and Fcgr1. Together these data suggest not only a possible role of SEZ6L in AD and immunity, but are pointing to a fundamental role of SEZ6L in the brain.

In conclusion, this study contributes to the understanding of the alterations occurring upon BACE1 inhibition. This may further have an impact on comprehending the side effects that the drugs may have in clinical trials, but also to investigate the understudied basic biology of this protease.

ZUSAMMENFASSUNG

Bei der Alzheimer Krankheit handelt es sich um eine fortschreitende neurodegenerative Erkrankung, welche die meistverbreitete Ursache für altersbedingte Demenz darstellt. Trotz immenser Bemühungen, die zugrundeliegenden molekularen und pathophysiologischen Mechanismen zu verstehen, gibt es bis heute keine wirkungsvolle Behandlung. Die Prozessierung des *amyloid precursor proteins* (APP) durch die Protease *β -site amyloid precursor protein cleaving enzyme 1* (BACE1) ist eines der frühen Ereignisse in der Entstehung der Alzheimer Krankheit und führt zur Produktion von Amyloid- β (A β). Folglich ist die Inhibition von BACE1 ein viel versprechender Ansatz in der Wirkstoff Entwicklung, und BACE1 inhibierende Wirkstoffe befinden sich zurzeit in klinischen Studien. Wurde BACE1 Inhibition zunächst als unbedenklich eingestuft, haben mittlerweile mehrere Forschungsarbeiten über BACE1-defiziente (BACE1^{-/-}) Mäuse eine Reihe unterschiedlicher Substrate von BACE1 aufgedeckt und deren physiologische Funktionen erläutert. Dazu zählen Funktionen bei der Synapsen-Verknüpfung, der Neurogenese und dem Auswachsen von Axonen. Folglich ist Vorsicht in der Entwicklung von Wirkstoffen geboten, da die therapeutische Manipulation von BACE1 durch ungewollte Beeinträchtigung seiner physiologischen Funktionen zu bedeutenden Nebenwirkungen führen könnte. Aus diesen Gründen ist es essentiell, die Biologie von BACE1 besser zu verstehen, insbesondere durch Untersuchung von dessen Substraten und deren Funktionen.

Hierfür habe ich zunächst die Proteine CACHD1, GLG1 und LRRN1 als neue BACE1 Substrate validiert und somit belegt, dass weitere BACE1 Substrate mit unbekanntem Funktionen existieren, welche wiederum durch die Manipulation von BACE1 zu ungeahnten Konsequenzen führen könnten. Des Weiteren habe ich eine neue proteomische Methode namens *Surface-Spanning Protein Enrichment with Click Sugars* (SUSPECS) etabliert, welche verwendet werden kann, um glykosylierte Proteine von der Zelloberfläche anzureichern. Diese Methode habe ich verwendet, um die Änderung im Zelloberflächenproteom von kultivierten murinen Primärneuronen zu beschreiben, nachdem diese mit einem BACE1 Inhibitor behandelt wurden. Diese pharmakologische Inhibition führte zu Änderungen in der Zusammensetzung der Oberflächenproteine und insbesondere zu einer Zunahme der Menge an BACE1 Substraten. Auch Proteine, bei denen es sich wahrscheinlich nicht um BACE1 Substrate handelt, nahmen hierbei zu, was wiederum auf sekundäre Effekte der BACE1 Inhibition deutet. Zuletzt befasst sich diese Arbeit mit der biologischen Rolle des BACE1 abhängigen Substrates *Seizure-6-like protein* (SEZ6L). Hierfür wurden proteomische und verhaltensbasierte Experimente durchgeführt. SEZ6L defiziente Mäuse (SEZ6L^{-/-}) wiesen hierbei verschlechterte Motorkoordination im Zuge des Rotarod Leistungstestes auf und zeichneten sich durch veränderte Gangzyklus Muster während einer DigiGait Analyse aus. Obwohl bei SEZ6L^{-/-} Mäusen auf den ersten Blick kein BACE1 abhängiger Phänotyp festgestellt werden konnte, zeigte die proteomische Analyse von deren Cerebella eine Reduktion verschiedener Proteine, u.a. von CaMKIV, KHDRBS1, Syngap1 und OLFM1. Diese tragen zu neurodegenerativen Prozessen, synaptischer Plastizität und der Entwicklung des Cerebellums bei. Des Weiteren, habe ich complement C3 und Fcgr1 als neue mögliche Interaktionspartner für SEZ6L identifiziert. Diese Ergebnisse weisen nicht nur auf eine mögliche Rolle von SEZ6L in der Alzheimer Krankheit und im Immunsystem hin, sondern belegen auch, dass SEZ6L eine fundamentale Rolle im Gehirn spielen könnte.

Zusammenfassend lässt sich sagen, dass diese Arbeit dazu beiträgt, die Auswirkungen veränderter BACE1 Aktivität zu verstehen. Dieses Verständnis könnte einerseits dazu beitragen, die Nebenwirkungen von Wirkstoffen in klinischen Studien besser zu verstehen, aber auch dabei helfen bisher unbekannt biologische Grundlagen dieser Protease aufzuklären.

LIST OF ABBREVIATIONS

AD	Alzheimer's disease
ADAM10	A disintegrin and metalloprotease 10
AICD	APP intracellular domain
AMPA	α -amino-3-hydroxy-5-methylisoxazole-4-propionate
AMPAR	AMPA receptor
APLP1	Amyloid precursor-like protein 1
APLP2	Amyloid precursor-like protein 2
APP	Amyloid precursor protein
A β	Amyloid beta
BACE1	β -site amyloid precursor protein cleaving enzyme 1
BACE2	β -site amyloid precursor protein cleaving enzyme 2
BSRP	Brain specific receptor-like protein
C3	β -secretase inhibitor IV
CACHD1	VWFA and cache domain-containing protein 1
CaMKIV	Calcium/calmodulin-dependent protein kinase type IV
CHL1	Neural cell adhesion molecule close homolog of L1
CSF	Cerebrospinal fluid
CTF	C-terminal fragment
CTR	Control
CUB	Complement proteases C1r and C1s, embryonic sea urchin protein Uegf, bone morphogenetic protein-1 (BMP-1)
DBCO	Dibenzylcyclooctyne
DIAN	Dominantly Inherited Alzheimer Network
DMSO	Dimethyl sulfoxide
DNER	Delta and Notch-like epidermal growth factor-related receptor
ER	Endoplasmic reticulum
FAD	Familial Alzheimer's disease
FASP	Filter aided sample preparation
FDR	False discovery rate
GLG1	Golgi apparatus protein 1
GluR2	Glutamate receptor 2
GOI	Gene of interest
HET	Heterozygous
KO	Knockout
LRRN1	Leucine-rich repeat neuronal protein 1
ManNAz	Tetra-acetylated <i>N</i> -azidomannosamine
MAPT	Microtubule-associated protein tau
MT4MMP	Membrane-type matrix metalloproteinase 4
MT5MMP	Matrix metalloproteinase 5
NEO1	Neogenin
NFTs	Neurofibrillary tangles
NMDA	<i>N</i> -methyl-D-aspartate
NRG1	Neuregulin 1
NTM	Neurotrimin
o/n	Overnight
OLFM1	Noelin, Olfactomedin-1
PC	Purkinje cells
PET	Positron-emission tomography

PNS	Peripheral nervous system
PSEN1	Presenilin-1
PSEN2	Presenilin-2
RGMA	Repulsive guidance molecule A
RIP	Regulated intramembrane proteolysis
RT	Room temperature
sAPP α	Soluble APP alpha
sAPP β	Soluble APP beta
SCR	Short consensus repeats for complement C3b/C4b-binding site
SEZ6	Seizure protein 6
SEZ6L	Seizure 6-like protein
SEZ6L2	Seizure 6-like protein 2
SPECS	Secretome protein enrichment with click sugars
SUSPECS	Surface-spanning protein enrichment with click sugars
Tg	Transgenic
TGN	Trans-Golgi network
TKO	Triple knockout
TSPAN6	Tetraspanin-6
WT	Wild-type

1. INTRODUCTION

1.1. History of Alzheimer's disease

Alzheimer's disease (AD) is a progressive, irreversible neurodegenerative disorder and the most common form of dementia. It was first described in 1907 by a German psychiatrist Alois Alzheimer based on a 51-year-old patient Auguste Deter who afterwards died of the progressive behavioural and cognitive disorder. He reported the presence of the two nowadays well established hallmarks of the disease: abnormal intracellular aggregates – neurofibrillary tangles and miliary foci, later on known as neuritic plaques in Deter's brain (Alzheimer (1907); (Alzheimer et al., 1995). Alzheimer's miliary foci were represented as dystrophic neurites surrounding a "special substance in the cortex" (Alzheimer et al., 1995) that remained a mystery for decades. After the first isolation and purification in 1984, Glenner and Wong showed a novel, 4.2kDa cerebrovascular amyloid protein, speculated to be derived from a precursor protein (Glenner and Wong, 1984). Four years later amyloid precursor protein (APP) was finally cloned (Kang et al., 1987) and the previously isolated peptide was come to known as the amyloid- β peptide or shortly A β peptide.

The case of the Auguste Deter represented an unusual demented patient to Alois Alzheimer and only in the late 60s a relationship between the amount of A β plaques and the risk of dementia was established (Blessed et al., 1968). Today AD is recognized as one of the biggest health- and social-care priorities of the 21st century with many efforts being made to find a cure or a disease-modifying therapy (Scheltens et al., 2016).

1.2. Epidemiology of Alzheimer's disease

AD is one of the greatest burdens for the patients, their families and the world health-care. In 2010 it was estimated that worldwide 35.6 million people lived with dementia, with prognosis of doubling every 20 years, reaching 65.7 million by 2030 and 115.4 million by 2050 (Prince et al., 2013). The number of people that will develop the disease and the survival time of demented people are assumed to remain stable.

Assessment of the total payments in 2016 for health care, long-term care and hospital services for demented people in the United States alone showed the costs as high as \$236 billion (Alzheimer's Association, 2016). The main risk factor is age and there is an increase in incidence rates from approximately 0.5% per year among individuals aged 65–70 to approximately 6–8% for individuals over age 85 (Mayeux and Stern, 2012). Combination of the rising incidence of AD in elderly and considerably long progression of the disease is in large part a reason for the worldwide high prevalence.

1.3. Pathology of the disease

The main pathological lesions that characterize AD on the microscopic level are senile plaques, composed of extracellular A β deposits; neurofibrillary tangles (NFTs), made of intracellular aggregates of the microtubule-associated protein tau (MAPT) found in apical dendrites and cell bodies; and loss of synapses and neurons, in particular cholinergic neurons. Macroscopically, there is a large brain weight and volume loss, affecting structurally mostly

the (trans-)entorhinal and hippocampal regions, while functionally the inferior parietal lobules and precuneus (Schroeter et al., 2009).

Senile or neuritic plaques are composed of a heterogeneous population of proteolytically generated A β that are deposited outside neurons in dense formation. Among the different isoforms, A β 42 plays a crucial role in the pathogenesis of the disease due to its biochemical properties that are in favour of aggregating into insoluble, neurotoxic oligomers, and protofibrils.

NFTs are composed of the disrupted tau that before forming tangles undergoes a series of disease-related post-translational modifications like hyperphosphorylation (Grundke-Iqbal et al., 1986), acetylation (Min et al., 2010), *N*-glycosylation (Wang et al., 1996) and truncation (Mena et al., 1996). These modifications, together with the loss of microtubule binding, lead to elevated intracellular tau which in turn is facilitating tau-tau interactions and polymerization. Deposition of tau aggregates begins in the entorhinal cortex and hippocampus before spreading to other regions (Braak and Braak, 1991, 1997).

In clinics, the pathology of the disease can be monitored using established core cerebrospinal fluid (CSF) biomarkers: 42 amino acid form of A β , A β 42, showing cortical amyloid deposition; total tau (t-tau), reflecting the intensity of neurodegeneration; and phosphorylated tau (p-tau181 and p-tau231), correlating with neurofibrillary pathological changes (Blennow et al., 2010). From the imaging methods, the most innovative is positron-emission tomography (PET) with ligands for A β visualising amyloid burden. Currently, three ligands have been approved in clinical use: florbetapir, florbetaben, and flutemetamol (Herholz and Ebmeier, 2011). These ligands can assess cortical amyloidosis with high accuracy, as evaluated by studies of elderly patients showing pathological changes just before death (Clark et al., 2012).

1.4. Familial and sporadic Alzheimer's disease

There is a complex interaction among genetic and environmental factors that causes the disease. Most of the AD cases are sporadic. However, there are some known mutations that lead to early-onset familial AD (FAD).

Autosomal dominant mutations in APP, presenilin PSEN1 and PSEN2 causes AD before the age of 60 and are found in less than 1% of patients (Campion et al., 1999). Those mutations are influencing APP processing and altering the levels of A β 42 or A β 43 (Scheuner et al., 1996) that are highly self-aggregating, compared to A β 40 that actually may be anti-amyloidogenic (Kim et al., 2007). An extra copy of the APP gene in Down's syndrome patients also leads to AD (Wisniewski et al., 1985), concluding that life-long overexpression of APP is causing AD. One of the well described FAD mutations is the Swedish double mutation (K670N/M671L) that is located adjacent to the β -secretase site found in two large Swedish families (Mullan et al., 1992) and known to increase the production of total A β . Mutations localized C-terminally of the A β sequence, including Florida (I716V), Indiana (V717F), London (V717I), and many others increase the A β 42/A β 40 ratios in favour of more toxic A β 42 (Eckman et al., 1997; Goate et al., 1991; Murrell et al., 1991).

Sporadic Alzheimer's disease patients have an unknown cause and the onset is above the age of 60 (late-onset). Apolipoprotein E4 (ApoE4, ϵ 4 allele) is a major genetic risk factor found in most AD cases. Its gene-dosage is increasing the risk and decreasing the age of onset of the

disease (Corder et al., 1993). On the other hand, $\epsilon 2$ allele, ApoE2 may be protective for AD (Farrer et al., 1997). Genome-wide association studies identified many other genes that affect the late-onset AD, including ABCA7, BIN1, CASS4, CD33, CD2AP, CELF1, CLU, CR1, DSG2, EPHA1, FERMT2, HLA-DRB5-DBR1, INPP5D, MS4A, MEF2C, NME8, PICALM, PTK2B, SLC24H4-RIN3, SORL1, ZCWPW1, PLD3 and TREM2 (Karch and Goate, 2015).

Other risk factors for late-onset disease include age as the major non-genetic risk, head injury, low educational levels, hyperlipidemia, hypertension, homocysteinemia, diabetes mellitus, and obesity (Huang and Mucke, 2012). Additional lifestyle-related factors that suggest the risks for dementia are diabetes, obesity, physical and mental inactivity, depression, smoking, and diet (Norton et al., 2014).

1.5. The amyloid hypothesis of Alzheimer's disease

The consensus of the onset of the disease is that the trigger is the accumulation of A β to high levels in the brain leading to a pathogenic cascade event and driving the severe memory deficits (Hardy and Selkoe, 2002). The proposed imbalance of the A β production and clearance is promoting the formation of neurofibrillary tangles in the well-established amyloid hypothesis that nowadays is the dominant model of AD pathogenesis (Beyreuther and Masters, 1991; Hardy and Allsop, 1991; Selkoe, 1991; Selkoe and Hardy, 2016)(Fig. 1).

There are many evidences to support the amyloid hypothesis, both at the gene and protein level. Firstly, the discovery of the γ -secretase's catalytic site presenilin and its dominant mutations, leading to a higher A β 42/A β 40 ratio, are found to cause early-onset AD. Mutations within or in close proximity of A β region of APP also causes early-onset AD and the 3 copies of the APP gene in Down's syndrome leads to early A β deposits, microgliosis, astrocytosis and NTF formation, all characteristic for AD. Supporting the amyloid hypothesis, rare Down's syndrome individuals with only partial trisomy of chromosome 21 excluding APP gene, have the syndrome but do not develop AD (Prasher et al., 1998). Another missense mutation of APP, Icelandic A673T, adjacent to the β -site amyloid precursor protein cleaving enzyme 1 (BACE1) cleavage site results in an approximately 40% reduction of amyloidogenic peptides and has shown to be protective of AD (Jonsson et al., 2012). Furthermore, the major risk factor of AD, ApoE4 was found to impair the clearance of the A β from the brain (Castellano et al., 2011). Soluble A β 42 oligomers isolated from AD patients can cause severe impairments of hippocampus and memory in rodents, while it can induce hyperphosphorylation of tau in cultured neurons. Low CSF levels of A β 42 in humans together with the positive amyloid-PET precede other pathological lesions for years. Moreover, passive immunotherapy for A β with different antibodies that is now in phase 3 of the clinical trials (crenezumab, gantenerumab and aducanumab) suggests a potential treatment effect in patients (Arndt et al., 2018; Cummings et al., 2018; Ostrowitzki et al., 2017).

Taken together, dyshomeostasis of A β is preceding other pathological events that lead to AD phenotype.

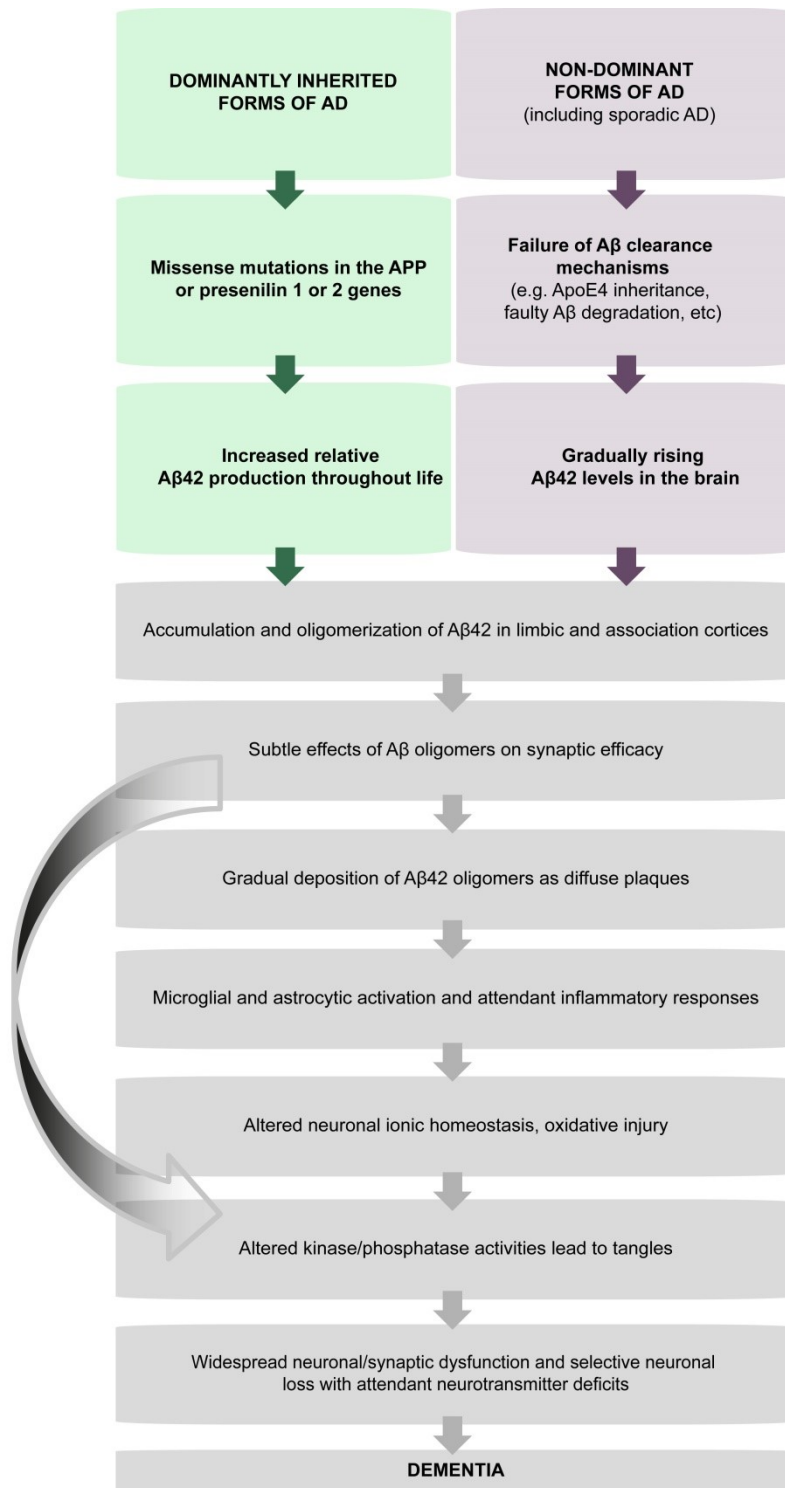


Figure 1. Amyloid hypothesis of AD. Proposed cascade of pathogenic events that leads to AD. The curved black and gray arrow is showing that Aβ oligomers may act in a direct way by affecting synapses and neurites as well as activating microglia and astrocytes. Modified from Selkoe and Hardy, 2016 (Selkoe and Hardy, 2016).

1.6. Amyloid precursor protein (APP) and its processing

The amyloid precursor protein (APP) is a single-pass transmembrane protein and member of a family of related proteins that includes the amyloid precursor-like protein 1 and 2 (APLP1 and APLP2). All have large extracellular domains processed in a similar manner, but only APP has the A β sequence and is involved in AD (O'Brien and Wong, 2011). The precise physiological function of APP to date is not fully understood. The ectodomain was shown to improve cognitive function and synaptic density in adult animals (Meziane et al., 1998; Roch et al., 1994), while the intracellular region serves as a transcriptional regulator, but also with the YENPTY amino acid domain as an intracellular sorting regulator (Chen et al., 1990; O'Brien and Wong, 2011). The APP product A β plays a role in synapses by regulating synaptic scaling and vesicle release (Abramov et al., 2009; Kamenetz et al., 2003). APP-deficient mice exhibit almost no phenotype, however, triple deletion of APP and other two members of the family, APLP1 and APLP2 have cortical dysplasia and die shortly after birth (Herms et al., 2004), while the double APP and APLP2 knockout mice have defective neuromuscular synapses (Wang et al., 2005). Similar to the single APP, the double APP and APLP1 knockout mice did not have any additional abnormalities and were fertile and viable (Heber et al., 2000).

The canonical processing of APP on or close to the cell surface is described as the non-amyloidogenic pathway that begins with α -secretase activity, mainly A Disintegrin and Metalloprotease 10 (ADAM10) in neurons (Kuhn et al., 2010; Lammich et al., 1999). The proteolytic event is happening within the A β sequence, resulting in the secretion of soluble APP α (sAPP α) and generation of the membrane bound 83 amino acids long C-terminal fragment (CTF), referred as C83 or α -CTF (Fig. 2). Further processing of C83 is mediated by the γ -secretase complex. This multiprotein complex consisting of four subunits: presenilin 1 or 2, nicastrin, APH-1 and PEN-2 is cleaving within the transmembrane domain, in a process termed regulated intramembrane proteolysis (RIP) (De Strooper, 2003). APP CTFs are cleaved at three positions: ϵ -, ζ - and γ -cleavage site generating the short secreted p3 peptide and the APP intracellular domain (AICD) fragment.

APP can be reinternalized from the surface in clathrin-coated pits into endosomal compartment and processed by the protease BACE1 in the amyloidogenic pathway. The first cleavage occurs N-terminally of the A β sequence resulting in the soluble APP β (sAPP β) ectodomain and the 99 amino acids large CTF (C99 or β -CTF). Like C83, C99 can also be cleaved by γ -secretase and thus release A β and AICD. The processing by γ -secretase starts with the ϵ -cleavage that occurs mainly at the carboxyl side of leucine 49 of the A β sequence yielding A β 49, followed by A β 46 ζ -cleavage and A β 43, ending in the secretion of A β 40. Less frequently it starts at threonine 48 subsequently generating A β 48, A β 45, A β 42 and A β 38 (Bolduc et al., 2016). Of all secreted A β peptides A β 40 are the most common, around 90%, followed by A β 42, which is more prone to aggregation (Qi-Takahara et al., 2005). Different FAD mutations lead to higher A β 42 abundance which increases A β aggregation and plaque formation.

Non-canonical processing of APP is happening N-terminally of the β -secretase cleavage site at recently identified η -cleavage site (504/505) by matrix metalloproteinase 5 (MT5). β - or α -secretase can further process it into A η - β or A η - α peptides, respectively (Willem et al., 2015). Another cleavage is at δ -site processed by asparagine endopeptidase (AEP) at three different positions: 584, 373 and 585 (Zhang et al., 2015). Additional competing protease Meprin- β can also shed APP at the cell surface at three positions: 124/125, 380/381 and 383/384 (Jefferson et al., 2011).

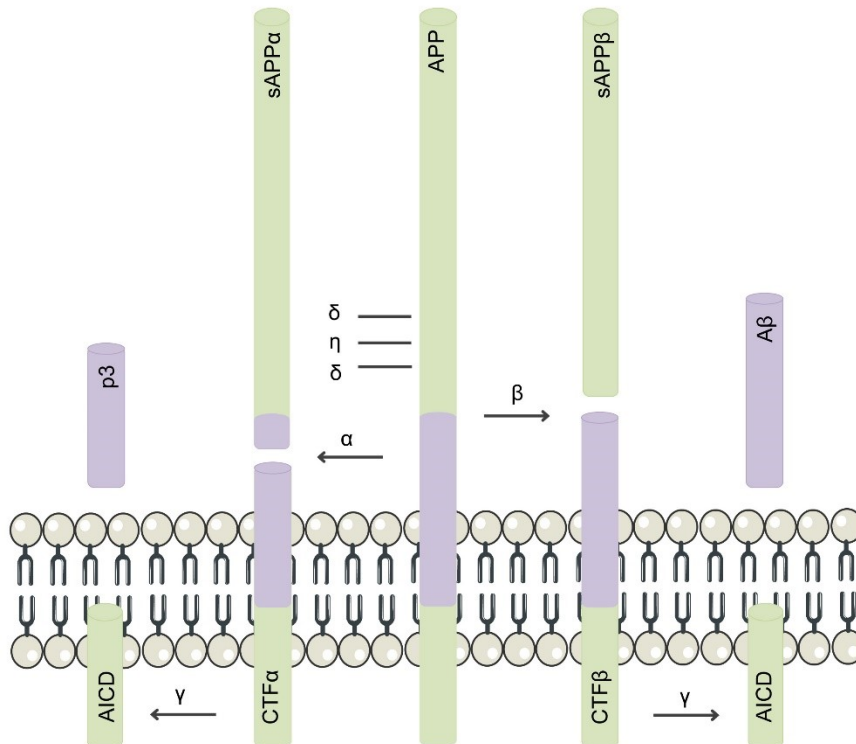


Figure 2. APP processing. APP is processed in non-amyloidogenic pathway with α - and γ -secretases, yielding sAPP α with CTF α and p3 with AICD, respectively. In amyloidogenic pathway, β -secretase is cleaving on the N-terminal side of A β peptide resulting in the sAPP β and CTF β . The latter is further processed by γ -secretase releasing the A β and AICD. Non-canonical processing of APP includes η -secretase, δ -secretase and Meprin- β .

1.7. The β -site amyloid precursor protein cleaving enzyme 1 (BACE1)

Using different experimental procedures of expression cloning, genomic strategies, and biochemical purification, five independent groups discovered the β -secretase of the APP in 1999 and named it β -site amyloid precursor protein cleaving enzyme (BACE), β -secretase, Asp2 or memapsin 2 (Hussain et al., 1999; Lin et al., 2000; Sinha et al., 1999; Vassar et al., 1999; Yan et al., 1999). All came down to the same 501 amino acid sequence assuring the validity of nowadays well recognized β -secretase or BACE1.

BACE1 is a type I transmembrane aspartic protease related to the pepsin family and the retroviral aspartic proteases with low pH optimum and predominantly localized in acidic intracellular compartments like endosomes or trans-Golgi network (TGN) (Vassar et al., 2009). Its catalytic domain is in the lumen of the vesicles and contains two aspartic acid active site motifs (DT/SGS/T) with approximately 200 residues apart. Synthesized as zymogen, in the endoplasmic reticulum (ER) and TGN, its pre- and pro-peptide domains are removed by signal peptidase and pro-protein convertase, respectively (Benjannet et al., 2001; Bennett et al., 2000b). It has 4 N-glycosylation sites (N153, N172, N223, N354) and its catalytic domain is crosslinked with 3 disulphide bonds (C216-C420, C278-C443, C330-C380) (Capell et al., 2000; Haniu et al., 2000). Other post-translational modifications include: phosphorylation at Ser498 (Pastorino et al., 2002), ubiquitination at Lys501 (Kang et al., 2012), S-palmitoylation at 4 cysteine residues (C474, C478, C482, and C485) (Vetrivel et al., 2009) and acetylation at several arginine residues in the catalytic site (Ko and Puglielli, 2009)(Fig. 3).

The expression of BACE1 is high in brain, particularly in neurons, as compared to the other cell types of the body. The cleavage of APP by BACE1 occurs at amino acid Asp+1 and Glu+11 of the A β sequence and its sequence specificity at P1 is Leu>>Met>Val. When overexpressing it increases, while knocking down BACE1 it decreases sAPP β , C99 and A β generation. All above mentioned featured made BACE1 a valid candidate for β -secretase (Vassar et al., 2014).

A year after the discovery of BACE1, its homolog BACE2 was identified (Bennett et al., 2000a; Farzan et al., 2000). With 64% similarity, this aspartyl protease raised the possibility of also having β -secretase activity; however, it was soon shown to promote the non-amyloidogenic pathway of APP and being more of an alternative secretase (Basi et al., 2003; Farzan et al., 2000; Fluhner et al., 2002; Yan et al., 2001).

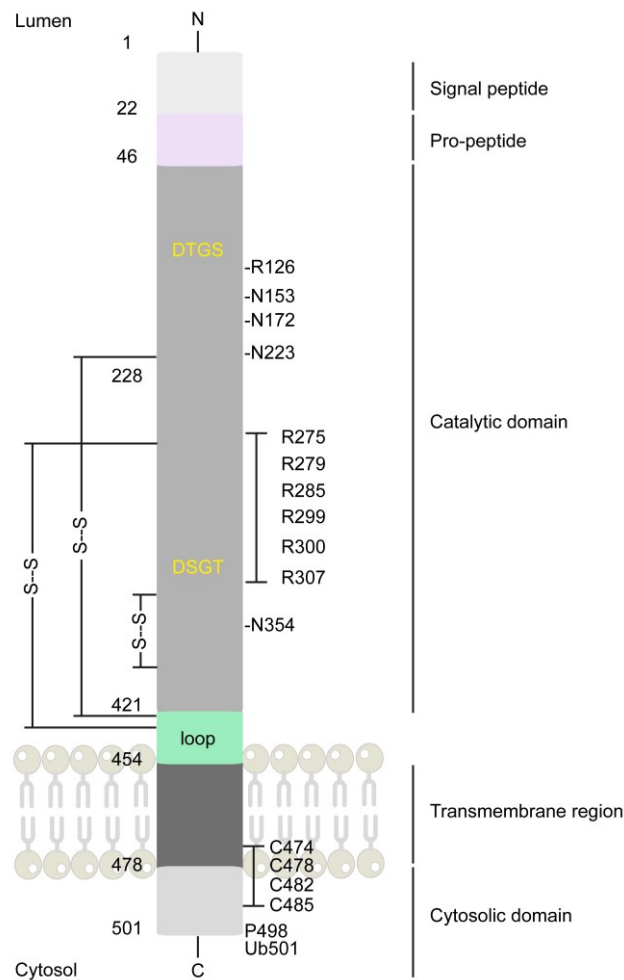


Figure 3. BACE1 schematic view. Schematic representation of different domains and post-translational modifications of BACE1. In yellow are two active sites at positions 93 and 289. Letters are referring to the amino acid code, while numbers to their position. S-S – disulphide bridges within the catalytic domain; N – N-linked glycosylation sites; R – acetylated arginine residues; C – cysteine residues at S-palmitoylation site; P – serine 498 phosphorylation site; Ub – ubiquitination at lysine 501 site. Modified from Vassar *et al.*, 2014 (Vassar et al., 2014).

1.8. BACE1 cellular localization and trafficking

BACE1 can be localized in different organelles, but its activity is the highest in endosomes, in particular early endosomes (Kinoshita et al., 2003; Rajendran et al., 2006; Sannerud et al., 2011) and to a lower extent to TGN due to the acidic pH (4.5-6) of these compartments. Its cleavage activity for APP is correlating with lipid raft localization (Kalvodova et al., 2005). Intracellular sorting to the early endosomes of APP and BACE1 is not completely understood. BACE1 requires Arf6 (Prabhu et al., 2012; Sannerud et al., 2011), while APP is using cholesterol-dependent clustering and adaptor protein-2 for its sorting (Perez et al., 1999; Schneider et al., 2008). After internalization, BACE1 can be transported: in a retrograde manner to the Golgi with its acidic cluster dileucine binding motif through the GGA protein family members (He et al., 2005; Tesco et al., 2007; von Arnim et al., 2006); to the lysosomes for degradation (Koh et al., 2005); through recycling endosomes via Rab11 to the cell surface and re-internalized back to endosomes (Udayar et al., 2013); or through retrograde transport to the soma with the help of Eps15-homology-domain-containing (EHD) 1 and 3 proteins (Buggia-Prevot et al., 2013).

1.9. BACE1 deficient mice

The final proof of BACE1 as the major β -secretase came after the generation and characterization of BACE1-deficient mice (BACE1^{-/-}), which was performed by several independent research groups (Cai et al., 2001; Dominguez et al., 2005; Luo et al., 2001; Roberds et al., 2001). In these studies, the mice were shown to be viable, fertile and appearing normal in tissue morphology, histology, haematology, clinical chemistry and gross behaviour. On the other hand, they completely lack β -cleavage products like A β , C99 and sAPP β . Further studies aimed to show the importance of BACE1 in APP transgenic (Tg) lines, where APP Tg/BACE1^{-/-} mice lacked A β production and amyloid deposition, and showed improvement of learning and memory deficits (Laird et al., 2005; Luo et al., 2003; McConlogue et al., 2007; Ohno et al., 2007; Ohno et al., 2004). The conclusion that arose indicated that BACE1 is a valid drug target for inhibition with minor mechanism-based side-effects, to lower levels of A β in patients.

The initially positive findings of BACE1^{-/-} mice were questioned by later evidences that BACE1 cleaves many more substrates beside APP and that mice have more phenotypes than originally considered (Table 1). The addition to the growing list of BACE1 substrates came with the large-scale proteomic studies that identified over 30 novel candidates in BACE1 overexpressing HEK and HeLa cells (Hemming et al., 2009), cell cultures of primary mouse neurons (Kuhn et al., 2012; Zhou et al., 2012) and β -islet cells (Stutzer et al., 2013).

1.10. BACE1 substrates and functions

The most severe developmental phenotype of BACE1^{-/-} mice are myelination abnormalities, which led to the discovery of one of the best studied substrate neuregulin 1 (NRG1) type III (Fleck et al., 2012; Hu et al., 2006; Willem et al., 2006). Detailed analysis of sciatic nerves showed hypomyelination and the number of axons within Remak bundles were significantly increased (Hu et al., 2006; Willem et al., 2006). Although other proteases can also cleave NRG1 type III, BACE1 seems to be the dominant one and activating signalling in the peripheral nervous system (PNS) (Fleck et al., 2012). Another family member, NRG1 type I

is also proteolytically cleaved by BACE1 and its reduction in neurons or reduction of its receptor ErbB2 in muscles reduces muscle spindle formation (Andrechek et al., 2002; Hippenmeyer et al., 2002; Leu et al., 2003), the same phenotype observed with pharmacological inhibition in adult mice (Cheret et al., 2013). Besides hypomyelination, the lack of NRG1 processing has also been associated with schizophrenia-like phenotypes observed in the BACE1^{-/-} mice (Savonenko et al., 2008).

Some of the BACE1^{-/-} phenotypes may also come from the reduced cleavage of neurexin 1 alpha, the neuroligin family and the latrophilin family of proteins, known to interact with one another (Boucard et al., 2012), and needed for synapse function and excitatory synaptic strength. Neurexin 1 alpha and neuroligin-deficient mice recapitulate some of the phenotypes found in the BACE1^{-/-} mice (Bang and Owczarek, 2013; Etherton et al., 2009; Xu et al., 2012).

Another BACE1 substrate seems to be β -subunits of the voltage-gated sodium channels (Nav) that is suggested to be controlled by BACE1 and regulating density, neuronal excitability and seizure susceptibility (Kim et al., 2011). BACE1^{-/-} mice develop significant retinal pathology and this phenotype might be a result of decreased processing of vascular endothelial growth factor receptor 1 (VEGFR1) (Cai et al., 2012). The mice also exhibit axon guidance defects in the hippocampus and olfactory system (Cao et al., 2012; Hitt et al., 2012; Rajapaksha et al., 2011), that may in part be explained by yet another substrate, neural cell adhesion molecule close homolog of L1 (CHL1), whose knockout mice have axon guidance defects in the same areas (Heyden et al., 2008; Montag-Sallaz et al., 2002). Reduced BACE1 cleavage of CHL1 was as well correlated with the defects in axonal organization in hippocampus when BACE1 is deleted in the adult stage (Ou-Yang et al., 2018). Shedding of Jagged 1 (Jag1) protein in BACE1^{-/-} mice is reduced and appears to increase astrogenesis with corresponding decrease in neurogenesis during the hippocampal early development (Hu et al., 2013).

Contactin-2, an *in vitro* and *in vivo* confirmed substrate (Dislich et al., 2015; Kuhn et al., 2012; Zhou et al., 2012), is maintaining voltage-gated potassium channels in juxtaparanodes of myelinated axons (Poliak et al., 2003; Traka et al., 2003) and its knockout has cognitive impairments, shorter internodes, and disrupted juxtaparanodes (Savvaki et al., 2008). It may be possible, but yet necessary to prove, that BACE1 is modulating the concentration and function of juxtaparanodal potassium channels through processing of contactin-2 (Vassar et al., 2014).

Another confirmed BACE1 substrate, seizure protein 6 (SEZ6) (Kuhn et al., 2012; Pigoni et al., 2016), is also thought to have BACE1 related functions. The SEZ6^{-/-} mouse phenotypes are comparable to those observed in the BACE inhibitor treated mice as the inhibitor does not affect dendritic spine density nor plasticity of SEZ6^{-/-} mice like it does in the WT treated mice, concluding that the SEZ6 is responsible for maintaining normal dendritic spine dynamics (Zhu et al., 2018b).

Not all phenotypes could be connected to a substrate: sensorimotor impairments, spatial and temporal hippocampus-dependent memory deficits (Ohno et al., 2006; Ohno et al., 2007; Ohno et al., 2004), spontaneous seizures and increased neuron loss with age in hippocampus (Hitt et al., 2010; Hu et al., 2010; Kobayashi et al., 2008), hippocampal synaptic plasticity and performance on tests of cognition and emotion alterations (Laird et al., 2005), anxious and less exploratory phenotype, decrease in serotonin levels and dopamine turnover in the hippocampus, decrease in dopamine in the striatum (Harrison et al., 2003), postnatal lethality and differences in growth (Dominguez et al., 2005).

In conclusion, numerous observed phenotypes of the central nervous system are suggesting that BACE1 indeed has a diverse physiological function and that its growing list of substrates might be related to those (Table 1).

Table 1. BACE1 phenotypes and substrates. List of BACE1 phenotypes from the BACE1^{-/-} mouse brain and their known substrates. Modified from Vassar *et al.* 2014 (Vassar *et al.*, 2014).

Phenotype	Substrate	References
Astrogenesis increase, neurogenesis decrease	Jag1	(Hu <i>et al.</i> , 2013)
Axon guidance defects	CHL1	(Cao <i>et al.</i> , 2012; Hitt <i>et al.</i> , 2012; Rajapaksha <i>et al.</i> , 2011)
Hyperactivity	NRG1	(Dominguez <i>et al.</i> , 2005; Savonenko <i>et al.</i> , 2008)
Hypomyelination	NRG1	(Hu <i>et al.</i> , 2008; Hu <i>et al.</i> , 2006; Willem <i>et al.</i> , 2006)
Memory deficits	-	(Laird <i>et al.</i> , 2005; Ohno <i>et al.</i> , 2006; Ohno <i>et al.</i> , 2007; Ohno <i>et al.</i> , 2004)
Neurochemical deficits	-	(Harrison <i>et al.</i> , 2003)
Neurodegeneration w/ age	Na _v β2	(Hu <i>et al.</i> , 2010)
Post-natal lethality, growth retardation	-	(Dominguez <i>et al.</i> , 2005)
Retinal pathology	VEGFR1	(Cai <i>et al.</i> , 2012)
Schizophrenia endophenotypes	NRG1	(Savonenko <i>et al.</i> , 2008)
Seizures	Na _v β2	(Hitt <i>et al.</i> , 2010; Hu <i>et al.</i> , 2010; Kim <i>et al.</i> , 2007; Kobayashi <i>et al.</i> , 2008)
Spine density reduction	NRG1	(Savonenko <i>et al.</i> , 2008)

1.11. BACE1 as a drug target in Alzheimer's disease

AD is an incurable disease and to date the drugs that are approved by the FDA are only supportive or palliative rather than disease-modifying or curable. Five drugs are currently widely utilized; four are classified as cholinesterase inhibitors approved in mild-to-moderate stages: donepezil (Aricept, Eisai/Pfizer), rivastigmine (Exelon, Novartis), galantamine (Razadyne, formerly Reminyl, Ortho-McNeil), and the rarely used tacrine (Cognex, First Horizon). The fifth drug is the *N*-methyl-D-aspartate (NMDA) receptor antagonist memantine (Namenda, Forest), that opposes glutamate activity by blocking NMDA receptors (Casey *et al.*, 2010). None of the five drugs are altering the final outcome of the disease and there is an urgent need of developing an effective and mechanism-targeted therapy.

The amyloid hypothesis puts Aβ as a major culprit in the pathology of the disease. The support of the hypothesis that Aβ deposition is the earliest initiating event driving the tau pathology, inflammation and concomitant synapse dysfunction together with cell loss come from the studies of Dominantly Inherited Alzheimer Network (DIAN) (Bateman *et al.*, 2012; Jack *et al.*, 2012). Consequently, as the rate limiting enzyme in the generation of Aβ, BACE1 is a promising drug target and currently in clinical trials. The rare mutation of APP (A673T) that was recently described to protect of AD due to life-long reduced β-cleavage further supports the idea of BACE1 inhibition (Jonsson *et al.*, 2012). Partial reduction of BACE1 has dramatic effects on the plaque load and synaptic pathology, which has been shown in Alzheimer mouse models lacking one copy of BACE1 (McConlogue *et al.*, 2007). Initial

reports of BACE1^{-/-} mice showed no gross phenotypes (Cai et al., 2001; Dominguez et al., 2005; Luo et al., 2001; Roberds et al., 2001). However, detailed analysis of the mice proved that BACE1^{-/-} mice suffer from different phenotypes. Although these results may raise concerns regarding the safety of BACE1 inhibition, many of BACE1^{-/-} phenotypes are associated with developmental processes which is consistent with the high BACE1 expression after birth followed by strong decrease during the first few postnatal weeks and are mostly absent in heterozygous mice suggesting that 50% loss of BACE1 function would be tolerated (Vassar et al., 2014).

Initially, due to the large active site of BACE1, it had been challenging to develop small-molecule inhibitors that can both efficiently cross the blood-brain barrier and be large enough to block the substrate-binding site (Ohno, 2016). Advances in medicinal chemistry led to the development of potent inhibitors. Currently, there are 2 that are remaining in the phase 3: E2609 (Eisai) and CNP520 (Novartis) (Table 2). The development of some of the inhibitors were recently terminated due to hepatotoxicity (JNJ-54861911, Janssen, Shionogi), did not meet the endpoints (LY3314814, Eli Lilly) or the benefit to risk ratio criteria was not met (MK-8931, Merck) (Das and Yan, 2019). The discouraging reports were speculated to be expected, since the introduction of the drug is likely to be given at the too late stage of the disease when the lowering of A β no longer has a cognitive improvement. Novel clinical strategies are aiming at the pre-symptomatic stages and are thought to be given as a primary prevention.

Table 2. BACE inhibitors in clinical trials. Overview of the ongoing and discontinued clinical trials of BACE inhibitors (Sources: clinicaltrials.gov, alzforum.org, accession date: 04.03.2019.).

Company	Compound	Clinical trial	Trial Phase	Patients
Eisai, Biogen	Elenbecestat, E2609	NCT02956486	3	Early AD, including MCI or mild AD
		NCT03036280		
Novartis, Amgen	CNP520 with CAD106 A β immunotherapy	NCT02565511	2/3	Cognitively unimpaired, homozygous APOE4
	CNP520	NCT03131453		Cognitively unimpaired participants, at least one APOE4 allele, if heterozygotes – elevated brain amyloid
Eli Lilly	LY3202626	NCT02791191	Discontinued	Mild AD
Eli Lilly, AstraZeneca	Lanabecestat, AZD3293, LY3314814	NCT02972658	Discontinued	Early AD
		NCT02783573		Mild AD
Janssen, Shionogi Pharma	Atabecestat JNJ-54861911	NCT02260674	Discontinued	Early AD
		NCT02406027		Asymptomatic at risk for developing AD
		NCT02569398		
Merck	Verubecestat MK-8931	NCT01739348	Discontinued	Mild to moderate AD
		NCT01953601		Prodromal AD
Boehringer Ingelheim, Vitae Pharmaceuticals	BI 1181181 VTP 37948	-	Discontinued	Healthy volunteers (Phase 1)
Eli Lilly	LY2886721	-	Discontinued	MCI or mild AD
High Point	HPP854	-	Discontinued	MCI or mild AD
CoMentis	CTS2116	-	Discontinued	Healthy volunteers (Phase 1)
Roche	RG7129 RO5508887	-	Discontinued	Healthy volunteers (Phase 1)
Pfizer	PF-06751979	-	Discontinued	Healthy volunteers (Phase 1)
	PF-05297909	-	Discontinued	Healthy volunteers (Phase 1)

1.12. The Seizure protein family

The seizure protein family members were recently identified as BACE1 substrates (Kuhn et al., 2012; Pignoni et al., 2016). Known also as Brain Specific Receptor-like Proteins (BSRPs), this protein family contain the same structural features and include: Seizure protein 6 (SEZ6), Seizure 6-like protein (SEZ6L) and Seizure 6-like protein 2 (SEZ6L2). They are single-pass type I membrane proteins that have a signal sequence, large extracellular domain, a membrane spanning domain and an intracellular region with consensus NPXY motif, that binds proteins with phosphotyrosine binding domains (PTB). The extracellular domain contains multiple CUB (Complement proteases C1r and C1s, embryonic sea urchin protein Uegf, bone morphogenetic protein-1 (BMP-1)) and SCR (short consensus repeats for complement C3b/C4b-binding site) (also referred as CCP – complement control protein or Sushi) domains. CUB and SCR are highly conserved domains often found in proteins of the immune system and are considered to be involved in protein-protein interactions (Bork and Beckmann, 1993; Giannakis et al., 2001). Furthermore, SEZ6L has an additional subset of CUB domain, with the ability of binding calcium (cbCUB, Ca²⁺-binding CUB domain) known to be involved in different major biological functions, such as immunity, development and in various cancer types (Gaboriaud et al., 2011).

SEZ6 was first identified in a study using a seizure inducing convulsant drug pentylenetetrazol on cortical neurons and in mice, where it was shown that its expression was increased both *in vitro* and *in vivo* upon the stimulation (Shimizu-Nishikawa et al., 1995). Soon afterwards, the mapping of the other seizure-related genes was performed and shown to be upregulated as well (SEZ2, SEZ4, SEZ7, SEZ10, SEZ15), while some others downregulated (SEZ9, SEZ12 and SEZ17) following pentylenetetrazol treatment (Wakana et al., 2000).

The expression of the seizure proteins is found mostly in the brain, but also in other organs, including pancreas (Hald et al., 2012; Stutzer et al., 2013). On the mRNA level, SEZ6L and SEZ6L2 expression is overlapping, while SEZ6 has a distinct pattern in the brain. SEZ6L and SEZ6L2 are widely expressed in the gray matter of the brain, with high levels in the olfactory bulb, anterior olfactory nuclei, hippocampus, cerebellar cortex and low levels in the white matter, like the corpus callosum and cerebellar medulla. Furthermore, intense expression is found in Purkinje cells (PCs) and granule cells, together with the positive signal in interneurons. On the other hand, SEZ6 is restricted to the gray matter and has higher levels in forebrain, such as the olfactory bulb, anterior olfactory nuclei, olfactory tubercle, striatum, hippocampal CA1 pyramidal cell layer and cerebral cortex. In granule cells SEZ6 is only weakly expressed (Kim et al., 2002; Miyazaki et al., 2006; Osaki et al., 2011).

The function of this protein family is poorly understood. SEZ6 is a susceptibility gene for febrile seizures (Mulley et al., 2011), childhood-onset schizophrenia (Ambalavanan et al., 2016), and is associated with developmental delay, short stature, microcephaly and dysmorphic features (Xie et al., 2016). It was recently shown in an Italian family that a rare SEZ6 variant is associated with familial form of AD (Paracchini et al., 2018). On the protein level, SEZ6 is suggested to be a highly reliable biomarker candidate for depressed, bipolar and schizophrenic patients (Maccarrone et al., 2013), but also was discussed as a potential CSF biomarker for AD patients (Khoonsari et al., 2016).

The second family member SEZ6L was connected to different cancer types: lung cancer (Gorlov et al., 2007; Nishioka et al., 2000; Raji et al., 2010), gastric cancer (Kang et al., 2008; Sepulveda et al., 2016) and as a head and neck cancer progression gene (Bornstein et al., 2016). The mutation of the SEZ6L gene is found in multiple myeloma (Kamada et al., 2012),

but also is connected to the cholesterol-regulatory functions (Blattmann et al., 2013), associated with Interleukin-6 levels (Shah et al., 2013) and bipolar disorder I (Xu et al., 2013).

The third family member, SEZ6L2, is increased on the protein level in different lung cancers and therefore suggested to be a prognostic marker of lung cancers (Ishikawa et al., 2006), involved in mouse neural tube development (Yu et al., 2017), upregulated in osteosarcoma (Wang, 2017) and an autism candidate gene (Kumar et al., 2009) together with SEZ6L (Chapman et al., 2015). Another study showed involvement of SEZ6L2 in the Man-6-P-independent transport of cathepsin D, and the cleavage of SEZ6L2 by cathepsin D produces a neurite outgrowth stimulating soluble fragment (Boonen et al., 2016). It has also been suggested that SEZ6L2 is one of the auxiliary subunits of the AMPA receptor, acting as a scaffolding protein to link GluR1, and modulating AMPA-adducin signal transduction (Yaguchi et al., 2017).

A mouse model that lacks all three members of the family shows motor discoordination in fixed bar and rotarod (Miyazaki et al., 2006). The SEZ6, SEZ6L and SEZ6L2 triple-knockout (TKO) PCs in the cerebellum were often innervated by multiple climbing fibres that had different neuronal origins. Additionally, electrophysiological abnormalities of climbing fibre–Purkinje cell synapses were recorded. Furthermore, the cerebellum of SEZ6 TKO mice displays a downregulation of the phosphorylation levels of protein kinase C alpha (PKC α) (Miyazaki et al., 2006).

Of the single knockouts, only the SEZ6-deficient mouse model was further described showing function of SEZ6 in dendritic arborization of cortical neurons (Gunnensen et al., 2007). The lack of SEZ6 is causing mice to have an excess of short dendrites in the deep-layer pyramidal neurons in the somatosensory cortex. Moreover, SEZ6-deficient cultured cortical neurons have excessive neurite branching and by adding membrane-bound SEZ6 the effect is opposite. There is a reduction in the dendritic spine density and also reduced excitatory postsynaptic currents of the layer V pyramidal neurons in the deficient brain. The mice also exhibit exploratory, motor and cognitive deficits (Gunnensen et al., 2007).

1.13. Seizure protein family as the main BACE1 substrates

Recent unbiased proteomic analyses, that our lab and others performed, revealed new physiological substrates of BACE1 (Hemming et al., 2009; Kuhn et al., 2012; Stutzer et al., 2013; Zhou et al., 2012). To this end, the secretome protein enrichment with click sugars (SPECS) method was developed, which enables identification of large amount of proteins in the secretome of the primary cultures, with the advantage of having serum proteins or other medium supplements present. The method utilizes modified sugars that are metabolically labelling newly synthesized glycoproteins, which facilitates click chemistry mediated biotinylation and selective enrichment using streptavidin for quantitative proteomics (Kuhn et al., 2012). SPECS identified 34 neuronal membrane proteins that were significantly reduced upon BACE1 inhibition, which covers 19% of the 183 shed membrane proteins identified in neurons, making BACE1 a major sheddase in neurons (Kuhn et al., 2012).

Some of the substrates were shown to be mainly processed by BACE1, while others are likely also shed by additional proteases. The proteins for which BACE1 was the major sheddase included the seizure protein family members, SEZ6L and SEZ6, whose abundances were reduced by 96 and 92% in the secretome upon BACE1 inhibition, respectively. On the other hand, SEZ6L2 was just a partially processed by BACE1, resulting in 60% remaining

abundance. SEZ6 and SEZ6L were validated *in vitro* and *in vivo* which confirmed exclusive processing by BACE1 (Pigoni et al., 2016). Besides the cleavage by BACE1, SEZ6L and SEZ6L2 were shown to be also BACE2 substrates in pancreatic β -cells (Stutzer et al., 2013).

The influence of BACE1 cleavage on SEZ6 function was recently investigated in an *in vivo* study, where mice were treated with BACE1 inhibitor NB-360 (Novartis). The BACE1 inhibition caused a reversible spine density reduction in wild-type, without affecting the SEZ6-deficient mice (Zhu et al., 2018b). In addition, knocking out SEZ6 in a small subset of mature neurons prevented the BACE1 inhibition-induced changes. Using electrophysiological recordings in chronic BACE1 inhibitor-treated wild-type and vehicle-treated SEZ6-deficient mice showed decreased hippocampal long-term potentiation, but did not alter the long-term potentiation in CA1 neurons of SEZ6-deficient mice (Zhu et al., 2018b).

Although SEZ6 was described to play an important role in maintaining normal dendritic spine dynamics and involved in BACE1 inhibition-induced structural and functional synaptic alterations (Zhu et al., 2018a; Zhu et al., 2018b), to date, SEZ6L functions and BACE1-dependent phenotypes are still not elucidated.

2. AIM OF THE WORK

Alzheimer's disease is a devastating and incurable neurodegenerative disorder affecting millions of people worldwide. It is a great burden for world healthcare and patients often require constant supervision from medical personnel or family. There is an urgent need for an efficient and safe treatment. Many clinical trials are currently taking place targeting different aspects of the disease. One major drug target is BACE1, as its cleavage of APP is the rate-limiting step in A β production. Pharmacological inhibition of BACE1 however, may lead to undesired side-effects as this enzyme is involved in many fundamental processes in brain such as axon guidance, neurogenesis, myelination and neuronal network functions. Over the years many unbiased proteomic studies revealed that BACE1 has a broad range of physiological substrates that raised the concern of possible mechanism-based side effects that may result from the reduced cleavage of its substrates or subsequent accumulation on the cell membrane. It is therefore essential to understand how the function of substrates is altered upon inhibition and whether their loss of cleavage contributes to the phenotypes caused by BACE1 deficiency or inhibition.

Thus, to understand better the role of BACE1 and consequences of inhibition, the focus of this thesis was to identify, validate and investigate its substrates. To this end the following aims were addressed:

1. Validation of novel substrates of BACE1

Selected novel substrate candidates that were identified in different proteomic studies, including the approach using the SPECS method, were to be further validated using an independent biochemical method. Substrate candidates were selected based on the percentage of cleavage by BACE1 and are the following: CACHD1, GLG1, LRRN1, DNER and NTM.

2. Neuronal surface proteome upon pharmacological inhibition of BACE1

Pharmacological inhibition of BACE1 may lead to side effects due to loss of cleavage of BACE1 substrates followed by its accumulation on the cell surface. This may affect cell signalling and cell-cell interactions and communication. To investigate the role of BACE1 on the cell surface, a new method for cell surface proteome determination was to be developed and applied to BACE1 inhibited cortical neurons. The observed major changes were to be validated in an independent set of biological samples *in vitro* and *in vivo*.

3. Analyses of SEZ6L^{-/-} mice

SEZ6L was identified and validated as one of the exclusive BACE1 substrates in the murine brain whose function is poorly understood. To understand its function and how the reduced cleavage of SEZ6L upon BACE1 inhibition might cause unwanted side effects in patients it is necessary to investigate the protein. Therefore, SEZ6L^{-/-} mice were to be analysed first via behavioural tests and afterwards by proteomics to investigate which proteins have changed levels due to the loss of SEZ6L. Furthermore, an interactomic study was to be performed to identify binding partners of SEZ6L, which possibly helps to unravel its function.

3. MATERIAL AND METHODS

3.1. Material

3.1.1. General reagents and chemicals

Reagents used in this thesis are listed in the table 3.

Table 3. Reagents and chemicals used in this thesis. Overview of all reagents and chemicals used in the thesis.

Reagent	Catalogue number	Manufacturer
Acetic Acid	49199	Fluka
Acrylamide/Bis Solution, 37.5:1	10681.03	Serva
Agarose UltraPure	16500	Invitrogen
Ampicillin sodium salt	K029.2	Roth
B-27 Supplement (50×), serum free	17504044	Thermo Fisher Scientific
Bacto Agar	214030	BD
BC Accay Reagent A	UP95424A	Interchim
BC Accay Reagent A	UP95425A	Interchim
Biotin	B4501	Sigma Aldrich
Bovine Serum Albumin	A8022	Sigma Aldrich
BS3 crosslinker	ab145612	Abcam
C3 (β -secretase inhibitor IV)	565788	Merck
Concanavalin A from <i>Canavalia ensiformis</i>	C7555	Sigma Aldrich
CutSmart Buffer	B7204S	NEB
L-Cysteine hydrochloride monohydrate	C6852	Sigma Aldrich
Dimethylsulfoxid (DMSO)	4720.4	Roth
DMEM - Dulbecco's Modified Eagle Medium, high glucose, GlutaMAX Supplement, pyruvate	31966047	Thermo Fisher Scientific
DMEM - Dulbecco's Modified Eagle Medium, high glucose, GlutaMAX Supplement	61965059	Thermo Fisher Scientific
DNA Ladder 1 kb	N3232S	NEB
ECL Prime Western Blotting System	GERPN2232	Sigma Aldrich
ECL Western Blotting Reagents	GERPN2106	Sigma Aldrich
EcoRV-HF	R3195	NEB
Ethanol, 80% techn.	9474.3	Roth
FBS - Fetal Bovine Serum	10270-106	Thermo Fisher Scientific
GelRed Nucleic Acid Gel Stain	41003-1	Biotium
GlutaMAX Supplement	35050061	Thermo Fisher Scientific
GoTaq G2 DNA Polymerase	M784B	Promega
GoTaq Reaction Buffer 5×	M791A	Promega
HBSS - Hanks' Balanced Salt Solution	24020-091	Thermo Fisher Scientific
HEPES 1M	15630-056	Thermo Fisher Scientific
High Capacity Streptavidin Agarose	20361	Thermo Fisher Scientific
IGEPAL CA-630	I3021	Sigma Aldrich
Immobilon-P PVDF Membrane	IPVH00010	Merck
Isopropanol	L311393	Thermo Fisher Scientific
rLys-C, Mass Spec Grade	V1671	Promega

Lipofectamine 2000, Transfection reagent	11668027	Thermo Fisher Scientific
MEM Non-Essential Amino Acids Solution	11140-035	Thermo Fisher Scientific
2-Mercaptoethanol	4227.1	Roth
NAD	N7004	Sigma
NEB 5-alpha Competent <i>E. coli</i> (High Efficiency)	C2987	NEB
Neurobasal medium	21103049	Thermo Fisher Scientific
O.C.T. Compund	4586	Tissue-Tek
Opti-MEM, Reduced Serum Medium, GlutaMAX Supplement	51985042	Thermo Fisher Scientific
Papain, from papaya latex, buffered aqueous suspension	P3125	Sigma Aldrich
Paraformaldehyde	1.04005	Merck
PCR Nucleotide Mix	11814362001	Roche
PBS - Phosphate-Buffered Saline, pH 7.4	10010056	Thermo Fisher Scientific
Penicillin/Streptomycin (5000 U/mL)	15070-063	Thermo Fisher Scientific
Phusion DNA polymerase 2000 U/ml	M0530S	NEB
Pierce 660 nm Protein Assay Reagent	22660	Thermo Fisher Scientific
Poly-D-Lysine Hydrobromide, Mol wt 70-150 tsd	P6407	Sigma Aldrich
Precision Plus Protein Dual Xtra Prestained Protein Standards	161-0377	Bio-Rad
Protease Inhibitor Cocktail	P8340	Sigma Aldrich
Protein G Sepharose 4 Fast Flow	17-0618-06	GE Healthcare
Proteinase K, recombinant, PCR Grade	03115828001	Sigma Aldrich
Pwo-DNA-Polymerase	732-3262	Peqlab
Puromycin Dihydrochloride	A1113803	Thermo Fisher Scientific
Recombinant Protein G - Sepharose 4B	101243	Thermo Fisher Scientific
ReproSil-Pur 120 C18-AQ, 1.9 µm	r119.aq.	Dr. Maisch
SDS, Molecular Biology Grade	20765.03	Serva
Skim Milk Powder	70166	Sigma Aldrich
Sodium azide	1.06688	Merck
Sodium chloride	3957.2	Roth
Sodium hydroxide 1.0 N solution	S2770	Sigma Aldrich
Sucrose (saccharose)	1.07687	Merck
Sulfo-dibenzylcyclooctyne-biotin (Sulfo-DBCO-Biotin)	CLK-A116-10	Jena Bioscience
Taq DNA ligase 40000 U/ml	M0208L	NEB
T5 Exonuclease 10000 U/ml	M0363S	NEB
TEMED, 99% p.a.	2367.2	Roth
tetraacetylated N-azidoacetylmannosamine (Ac4-ManNAz)	-	Provided by Stefan Bräse
Tris ultrapure, 5 kg	A1086	Applichem
Triton X-100	1.08603	Merck
0.05% Trypsin-EDTA 1×	25300-062	Thermo Fisher Scientific
Trypsin, Sequencing Grade Modified	V5111	Promega
Tween 20	8.22184	Merck
Urea	1.08487	Merck
Zeocin	R25005	Thermo Fisher Scientific

3.1.2. Primers

The primers used in this thesis are summarized in the table 4:

Table 4. Primers used in this thesis. Overview of all primers used in the thesis for cloning, sequencing and genotyping of mouse lines.

Protein	Primer	Sequence (in 5' - 3' order)	Usage
mmBACE1	BACE1 wt fw	AGGCAGCTTTGTGGAGATGGTG	genotyping
	BACE1 rev	CGGGAAATGGAAAGGCTACTCC	
	NEO BACE1 fw	TGGATGTGGAATGTGTGCGAG	
mmCACHD1	mmCACHD1 fl RHA rev	CAAGCCTAACGAGGAGGAGAGGATTTAG CACTCAGCATCCACAGTGTGC	cloning
	mmCACHD1 LHA fw	TCAGGAGCAGGAGGATCATCGGATGACGC CGACTTCTCCATCCTG	
	CACHD1 seq 1 fw	CAGATTGCCAAGGACGC	sequencing
	CACHD1 seq 2 fw	CCTCATAGATGACAAAGG	
	CACHD1 seq 3 fw	TGGCTATGTCGTGACAATC	
mmGLG1	mmGLG1 LHA neu fw	TCAGGAGCAGGAGGATCATCGGATCAGA ATGGTCACGGTCAGGG	cloning
	mmGLG1 R* FL RHA neu rev	CAAGCCTAACGAGGAGGAGAGGATCCTGT CCTTCAGCTCTCGTGTC	
	mmGLG1 seq 1 new fw	GCTTGATCTGCGGCTTCATG	sequencing
	mmGLG1 seq 2 new fw	CTGGATTACATCGGAAAGG	
	mmGLG1 seq 2/3 fw	ACAGAAGAGCAAGGAAGGAGG	
	mmGLG1 seq 3 new fw	TGGCAGACAACCAGATCGAC	
mmLRRN1	mmLRRN1 LHA fw	TCAGGAGCAGGAGGATCATCGGATTCCAT ACTGACTAGTGAG	cloning
	mmLRRN1 RHA rev	CAAGCCTAACGAGGAGGAGAGGATCCAC ATGTAATAGCTTCT	
	mmLRRN1 seq 1 fw	GTCCCCAGCTTTGTGTTTGT	sequencing
	mmLRRN1 seq 2 fw	CCCTGGATAACTTGCCAGAA	
	mmLRRN1 seq 3 fw	CCGTGGAAACTCTTTCAGACA	
mmDNER	mmDNER LHA fw neu	TCAGGAGCAGGAGGATCATCGGATGCTGG GCCCAAAGCGGCTGCTTG	cloning
	mmDNER RHA rev	CAAGCCTAACGAGGAGGAGAGGATCAAA TCTTTTGTTTAATCA	
	mmDNER seq 1 neu fw	CCAGGAGCCTGACATAATCC	sequencing
	mmDNER seq 2 neu fw	ATGGCGTGCATTTACCT	
mmNTM	mmNeurotrimin fl RHA rev	CAAGCCTAACGAGGAGGAGAGGATTCAA AATTTGAGGAGCAGG	cloning
	mmNeurotrimin LHA fw	TCAGGAGCAGGAGGATCATCGGATGGAG ATGCCACCTTTCCCAAAGC	
mmSEZ6	SEZ6 fw	GAGTGAGCAGAATCCATCAAGAGG	genotyping
	NEO SEZ6 fw	CGCTATCAGGACATAGCGTTGGCTACC	
	SEZ6 rev	CATCTTCACAGGTGATGCTGTGTC	

mmSEZ6L	SEZ6L fw	CGTCCCTGAAGCAACTCAACTCGG	
	SEZ6L rev	CCGTGGTGATGATGGTGGTAGTGAC	
	NEO SEZ6L rev	GCCACACGCGTCACCTTAATATGCG	
mmSEZ6L2	SEZ6L2 fw	CGTGGGCTTGACACCTTTCTCAGC	
	SEZ6L2 rev	CCCCAGTGAAATACTCCCCTGATCC	

3.1.3. Buffers

The following buffers were used and listed in the table 6:

Table 6. Buffers used in this thesis. Overview of all buffers used in the thesis.

Name	Composition
Blocking solution	Triton-X 0,5% (v/v), NGS 5% (v/v) in PBS pH 7,4
DEA buffer	50 mM NaCl, 2 mM EDTA, 0,2% Diethylamine
DNA sample buffer	30% Glycerol, 10 mM EDTA, 0,05% Orange G (Sigma)
Gibson assembly master mix 2X	5X Isothermal buffer, T5 Exonuclease 10000 U/ml, Phusion DNA polymerase 2000 U/ml, Taq DNA ligase 40000 U/ml
Isothermal reaction buffer 5X	25% PEG-8000, 500 mM Tris-HCl pH 7,5, 50 mM MgCl ₂ , 50 mM DTT, 4 mM (dNTP mix), 5 mM NAD
Laemmli buffer (4X)	8% SDS, 40% Glycerol, 0,025% Bromphenol blue, 125 mM Tris pH 6,8, 10% β-Mercaptoethanol
LB medium	10g Bacto-Tryptone, 5 g Yeast extract, 5 g NaCl in 1 l of H ₂ O
Lower Tris buffer	1,5 M Tris pH 8,8, 0,4% SDS
Neutralization buffer	0,5 M Tris pH 6,8
PBS	140 mM NaCl, 10 mM Na ₂ HPO ₄ , KCL, 1,75 mM KH ₂ PO ₄ pH 7,4 autoclaved at 120°C and 1,2 bar for 20 min
RIPA buffer	10 mM PBS pH 7,4, 150 mM NaCl, 1% Triton X-100 (v/v), 1% Sodium deoxycholate, 0,1% SDS, 2 mM EDTA
SDS Running buffer	25 mM Tris, 192 mM Glycin, 0,1% SDS
SOC medium	2% Bacto-Trypton, 0,5% Yeast extract, 10 mM NaCl, 10 mM MgSO ₄ , 10 mM MgCl ₂ , 2,5 mM KCl, 0,5% Na-Succinat, 20 mM Glucose
STEN	51 mM Tris pH 7,5, 150 mM NaCl, 2 mM EDTA, 1% Igepal CA-630
STET	50 mM Tris pH 7,5, 150 mM NaCl, 2 mM EDTA, 1% Triton X-100
TAE buffer	40 mM Tris, 20 mM Acetic acid, 1 mM EDTA
Tail lysis buffer	100 mM Tris pH 8,5, 200 mM NaCl, 5 mM EDTA, 0,2% SDS
Transfer buffer	25 mM Tris, 240 mM Glycin
Upper Tris buffer	0,5 M Tris pH 6,8

3.1.4. Kits

The kits used in this thesis are the following (Table 7):

Table 7. Kits used in this thesis. Overview of the kits used in the thesis.

Name	Catalogue number	Manufacturer
DNA, RNA and protein purification kit	MN740588	Macherey-Nagel
Plasmid DNA purification	MN740410	Macherey-Nagel
BC Assay Kit	UP40840A	Interchim

3.1.5. Equipment

The equipment used in this thesis is listed here (Table 8):

Table 8. Equipment used in this thesis. Overview of the equipment that was necessary to carry out this thesis.

Name	Manufacturer	Type
Avanti J-26XP, High-Speed Centrifuge	Beckman Coulter	Centrifuge
CKX53 Inverted Microscope	Olympus	Microscope
CryoStar™ NX70 Cryostat	Thermo Fisher Scientific	Cryostat
EASY-nLC 1000 Liquid Chromatograph	Thermo Fisher Scientific	Chromatograph
Hei-Tec, Magnetic Stirrer	Heidolph	Magnetic stirrer
Heracell 150i CO2 Incubators with Stainless-Steel Chambers	Thermo Fisher Scientific	Incubator
HERAFreeze HFU B Series -86°C Upright Ultra-Low Temperature Freezers	Thermo Fisher Scientific	Freezer
Heraeus Fresco 17 Microcentrifuge	Thermo Fisher Scientific	Centrifuge
Heraeus Megafuge 16 Centrifuge Series	Thermo Fisher Scientific	Centrifuge
ImageQuant LAS 4000 series	GE Healthcare	
Incubation/Inactivation Water Bath 1008	GFL	Water bath
Infinite 200 PRO	Tecan	Plate reader
KL 1600 LED	Olympus	Light source
Leica MZ75 Stereomicroscope	Leica	Microscope
Liebherr™ G Series Refrigerator	Thermo Fisher Scientific	Refrigerator
Liebherr GNP 1956 Premium NoFrost	Thermo Fisher Scientific	Freezer
Multi Controller and Cryo System	Cryo Anlagenbau	Cryo preservation
Multitron Pro	Infors	Incubation shaker
Nano Electrospray source (Thermo Proxeon)	Thermo Fisher Scientific	
Optima MAX-XP	Beckman Coulter	Ultracentrifuge
Orbital-Rocking Shaker 3011	GFL	Shaker
PowerPac Basic Power Supply	Bio-Rad	Power supply
Safe 2020 Class II Biological Safety Cabinets	Thermo Fisher Scientific	Hood
ScanSpeed MaxiVac	ScanVac	Vacuum centrifuge
TC20 Automated Cell Counter	Bio-Rad	Cell counter
ThermoMixer comfort	Eppendorf	Thermomixer
UP200St – Powerful Ultrasonic Lab Homogenizer	Hielscher	Ultrasonic homogenizer

UV HEPA PCR Systems	UVP	Hood
Velos Pro Orbitrap Mass Spectrometer	Thermo Fisher Scientific	Mass spectrometer
Veriti 96-Well Thermal Cycler	Thermo Fisher Scientific	PCR
Vortex mixer, peqTWIST	Peqlab	Vortex
ZIEGRA Ice Maker	Ziegra Eismachinen	Ice machine

3.2. DNA methods

3.2.1. Polymerase Chain Reaction (PCR)

Reaction mix for PCR was prepared on ice according to the table 9:

Table 9. PCR reaction mix. Summary of the reagents used in PCR reaction for DNA cloning.

Reagents	Amount
Nucleotide Mix (dNTPs)	1 μ l
Forward primer (10 μ M)	4 μ l
Reverse primer (10 μ M)	4 μ l
PWO Polymerase	1 μ l
Template DNA (100 ng)	1 μ l
Poly buffer complete (10 \times)	2.5 μ l
Autoclaved dH ₂ O	10.875 μ l
DMSO (2.5%)	0.625 μ l
Total	25 μ l

Samples were run in the Thermal Cycler using gradient program (Table 10):

Table 10. Gradient program. Overview of the program used in PCR reaction for DNA cloning.

Stage	Temperature	Duration
Stage 1 \times 1	95°C	5 min
Stage 2 \times 30	95°C	30 s
	55/58/63/66/69/72°C	30 s
	72°C	7 min
Stage 3 \times 1	72°C	7 min
	10°C	∞

PCR products were run on the 1% or 2% agarose gel (according to the size of DNA). For 1% gel, 1 g of agarose was dissolved in 100 ml of TAE buffer together with the GelRed Nucleic Acid Gel Stain (1:10000) for visualisation of DNA. DNA ladder 1 Kb was loaded together with the samples mixed in sample buffer and ran 45 min, 120 V.

3.2.2. Cloning of DNA constructs

All the created plasmids were first digitally made in Vector NTI Advance 11.5.3 software (Life Technologies) and the cDNA was sequenced for the internal control. Gene of interest (GOI) was multiplied with the flanking left and right homology arms (LHA and RHA) with polymerase chain reaction (PCR) from the annotated cDNA (Table 12). PCR products were run on the 1% agarose gel (30 min, 120 V), and the bands at the right molecular height were cut so that GOI can be purified. DNA extraction was done with the DNA, RNA and protein purification kit for clean-up of the DNA from the agarose gel (MN 740609). Plasmid

backbone (F2KP-5XUAS-E1b or pcDNA3.1-Zeo(+)) containing LHA and RHA was linearized with EcoRV-HF (EcoRV specific cleavage of both plasmid backbones occurs between LHA and RHA) according to the manufacturer's instructions (Table 11).

Table 11. Purification of DNA. Overview of the reagents used for DNA purification.

Name of the plasmid	F2KP-5XUAS-E1b	pcDNA3.1-Zeo(+)
Amount	6982 bp / 100 ng/μl	5253 bp / 100 ng/μl
Buffer Cutsmart 10×	2 μl	2 μl
EcoRV-HF	1 μl	1 μl
Plasmid 1 μg	10 μl	10 μl
Autoclaved dH ₂ O	7 μl	7 μl
Total	20 μl	20 μl

Purified GOI and the linearized plasmid backbone were brought together with Gibson's assembly. Competent *E. coli* were transformed and plated on agar plates with Ampicillin resistance overnight (o/n), 37°C. Next day the single colonies were picked and grown o/n, 37°C, with shaking. From the grown colonies DNA was prepared using Isolation of high copy plasmid DNA from *E. coli* kit (MN 740588.250) according to the manufacturer's instructions. Plasmids from each colony were digested with suited restriction enzyme (restriction sites that cleaves the plasmid only once in the sequence of GOI and once within the plasmid backbone were analysed according to the Vector NTI), ran on 1% agarose gel (30 min, 120 V) and selected ones containing the insert GOI band were sent for sequencing. Only sequenced plasmid that matched the sequence from the digitally created Vector NTI files were used for experiments (Table 12). In the case of both CACHD1 vectors there were two silent mutations that did not change the amino acid sequence. Additionally, the same vectors contained STOP codon before the FLAG tag, but the N-terminally HA tag however could still be detected via Western blotting.

Table 12. Plasmids. Overview of plasmids generated and used in this thesis.

Plasmid	Vector	cDNA	Source
F2KP-5XUAS-E1b-CD5-HA-SLIC-FLAG-mmCACHD1fl	F2KP-5XUAS-E1b	mmCachd1 full-length protein	Cloned in this study
pcDNAT3.1_Zeo(+)-CD5-HA-SLIC-FLAG-mmCACHD1fl	pcDNA3.1-Zeo(+)	mmCachd1 full-length protein	Cloned in this study
F2KP-5XUAS-E1b-CD5-HA-SLIC-FLAG-mmGLG1fl	F2KP-5XUAS-E1b	mmGLG1 full-length protein	Cloned in this study
pcDNAT3.1_Zeo(+)-CD5-HA-SLIC-FLAG-mmGLG1fl	pcDNA3.1-Zeo(+)	mmGLG1 full-length protein	Cloned in this study
F2KP-5XUAS-E1b-CD5-HA-SLIC-FLAG-mmLRRN1fl	F2KP-5XUAS-E1b	pYX Asc 1-mmLRRN1 full-length protein	Cloned in this study
pcDNAT3.1_Zeo(+)-CD5-HA-SLIC-Flag-mmLRRN1fl	pcDNA3.1-Zeo(+)	pYX Asc 1-mmLRRN1 full-length protein	Cloned in this study
F2KP-5XUAS-E1b-CD5-HA-SLIC-FLAG-mmDNERfl	F2KP-5XUAS-E1b	pFLCI-mmDNER full-length protein	Cloned in this study
pcDNAT3.1_Zeo(+)-CD5-HA-SLIC-FLAG-mmDNERfl	pcDNA3.1-Zeo(+)	pFLCI-mmDNER full-length protein	Cloned in this study
F2KP-5XUAS-E1-CD5-HA-SLIC-mmNeurotriminfl	F2KP-5XUAS-E1b	mmNTM full-length protein	provided by Peer-Hendrik Kuhn

3.2.3. Gibson assembly

Linearized plasmid backbone and the insert containing GOI were brought together using the formula to get the proper ratio of the insert and the plasmid (Table 13):

PLASMID: $A (0.02 \text{ pmol}) = X \text{ ng} \times 1000 / (YY \text{ bp} \times 650 \text{ Da})$

INSERT: $B (0.06 \text{ pmol}) = X \text{ ng} \times 1000 / (YY \text{ bp} \times 650 \text{ Da})$

Table 13. Gibson assembly. Gibson assembly mixture used to join the insert with the plasmid.

Reagents	Amount
Gibson assembly master mix 2×	5 μ l
Plasmid 0.02 pmol	A
Insert 0.06 pmol	B
Autoclaved dH ₂ O	10-(5+A+B) μ l
Total	10 μ l

Samples were incubated for 50 min at 50°C. Following incubation, samples were stored on ice or at 20°C for subsequent transformation.

3.2.4. Transformation of competent *E. coli* bacteria

Highly efficient NEB 5-alpha Competent *E. coli* were thawed on ice and 25 μ l was used together with the 4 μ l of DNA (obtained from the Gibson assembly) for 15 min incubation on ice. The transformation was done using heat shock at 42°C for 30 s following 2 min on ice. Afterwards, 500 μ l of SOC medium was added to the transformed bacteria and allowed to recover 1 h at 37°C in the shaking incubator at 200 rpm. The transformed bacteria were plated on LB agar plates with ampicillin (100 μ g/ml) and incubated o/n at 37°C.

3.2.5. Mini preps – preparation of DNA for construct screening

Single colonies were picked up from the agar plates and placed in the 5 ml of LB medium supplemented with ampicillin (100 μ g/ml) and grown o/n at 37°C in the shaking incubator at 200 rpm. The bacteria were pelleted by centrifuging at 4500 rpm and 4°C for 15 min. DNA was extracted using Plasmid DNA purification kit (Macherey-Nagel) following the manufacturer instructions. The extracted DNA was digested with the corresponding restriction enzyme and ran on an agarose gel to prove the presence of the insert. Positive clones were sent for sequencing to control the accuracy of the sequence.

3.2.6. Midi preps – preparation of DNA for transfection

Plasmids used for the transfections were transformed in the highly efficient NEB 5-alpha Competent *E. coli* and incubated o/n in 200 ml of LB medium supplemented with ampicillin (100 μ g/ml) at 37°C in the shaking incubator, at 200 rpm. The transformed bacteria was centrifuged at 4500 rpm at 4°C for 15 min and the DNA was extracted using Plasmid DNA purification kit (Macherey-Nagel) following the instructions of the manufacturer. DNA was measured with the Infinite 200 PRO (Tecan).

3.2.7. Sequencing of cloned DNA constructs

The sequencing service was provided by GATC Biotech by sending 200 to 300 ng of DNA and the respective sequencing primers that are not offered by the company. All the constructs used in this thesis were sequenced with the primers annotated in the table 4.

3.2.8. DNA isolation

DNA was isolated from tail or ear tissue, using 500 μ l of tail lysis buffer with 100 μ g/ml of Proteinase K per biopsy. Tissue was incubated o/n, shaking at 650 rpm, 55°C. Samples were centrifuged at 16000 \times g for 5 min, and subsequently, supernatants were collected and mixed with 400 μ l of isopropanol. Mixture was centrifuged at 16000 \times g for 20 min and DNA pellet was washed with 500 μ l of ice cold 70% ethanol. Samples were centrifuged at 16000 \times g for 5 min, supernatants discarded and pellet was dried at 55°C to remove ethanol. DNA was resuspended in 200 μ l of H₂O and incubated for 30 min, 55°C with shaking at 650 rpm.

3.2.9. Genotyping

Isolated DNA from B6.129-*Bace1*^{tm1Pcw}/J was amplified with PCR using following reaction mixture (Table 14):

Table 14. BACE1 genotyping. Summary of reaction used to genotype BACE1^{-/-} mice.

Reagents	Amount
Nucleotide Mix (dNTPs)	0.5 μ l
BACE1 wt fw (10 μ M)	0.2 μ l
BACE1 rev (10 μ M)	0.2 μ l
NEO BACE1 fw (10 μ M)	0.2 μ l
GoTaq G2 DNA Polymerase	0.1 μ l
Template DNA	1 μ l
GoTaq buffer 5 \times	4 μ l
Autoclaved dH ₂ O	13.8 μ l
Total	20 μ l

Samples were run in the Thermal Cycler using the program annotated in table 15.

Table 15. PCR reaction for BACE1 genotyping. Program used to amplify BACE1 DNA.

Stage	Temperature	Duration
Stage 1 \times 1	94°C	5 min
Stage 2 \times 30	95°C	30 s
	55/58/63/66/69/72°C	30 s
	72°C	7 min
Stage 3 \times 1	72°C	7 min
	10°C	∞

For B6.129-SEZ6TKO genotyping 3 separate reaction mixtures for each gene (SEZ6, SEZ6L and SEZ6L2) were prepared (Table 16, 17 and 18):

Table 16. SEZ6 TKO genotyping. Summary of reaction used to genotype SEZ6 TKO mice for SEZ6 gene.

Reagents	Amount
Nucleotide Mix (dNTPs)	0.5 μ l
SEZ6 fw (10 μ M)	1 μ l
SEZ6 rev (10 μ M)	1 μ l
NEO SEZ6 fw (10 μ M)	1 μ l
GoTaq G2 DNA Polymerase	0.5 μ l
Template DNA	1 μ l
GoTaq buffer 5 \times	4 μ l
Autoclaved dH ₂ O	11 μ l
Total	20 μ l

Table 17. SEZ6 TKO genotyping. Summary of reaction used to genotype SEZ6 TKO mice for SEZ6L gene.

Reagents	Amount
Nucleotide Mix (dNTPs)	0.5 μ l
SEZ6L fw (10 μ M)	1 μ l
SEZ6L rev (10 μ M)	1 μ l
NEO SEZ6L rev (10 μ M)	1 μ l
GoTaq G2 DNA Polymerase	0.5 μ l
Template DNA	1 μ l
GoTaq buffer 5 \times	4 μ l
Autoclaved dH ₂ O	11 μ l
Total	20 μ l

Table 18. SEZ6 TKO genotyping. Summary of reaction used to genotype SEZ6 TKO mice for SEZ6L2 gene.

Reagents	Amount
Nucleotide Mix (dNTPs)	0.5 μ l
SEZ6L2 fw (10 μ M)	1 μ l
SEZ6L2 rev (10 μ M)	1 μ l
GoTaq G2 DNA Polymerase	0.5 μ l
Template DNA	1 μ l
GoTaq buffer 5 \times	4 μ l
Autoclaved dH ₂ O	12 μ l
Total	20 μ l

Samples were run in the Thermal Cycler using the program (Table 19):

Table 19. PCR reaction for SEZ6 TKO genotyping. Program used to amplify SEZ6, SEZ6L and SEZ6L2 DNA.

Stage	Temperature	Duration
Stage 1 \times 1	95°C	5 min
Stage 2 \times 30	95°C	30 s
	SEZ6: 57°C /SEZ6L: 64°C /SEZ6L2: 62°C	30 s
	72°C	30 s
Stage 3 \times 1	72°C	7 min
	10°C	∞

PCR products were then run on agarose gel 45 min, 120 V and visualized with the GelRed Nucleic Acid Gel Stain (1:10000).

3.3. Cell culture methods

3.3.1. Cell culture

The cell culture passaging was done under sterile condition in the cell culture hood. The immortalized cell lines were first rinsed one time with 5 ml PBS and incubated for 2 to 3 minutes with 1.5 ml of Trypsin-EDTA to detach the cells from the plastic surface. Cells were collected in culturing medium and centrifuged at $1000 \times g$, room temperature (RT), for 5 min. Cell pellet was re-suspended in the culturing media and one fourth of the amount is plated. The procedure was repeated every 3 to 4 days, according to the confluency. Cell viability and confluency were regularly controlled under the light microscope.

3.3.2. Cell lines

The only immortalized cell line used in this thesis was Human Embryonic Kidney HEK293T (immortalized with SV40 large T-Antigen). HEK293T were cultured in DMEM supplemented with 10% FCS and 1% Penicillin/Streptomycin (5000 U/mL) (v/v).

The only primary culture used was the primary culture of cortical neurons prepared from embryonic 16 day (E16) and cultured in Neurobasal medium with 500 μ M GlutaMAX supplement, 1% Penicillin/Streptomycin (5000 U/mL) (v/v) and $1 \times$ B27 supplement.

Both cell types were grown in the incubator at 37°C and 5% CO₂.

3.3.3. Cryopreservation

Immortalized cell lines were cryopreserved at -80°C or in liquid nitrogen. Cells were pelleted and resuspended in the cold FBS supplemented with 10% DMSO (v/v) in 1 ml aliquots and put to -80°C. For culturing, cells were partially thawed and collected in the culturing medium, centrifuged at $1000 \times g$, RT, 5 min and resuspended in the fresh medium to be plated. Cells were passaged one time before doing the experiments and controlled for viability and confluency at the light microscope.

3.3.4. Transient transfection

For transient transfection of cells, 4.5 μ l of Lipofectamine 2000 and 250 μ l of Opti-MEM was mixed and added per well of a 6-well plate and incubated 5 min at RT. 1.5 μ g of DNA was added to the mix and incubated 20 min at RT. The mixture is added to each well, together with cells in Opti-MEM media supplemented with 10% FBS (v/v). Cell lysates were collected after three days and further analysed.

3.3.5. Lentivirus production

Lentiviruses were produced from HEK293T cells by transiently transfecting GOI carrying UAS sequence together with the driving plasmid with Gal4-VP16 sequence and packaging

plasmids needed for virus assembly. The amount of plasmid needed per one 10-cm dish was used as listed in table 20.

Table 20. Plasmids used for lentiviral production. Overview of the plasmids and its amount used to produce GOI in a lentivirus.

Type	Plasmid	µg/ 10-cm dish
responder	F2KP-5XUAS-E1b-CD5-HA-SLIC-FLAG	7,75
activator	FU-ΔZeo-Gal4-VP16	5,5
packaging	pCMV R8.91-psPAX2	5
	pcDNA3.1-Δzeo(-)-VSV-G	2,7

For each dish, the DNA mixture was added to 750 µl of Opti-MEM medium and separately another 750 µl of Opti-MEM was mixed with 38 µl of Lipofectamine 2000 and incubated 5 min, RT. DNA and Lipofectamine mixture in Opti-MEM was then mixed together and incubated for additional 20 min, RT. Afterwards, the transfection mixture was added to the cell suspension and 9 million cells per dish were plated in Opti-MEM supplemented with 10% FBS (v/v). One day after transfection, Opti-MEM medium was replaced with 8.5 ml of packaging medium (DMEM - Dulbecco's Modified Eagle Medium, high glucose, GlutaMAX Supplement, pyruvate; MEM Non-Essential Amino Acids Solution 1×; 10% FBS (v/v)). After 24 h, conditioned media with virus particles was collected for purification and making the highly potent stock of lentiviruses for transduction or directly transferred to the target cells.

Collected conditioned media was first centrifuged at $3000 \times g$, for 15 min at 4°C to remove cellular debris. The supernatant was filtered through a sterile 0.45 µm filter for removing additional contaminants and smaller cellular debris. Subsequently, filtered supernatants containing the viruses were either directly put to the targeting cells or further ultracentrifuged at 22000 rpm in a SW28 rotor for 2 h, 4°C. Pellets from the ultracentrifugation were resuspended in 250 µl of TBS-5 buffer and incubated o/n at 4°C. The viral suspension was then aliquoted and stored at -80°C.

3.3.6. Stable cell line production

Stable cell lines were produced by either transient transfecting with pcDNA3.1-Zeo(+) or by lentiviral transduction of F2KP-5XUAS-E1b carrying corresponding GOI in the HEK293T cells.

Two days after transfection, cells were passaged from the 6-well to the 25 cm² flask format and left for an additional day in the culturing medium. Afterwards, culturing medium was exchanged for the selection medium (DMEM - Dulbecco's Modified Eagle Medium, high glucose, GlutaMAX Supplement, 10% FBS (v/v), 1% Penicillin/Streptomycin (5000 U/mL) (v/v), 250 µg/ml Zeocin). Cells were controlled for growing, and when in stationary phase then passaged to stimulate growth. By stimulating growth, Zeocin is killing the untransfected cells and only the cells carrying the DNA construct with the resistance gene survive the selection. After a series of passaging, when the cell number was constant, the cells were considered to be stable and the expression of the GOI was tested via Western blot.

Stable cell lines produced with lentiviruses were transduced by transferring the conditioned media (as described above in the Lentiviral production) containing viral particles carrying GOI and the procedure of selection was done in the same way with the selection media for the

F2KP-5XUAS-E1b construct (DMEM - Dulbecco's Modified Eagle Medium, high glucose, GlutaMAX Supplement, 10% FBS (v/v), 1% Penicillin/Streptomycin (5000 U/mL) (v/v), 1 µg/ml Puromycin).

When performing the experiment, selection antibiotic was omitted.

3.3.7. Primary cortical neurons isolation and culture

Cortices of the mice embryonic 16 day (E16) were collected without meninges in cold HBSS and the medium was exchanged for the activated digestion medium (activation: 30 min at 37°C) (Table 21) and incubated 15-20 min, 37°C. Cortices were then washed two times in dissociation medium and a third time were dissociated in the same medium using 2 ml graduate sterile pipette. Dissociated cortical neurons were collected in a new tube avoiding small undissociated pieces and centrifuged 3 min at 700 × g. Cortical neurons were resuspended in the plating medium, counted, plated on the poly-D-lysine coated dishes (25 µg/ml of poly-D-lysine per well) and cultured at 37°C, 5% CO₂. Plating medium was exchanged for the culturing medium after three hours. Fifth day *in vitro* (DIV 5), cortical neurons were treated with 2 µM C3 inhibitor or vehicle control (DMSO) and finally collected at DIV 7.

Table 21. Primary cortical neuron preparation. Overview of media used to prepare and culture primary cortical neurons.

Medium	Composition
Digestion medium	9.7 ml DMEM high glucose with GlutaMAX Supplement, 0.01 g L-Cystein, 200 U papain, pH 7.4
Dissociation medium	DMEM high glucose with GlutaMAX Supplement, 10% FBS
Plating medium	DMEM high glucose with GlutaMAX Supplement, 10% FBS (v/v), 1% Penicillin/Streptomycin (5000 U/mL) (v/v)
Culture medium	9.6 ml Neurobasal, 500 µM GlutaMAX supplement, 1% Penicillin/Streptomycin (5000 U/mL) (v/v), 1× B27 supplement

3.3.8. Compound treatment

Stable cell lines as well as neurons were treated with the 2 µM of the β-secretase inhibitor IV (C3) or the vehicle control (DMSO) 24 h after transient transfection with the BACE1 in the case of the stable cell lines or 5 DIV in case of primary cortical neurons. Both cell types were left 48 h with the compound and afterwards collected for lysing, while in the case of the stable cell lines, conditioned media was collected for concanavalin A enrichment.

3.4. Protein analysis methods

3.4.1. Cell lysis

Cells were kept on ice and washed three times with cold PBS without detaching them from the well. Lysis buffer supplemented with Protease inhibitor (1:500) was then added and the

cells were scraped to detach them from the surface of the well. Lysate was transferred to the tube, incubated 10 min on ice and centrifuged 10 min at $20000 \times g$ and 4°C to remove cell debris. Supernatants were collected and stored at -20°C .

3.4.2. Protein quantification

Proteins were quantified with two different colorimetric assays: the BC Assay Kit from Uptima, Interchim or with Pierce 660 nm Protein Assay. For the BC Assay Kit, a serial dilution of an albumin standard, a blank control (buffer used for cell/tissue lysing) and samples were loaded in duplicates on the microplate wells. $200 \mu\text{l}$ of A and B working reagent mixture was loaded on the samples and mixed. The plate was incubated 30 min at 37°C and the absorbance (OD) was read at 562 nm against the blank. The Pierce 660 nm Protein Assay was used when the detergent in the lysis buffer was too high and interfering with the BC Assay. In SDT buffer, there is 2% of SDS and therefore, the Ionic Detergent Compatibility Reagent was used by freshly dissolving 1 g in 20 ml of Assay solution. $10 \mu\text{l}$ of a serial dilution of an albumin standard, a blank control and samples were loaded on the microplate and $150 \mu\text{l}$ of prepared mix was added to each well. Plate was covered, put on a shaker for 1 min and afterwards incubated 5 min, RT. OD was measured at 660 nm to obtain the concentration levels.

3.4.3. Concanavalin A enrichment

Conditioned media containing secreted and cleaved proteins was enriched using Concanavalin A agarose conjugate. Concanavalin A slurry was first washed two times with PBS and rotating for 5 min. The sample input was normalized according to the protein amount in the total lysates, added to the $50 \mu\text{l}$ of the washed beads and incubated o/n at 4°C while rotating. Afterwards, enriched beads were centrifuged for 5 min at 4°C and $2500 \times g$. Unbound proteins in the supernatant were removed and the beads were washed two times in PBS, rotating for 5 min. Enriched proteins were eluted in $25 \mu\text{l}$ of the reducing protein sample buffer and boiled 5 min at 95°C .

3.4.4. Co-immunoprecipitation

SEZ6L co-immunoprecipitation was done using 21D9 monoclonal anti-SEZ6L antibody. Protein G Sepharose (PGS) beads were washed 2 times in PBS and $50 \mu\text{l}$ per sample was conjugated with $600 \mu\text{l}$ the 21D9 o/n, at 4°C , with rotation. Conjugated beads were washed 3 times with PBS and $50 \mu\text{l}$ of the bis(sulfosuccinimidyl)suberate (BS3) solution ($2.5 \mu\text{l}$ $20\times$ PBS, $38.5 \mu\text{l}$ H_2O , 2.5 mM of RT equilibrated BS3 in H_2O) was added and incubated 1 h, RT, rotating. BS3 crosslinked PGS beads were then washed in different solutions: three times with $50 \mu\text{l}$ of 100 mM glycine pH 2.8, two times with PBS supplemented with 1% Igepal CA-630 (v/v) and finally one time with PBS. After washing, crosslinked beads were incubated with the samples homogenized in the HEPES buffer o/n, at 4°C on rotator. Samples were washed three times with HEPES buffer and eluted in $30 \mu\text{l}$ of 8% formic acid for 10 min, RT.

3.4.5. Mouse brain fractionation: membrane and soluble fraction

Brain hemispheres, cortices or cerebella, were homogenized in DEA buffer with rotor stator homogenizer on ice. 1 ml of homogenate was neutralized with 110 μ l of neutralization buffer and mixed. Homogenates were centrifuged for 5 min at $4000 \times g$ and $4^{\circ}C$. From this step, pellets were further processed for the membrane fraction, while the supernatants for soluble fraction were transferred to the ultracentrifuge tubes to be centrifuged for 30 min at $136000 \times g$ at $4^{\circ}C$ using Optima MAX-XP ultracentrifuge and TLA-55 rotor. Ultracentrifuged supernatants were transferred in a new tube and used as soluble fraction. Pellets from the first centrifugation step were washed one time with PBS, centrifuged 10 min, $4000 \times g$, at $4^{\circ}C$ and the obtained pellets were resuspended in Triton X-100 lysis buffer (STET). Lysates were incubated on ice 1 h with occasional vortex and afterwards centrifuged for 10 min at $20000 \times g$ and $4^{\circ}C$. Supernatants were collected and used in experiments as membrane fraction (lysate fraction). Both membrane and soluble fraction were quantified to estimate the protein concentration using BCA method.

3.4.6. Crude membrane preparation

Crude membrane preparations of cerebella were prepared using repeated tissue homogenization with different buffers and solubilisation with SDS. Cerebella were homogenized on ice using 20-100 mg of tissue in 1 ml of high salt buffer with Protease inhibitor using rotor stator homogenizer. Homogenates were then centrifuged at $16000 \times g$, 15 min, $4^{\circ}C$ and supernatants were discarded. Pellets were rehomogenized in 1 ml of carbonate buffer with Protease inhibitor, incubated 15 min, at $4^{\circ}C$ and centrifuged at $16000 \times g$, 15 min, and $4^{\circ}C$. This step of rehomogenization of pellets in 1 ml of carbonate buffer was repeated and after centrifugation, pellets were homogenized in 1 ml of Urea buffer with Protease inhibitor. After 15 min of incubation at $4^{\circ}C$, homogenate pellets were centrifuged at $16000 \times g$, 15 min, at $4^{\circ}C$ and the pellets were rehomogenized two times in 0.1 M Tris/HCl pH 7.6 with Protease inhibitor. Finally, after last homogenization, samples were centrifuged at $16000 \times g$, 15 min, at $4^{\circ}C$ and the pellets were solubilized in 50 μ l of SDT lysis buffer with 5 min incubation at $95^{\circ}C$. Sample protein concentration was measured with Pierce 660 nm protein assay.

3.4.7. Surface Spanning Protein Enrichment with Click Sugars – SUSPECS

Primary cortical neurons were metabolically labelled with 50 μ M tetraacetylated N azidoacetylmannosamine (Ac4-ManNAz) at DIV 5. After 48 h of labelling, cortical neurons were washed one time with cold PBS followed by incubation for 2 h at $4^{\circ}C$ with 100 μ M sulfo-DBCO-biotin in PBS. After the click reaction, biotinylated primary neurons were lysed in STET lysis buffer with Protease inhibitor and cleared by centrifugation for 10 min at $20000 \times g$ and $4^{\circ}C$. A polyrep column filled with 300 μ l of high capacity streptavidin agarose was used with gravity flow to enrich biotinylated proteins. The lysates diluted to 10 ml with 2% SDS in PBS and applied twice onto the column for protein binding. Non-biotinylated proteins were removed with two washing steps of 10 ml 2% SDS in PBS. Afterwards, beads were transferred in 2% SDS in PBS into an Eppendorf tube and the supernatant was removed. The biotinylated proteins were eluted from the beads in 150 μ l Lämmli buffer supplemented with 8 M urea and 3 mM biotin and heating at $95^{\circ}C$ for 5 min.

3.4.8. Western blot analysis

Samples were diluted in sample buffer, boiled for 5 min, at 95°C and run on the polyacrylamide gels. Gels were run in the electrophoresis chamber filled with SDS running buffer, at constant 80 V throughout the stacking gel and afterwards 120 V until the dye was completely out of the gel. The separated proteins in the gels were transferred to the polyvinylidene difluoride (PVDF) membrane with the transfer buffer at constant 400 mA for 65 min. Membranes were blocked with 5% skim milk (w/v) in PBS with 0.05% Tween-20 (v/v) (PBS-T) for 45 min at RT with shaking. Afterwards, membranes were washed three times with PBS-T for 10 min while shaking and incubated with primary antibody (listed in table 22) diluted in PBS-T and 0.05% BSA (v/v), o/n, shaking at 4°C. Membranes were washed three times with PBS-T shaking for 10 min to remove unbound primary antibodies followed by incubation with secondary antibody diluted in PBS-T and 0.05% BSA (v/v) for 1 h at RT, shaking. After incubation, membranes were again washed three times with PBS-T, 10 min, shaking and developed using ECL Western Blotting Reagents and analysed with ImageQuant LAS 4000.

Table 22. List of antibodies. Overview of antibodies and their immunogens, species, dilutions and catalogue numbers used in this thesis.

Antibody	Clone	Immunogen	Host species	Dilution	Catalogue number	Source
anti-mouse IgG Alexa Fluor Plus 488	-	Gamma Immunoglobins Heavy and Light chains	goat	1:500	A32723	Thermo Fisher Scientific
anti-mouse IgG Alexa Fluor Plus 555	-	Gamma Immunoglobins Heavy and Light chains	goat	1:500	A32727	Thermo Fisher Scientific
anti-mouse IgG Alexa Fluor Plus 647	-	Gamma Immunoglobins Heavy and Light chains	goat	1:500	A32728	Thermo Fisher Scientific
APLP1	8G6	peptide immunization (AA75-EPDPQRSRRCLLD PQR-AA90) within APLP1 copper binding domain	mouse	1:10	-	Developed in collaboration with Regina Feederle
β -actin	AC-74	slightly modified β -cytoplasmic actin N-terminal peptide, Ac-Asp-Asp-Asp-Ile-Ala-Ala-Leu-Val-Ile-Asp-Asn-Gly-Ser-Gly-Lys, conjugated to KLH	mouse	1:1000	A5316	Sigma
BACE1	3D5	BACE1	mouse	1:1000	-	Provided by Robert Vassar
Calnexin	-	Synthetic peptide corresponding to the sequence near the C-terminus of dog calnexin	rabbit	1:2000	ADI-SPA-860	Enzo Life Sciences
CaMKIV	26	Human CaM Kinase IV aa. 1-241	mouse	1:1000	610276	BD Biosciences

DNER	-	Ala26-His637 mouse DNER	goat	1:1000	AF2254	R&D Systems
GluR2	6C4	Recombinant fusion protein TrpE-GluR2 (putative N-terminal portion, amino acids 175-430)	mouse	1:1000	MAB397	Millipore
Golgin-97	CDF4	Human golgin-97	mouse	1:1000	A21270	Invitrogen
HA	3F10	HA	rat	1:10	-	Developed in collaboration with Elisabeth Kremmer
HRP-coupled anti-goat	-	goat IgG	donkey	1:5000	sc-2020	Santa Cruz
HRP coupled anti-mouse	-	mouse IgG	goat	1:10000	W402B	Promega
HRP coupled anti-rabbit	-	rabbit IgG	goat	1:10000	W401B	Promega
HRP-coupled anti-rat	-	rat IgG	goat	1:5000	sc-2006	Santa Cruz
HRP-coupled anti-sheep	-	sheep IgG	donkey	1:5000	sc-2473	Santa Cruz
MT4MMP	EP1270Y	human MT4MMP peptide	rabbit	1:1000	ab51075	Abcam
NEO1	21A8	mouse NEO1	rat	1:10	-	Developed in collaboration with Elisabeth Kremmer
NeuN	-	GST-tagged recombinant mouse NeuN	rabbit	1:300	ABN78	Millipore
OLFM1	-	Ser2-Arg481 mouse OLFM1	sheep	1:1000	AF4636	R&D Systems
RGMa	-	Cys48-Gly421 mouse RGMa	goat	1:1000	AF2458	R&D Systems
SEZ6	14E5	mouse SEZ6 ectodomain	rat	1:10	-	Developed in collaboration with Elisabeth Kremmer
SEZ6L	-	Glu32-Ser889 mouse SEZ6L	sheep	1:1000	AF4804	R&D Systems
SEZ6L	21D9	mouse SEZ6L ectodomain	rat	1:10	-	Developed in collaboration with Elisabeth Kremmer
SEZ6L2	-	Leu28-Ser837 mouse SEZ6L2/BSRP-A	sheep	1:1000	AF4916	R&D Systems
TSPAN6	-	176-205 aa	rabbit	1:1000	AP9224b	Abgent

3.4.9. Quantification and statistical analysis

Quantification of Western blot analysis was done using Multi Gauge V3.0 and subsequent result was statistically analysed using GraphPad Prism 7.01 software. Statistical test used were: unpaired t-test, Kruskal-Wallis test, Mann-Whitney U test and the displayed graphs are showing mean \pm SEM in at least 3 biological replicates.

3.4.10. Brain slice preparation

Brains perfused with 4% paraformaldehyde (PFA) were collected and postfixed in 4% PFA for 24 h. After fixation, brains were put in the series of sucrose solution, each for 24 h or more, according to when the solution was completely exchanged for the previous one (when the brains sank down in the tube): 15%, 20% and finally 30%. Brains were frozen in the OCT medium, cut with cryostat in the sagittal sections and stored in PBS for immunostaining.

3.4.11. Immunostaining of brain sections

Brain sections were transferred from PBS to blocking solution and incubated for 1 h, RT. Then they were incubated o/n with primary antibody in blocking solution at 4°C. After incubation, sections were washed three times with PBS and 0.2% Triton-X (v/v) for 10 min. Secondary antibody diluted in Triton-X 0.2% (v/v), NGS 2% (v/v) in PBS was applied, together with the nuclear staining dye Hoechst (1:2500) and incubated for 2 h, RT, in dark. Sections were washed two times for 10 min with PBS and 0.2% Triton-X (v/v) and additionally one time in PBS for 10 min. Sections were transferred to the glass slides, dried, mounted and visualised with Axio Imager 2.

3.4.12. Sample preparation for mass spectrometric measurement

SUSPECS sample preparation was done by Dr. Julia Herber. Samples were separated by 10% SDS-PAGE. The gels were stained using Coomassie staining (0.025% (w/v) Coomassie Brilliant Blue in 10% acetic acid) for 15 min followed by three washing steps in 10% acetic acid. The gel lanes of the individual samples were cut into 14 fractions and subjected to in-gel digestion. Briefly, fractions were cut further into cubes of roughly 1 mm² and Coomassie staining was removed using 40% acetonitrile (ACN) in 50 mM ammonium bicarbonate (ABC). Disulfide bonds were reduced in 10 mM dithiothreitol (DTT) in 100 mM ABC for 30 min at 37°C and cysteine residues were alkylated using 55 mM iodoacetamide (IAA) 100 mM ABC for 30 min at RT in the dark. Next, the gel pieces were dehydrated in 100% ACN. The supernatant was discarded and gel pieces of each fraction were incubated over night with 150 μ g of trypsin in 50 mM ABC at 37°C. Samples were acidified with formic acid (FA) and tryptic peptides were extracted twice with 150 μ l of 40% ACN supplemented with 0.1% FA. The peptides of each fraction were collected in an Eppendorf tube and dried using vacuum centrifugation. Afterwards, samples were reconstituted in 30 μ l of 0.1% FA.

Brain lysates and Co-IP samples were processed together with the technical assistance provided by Anna Berghofer using filter aided sample preparation (FASP) protocol. 10 to 20 μ g of sample was mixed with 200 μ l of UA and transferred to a Vivacon 500 filter unit with a

10 kDa cut off. Samples were centrifuged at $14000 \times g$ for 30 min. Another 200 μl of UA was added and the centrifuged was repeated. The flow-through was discarded and 100 μl of IAA solution was added. Samples were mixed and incubated in a Thermomixer at 600 rpm for 1 min and additional 5 min without mixing in the dark. Afterwards, samples were centrifuged at $14000 \times g$ for 30 min and then 100 μl of UB was added with subsequent centrifugation at $14000 \times g$ for 30 min. Addition of UB and centrifugation step was repeated two more times and the flow-through was discarded. Filter units were transferred to a new collection tube and 40 μL of UC with LysC (enzyme to protein ratio 1:50) was added. Samples were mixed for 1 min at 600 rpm and put into a wet chamber, with o/n incubation at 37°C . Afterwards, 120 μl of 50 mM ABC with trypsin was added (enzyme to protein ratio 1:100). Samples were put into a wet chamber for 4 h at 37°C and then centrifuged at $14000 \times g$ for 60 min. To improve the peptide recovery, 50 μl of 0.5 M NaCl was added and centrifuged at $14000 \times g$ for 20 min. Digested samples in the collection tubes were acidified with 8% formic acid to a $\text{pH} < 3$ and desalted with C18 STAGE Tips.

3.4.13. LC-MS/MS analysis

SUSPECS mass spectrometric analysis was done by Dr. Julia Herber and Dr. Stephan Müller. The gel fractions of the SUSPECS study were analysed on an Easy nLC-1000 or -1200 nano UHPLC coupled online via a Nanospray Flex electrospray ion source equipped with a column oven (Sonation, Germany) to a Velos Pro Orbitrap mass spectrometer. Peptides from eight out of 30 μl per samples were separated on self-packed C18 columns (500 mm \times 75 μm , ReproSil-Pur 120 C18-AQ, 1.9 μm ; Dr. Maisch, Germany) using a binary gradient of water (A) and acetonitrile (B) supplemented with 0.1% FA (0 min, 2% B; 3:30 min 5% B; 48:30 min, 25% B; 59:30 min, 35% B; 64:30 min , 60% B) at a flow rate of 250 nL/min.

Brain samples and CO-IPs were analysed were analysed by Dr. Stephan Müller on an Easy nLC-1000 or -1200 nano UHPLC coupled online via a Nanospray Flex electrospray ion source equipped with a column oven (Sonation, Germany) to either a Q-Exactive or a Q-Exactive HF mass spectrometer, respectively. An amount of 1.3 μg of peptides were separated on self-packed C18 columns (500 mm \times 75 μm , ReproSil-Pur 120 C18-AQ, 1.9 μm ; Dr. Maisch, Germany) using a binary gradient of water (A) and acetonitrile (B) supplemented with 0.1% FA (0 min, 2% B; 5 min 5% B; 185 min, 25% B; 230 min, 35% B; 250 min , 60% B) at a flow rate of 250 nL/min. Half of the material was injected for Co-IP samples.

On the Velos Pro Orbitrap instrument, full MS spectra were acquired at a resolution of 70,000 (automatic gain control (AGC) target: $3\text{E}+6$). The ten most intense peptide ions per spectrum were chosen for collision-induced dissociation (CID) within the ion trap (maximum ion trapping time: 100 ms, isolation width: 2.0 m/z, AGC target: $1\text{E}+5$, activation time 10 ms, NCE: 35%). A dynamic exclusion of 90 s was applied for CID acquisition.

On the Q-Exactive instrument, full MS spectra were acquired at a resolution of 70,000 (AGC target: $3\text{E}+6$). The 10 most intense peptide ions were chosen for fragmentation by higher-energy collisional dissociation (resolution: 17,500, maximum ion trapping time: 100 ms, isolation width: 2 m/z, AGC target: $1\text{E}+5$, NCE: 25%). A dynamic exclusion of 120 s was applied for fragment ion spectra acquisition.

On the Q-Exactive HF mass spectrometer, full MS spectra were acquired at a resolution of 120,000 (AGC target: $3\text{E}+6$). The 10 most intense peptide ions were chosen for fragmentation by higher-energy collisional dissociation (resolution: 15,000, maximum ion trapping time:

100 ms, isolation width: 1.6 m/z, AGC target: 1E+5, NCE: 26%). A dynamic exclusion of 120 s was applied for fragment ion spectra acquisition.

3.4.14. LC-MS/MS data analysis and statistical evaluation

The MS raw data was analysed using the software Maxquant (version 1.5.5.1) (Cox et al., 2014) using the default settings with slight modifications. A reviewed canonical database of *Mus musculus* from Uniprot (CO-IP: download: 2017-01-11, entries: 16,843 proteins; brain lysates: download: 2018-07-23, entries: 16,989 proteins) was used for the database search. Trypsin was defined as protease. Two missed cleavages were allowed. The option first search was used to recalibrate the peptide masses within a search window of 20 ppm. For the main search, the peptide mass tolerance was set to 4.5 ppm. Tolerances for peptide fragment ions were set to 20 ppm for HCD (Orbitrap) and 0.5 Da (Ion Trap) for CID spectra, respectively. Carbamidomethylation of cysteine was defined as static modification. Acetylation of the protein N-terminus as well as oxidation of methionine were set as variable modifications. The false discovery rate for both peptides and proteins was adjusted to less than 1% using a target and decoy approach (concatenated forward and reversed database). Label free quantification (LFQ) of proteins required at least two ratio counts of razor peptides. Only unique and razor peptides were used for quantification. The option “match between runs” was enabled with a matching time of 1.5 or 0.7 min.

For SUSPECS, individual protein LFQ intensity ratios of BACE inhibitor and control treated neurons were calculated separately for each biological replicate to reduce the variation between the different experiments. Proteins that were relatively quantified in at least three out of six biological replicates were subjected to statistical analysis. The protein LFQ ratios (C3/Ctr) were log₂ transformed and a one sample Ttest was applied ($\mu_0 = 0$) to evaluate statistically significant changes of proteins. The p-value threshold was corrected according to Benjamini-Hochberg for multiple hypotheses (p = 5%).

For the other experiments, a log₂ transformation of protein LFQ intensities was applied and an average log₂ fold change was calculated for each protein. At least three quantifications per group were required for statistical testing. Changes in protein abundance were evaluated using a Student's Ttest between the log₂ LFQ intensities of the two experimental groups. A permutation based FDR estimation was used to account for multiple hypotheses (p=5%; $s_0=0.1$) using the software Perseus (Tusher et al., 2001; Tyanova et al., 2016).

3.5. Animal work

3.5.1. Mouse lines

Mouse lines used in this thesis were the following: wild type (WT) C57BL/6NCrl and C57BL/6J (Charles River), BACE1^{-/-} (Jackson Laboratory, strain B6.129-*Bace1*^{tm1Pcw/J}) and B6.129-SEZ6L^{-/-} (originally generated from B6.129-SEZ6TKO, provided by Jenny Gunnensen laboratory). Mice had water and food supplies ad libitum and were maintained on a 12/12 h light-dark cycle. All animal procedures were carried out in accordance with the European Communities Council Directive (86/609/EEC) as well as the Ludwig-Maximilians-University Munich and the government of Upper Bavaria.

The B6.129-SEZ6L^{-/-} line was produced by crossing out the SEZ6L^{-/-} from the B6.129-SEZ6TKO (triple knock-out mice for SEZ6, SEZ6L and SEZ6L2 genes, provided by Jenny Gunnensen laboratory, first generated on a mixed 129 strain and C57BL genetic background as described (Miyazaki et al., 2006)). THET (triple heterozygous) mice were bred with the C57BL/6J ((T)WT) to get single SEZ6L^{+/-} mice in the first generation (F1) with the probability of 12.5% (Table 23). In the second generation (F2) SEZ6L^{+/-} were mated together to produce SEZ6L^{-/-} offspring (Table 24). Mice were crossed up to 8 generations (F8) and HET × HET mating scheme was used to produce littermate controls.

Summary of the mating scheme:

F1 offspring of triple THET × (T)WT mating

Table 23. Mating scheme in F1 generation. Overview of the probable genotypes according to the Mendelian ratio.

SEZ6	SEZ6L	SEZ6L2	Genotype percentage
WT	WT	WT	12.5%
WT	WT	HET	12.5%
WT	HET	WT	12.5%
HET	WT	WT	12.5%
WT	HET	HET	12.5%
HET	WT	HET	12.5%
HET	HET	WT	12.5%
HET	HET	HET	12.5%

F2 offspring of WT/HET/WT × WT/HET/WT mating:

Table 24. Mating scheme in F2 generation. Overview of the probable genotypes according to the Mendelian ratio.

SEZ6	SEZ6L	SEZ6L2	Genotype percentage
WT	WT	WT	25%
WT	HET	WT	50%
WT	KO	WT	25%

3.5.2. Behavioural testing

All behavioural testing and analysis on B6.129-SEZ6L^{-/-} line were performed in collaboration with Jenny Gunnensen laboratory at the University of Melbourne. The B6.129-SEZ6L^{-/-} line was generated with the same scheme as described above. All experiments were done in accordance with the Australian Code of Practice for the Care and Use of Animals for Scientific Purposes and were approved by the Animal Ethics Committee of the University of Melbourne. Four to six months old mice were used, of both gender and all three genotypes (WT, HET, KO). All training and testing was done blinded to the genotype of the mice. One cohort of mice, between approximately four and six months of age was tested for forelimb grip strength, ledged beam, fixed beam and DigiGait (WT and SEZ6L^{-/-} mice only). Additional small number of mice was tested on the ledge beam. Another cohort, four to five months old was tested on the rotarod. Experiments were performed in the light cycle and mice were acclimatized to the testing room prior to behavioral testing.

3.5.3. DigiGait analysis

Gait analysis was performed with the DigiGait™ imaging apparatus and software (Mouse Specifics Inc., Boston, MA). Mice were placed in a 15 × 5 cm plexiglass compartment with a transparent treadmill and a video camera mounted underneath. The videos were taken of the ventral side of the mice running at the constant speed of 15 and 25 cm/s and captured for 4 s. The videos were analysed with DigiGait software. A total of 78 mice were tested (for 15 cm/s analysis, WT n=24, SEZ6L+/- n=29, SEZ6L-/- n=24; for 25 cm/s analysis, WT n=19, SEZ6L+/- n=28, SEZ6L-/- n=20), of which 10 were unable to run at 25 cm/s for an adequate time duration for analysis to be completed (3 male WT, 2 female WT, 1 male SEZ6L+/-, 2 male SEZ6L-/- and 2 female SEZ6L-/-) and an additional male SEZ6L+/- mouse was unable to run at both recorded speeds. DigiGait indices were statistically analysed by pooling the data from female and male mice and using 1-way ANOVA with the p-value less than 0.05.

3.5.4. Ledge beam analysis

Mice were placed on the 80 cm long black plastic beam that has the starting edge of 3.5 cm and is narrowing down to 1 mm. Below the beam there was a 0.5 cm wide clear plastic edge used as a support for the mice when the foot are slipping from the beam. Two cameras were placed on both sides to record mice traversals from the wider side of the beam to the narrower. Mice performed two days of trainings with three traversals per day and one traversal on the testing day. Left and right side videos were analysed for the forelimb and hindlimb foot faults, total number of steps (hindlimb placements) and total time (s) needed to traverse the beam. For statistical analysis 2-way ANOVA was used with the p-value less than 0.05. In total, 92 mice were tested: 29 WT (13 male, 16 female), 32 SEZ6L+/- (16 male, 16 female) and 31 SEZ6L-/- (16 male, 15 female).

3.5.5. Forelimb grip strength analysis

Forelimb grip strength was recorded using mouse grip strength meter (Ametek, USA). Mice were lifted by the tail, allowed to grasp the triangular pull bar with both forepaws and pulled backwards in the horizontal plane until the forepaws released the bar. Five successful tests performed 30 s apart were measured and the peak tension (kg) was recorded. From the five trials, the highest value was taken and normalized to the body weight. 2-way ANOVA was used with the p-value less than 0.05. In total, 77 mice were tested: 24 WT (9 male, 15 female), 30 SEZ6L+/- (15 male, 15 female) and 23 SEZ6L-/- (15 male, 8 female).

3.5.6. Rotarod analysis

Mice were placed on an accelerating rotarod with cylinders 3.2 cm in diameter. The rotarod speed was gradually increasing from 1 to 40 rpm over 5 minutes. Mice underwent 3 trials 10 minutes apart each day for 5 consecutive days. The time was recorded for each mouse until it either fell off the cylinder or alternatively, did one full passive rotation. At the end of the trial, if the mouse remained on the cylinder, the latency was recorded as 300 s. In total, 89 mice

were tested: 29 WT (15 male, 14 female), 24 SEZ6L^{+/-} (18 male, 16 female) and 36 SEZ6L^{-/-} (21 male, 15 female). The results were analysed by 2-way ANOVA with the p-value less than 0.05.

4. RESULTS

4.1. BACE1 substrates in secretome and surfaceome

4.1.1. BACE1 substrate shedding in the overexpressing system of HEK293T cells

BACE1 is the protease responsible for initiating A β generation and therefore, a key drug target in Alzheimer's disease. It is a major sheddase with a broad range of physiological substrates that possess different functions in neurobiology. The fact of having numerous substrates is raising concerns that possible mechanism-based side effects of BACE1 inhibition in patients may result from reduced cleavage of its substrates and their subsequent accumulation on the cell membrane.

Previous proteomic study done in our lab identified an increased number of BACE1 substrate candidates in neurons using secretome protein enrichment with click sugars (SPECS) (Kuhn et al., 2012). However, proteomic studies need further validation with an independent method to verify the validity of substrates candidates. Therefore, to target the first aim, validations of the top substrate candidates from the SPECS method were performed. Since many of the identified proteins are little characterized, particularly in the brain, the availability of suitable antibodies against endogenous proteins is scarce. For this reason, HEK293T cells were used to overexpress the proteins of interest with lentiviral approach. Five proteins were chosen that exhibited at least 40% reduction of the shedded ectodomain in the secretome upon BACE1 inhibition, ranging from the high to the low abundance reduction (Kuhn et al., 2012). The following murine proteins were cloned into lentiviral vector bearing HA on the N-, and FLAG on the C-terminus of the protein: VWFA and cache domain-containing protein 1 (CACHD1) with 88%, Golgi apparatus protein 1 (GLG1) with 79%, Leucine-rich repeat neuronal protein 1 (LRRN1) with 75%, Neurotrimin (NTM) with 67% and Delta and Notch-like epidermal growth factor-related receptor (DNER) with 43% reduction of its secreted ectodomain upon BACE1 inhibition as observed in the SPECS study (Table 25).

Table 25. Overview of BACE1 substrate candidates identified in different proteomic analysis and evaluated in this study. Overview of BACE1 substrates evaluated in this study with its gene name, protein type and identification in annotated proteomic studies.

Gene name	Protein type	SPECS study ^a	Human cell lines study ^b	Study in neurons ^c	Study in β -cells ^d
Sez6l	Type I	0.04	-	-	BACE2
Cachd1	Type I	0.12	+ (HEK)	-	-
Glg1	Type I	0.21	+ (HeLa)	+	BACE1/2
Lrrn1	Type I	0.25	-	-	BACE2
Ntm	GPI	0.33	-	-	-
Dner	Type I	0.57	-	-	BACE1/2

^aMean ratio of identified substrates between BACE1 inhibitor (C3) and control (DMSO) treated WT neurons (Kuhn et al., 2012)

^bIdentification of substrates in HEK or HeLa cell lines overexpressing BACE1 (Hemming et al., 2009)

^cIdentification of substrates in neurons treated with BACE1 inhibitor (Zhou et al., 2012)

^dBACE1 and BACE2 targets in pancreatic β -cell sheddome (Stutzer et al., 2013)

Stable HEK293T cell lines overexpressing proteins of interest were then established using the puromycin selection. For the control experiment of the expression of all the constructs, Western blotting of the cell lysates and conditioned media with and without the construct was performed using the anti-HA antibody (Fig. 4A). Non-transfected cells showed only non-specific bands, while in transfected ones the full-length proteins were observed in total lysates

together with their ectodomain in conditioned media. Based on the amino acid sequence, all proteins showed a higher molecular weight than expected, presumably for the added weight of glycosylations that are often occurring in the GPI-anchored and single-pass type I membrane proteins. Full length proteins were observed in lysates (Fig. 4A): CACHD1 double band at ~150 and ~160 kDa, DNER at ~140 and ~160 kDa, GLG1 had only one band at ~150 kDa, LRRN1 one at ~95, one at ~110 kDa and additional faint band at ~160 kDa and NTM double band at ~60 and ~65 kDa. Observed double bands might come from the immature and mature version of the protein. In the conditioned media, all ectodomains beside NTM and additional LRRN1 band were detected at the same or slightly lower molecular weight than the full length protein, which fits to the possible BACE1 cleavage site that is usually occurring in the proximity of the transmembrane domain. Interestingly, specific signals for NTM in the conditioned media were ~20 kDa lower than the full length protein detected in the lysates that might come from truncation of the ectodomain. Furthermore, LRRN1 had a dominant band at ~150 kDa that might come from the added post-translational modifications (Fig. 4A, marked with #).

Since HEK293T cells express little endogenous BACE1, stable cell lines were subjected to transient transfection of the human BACE1 in order to see whether the increase in BACE1 can lead to the increase of shedding of protein ectodomains. Inhibition of BACE1 activity with the inhibitor C3 was used as an additional control to test if the change is depending on the BACE1 activity. Upon BACE1 overexpression, CACHD1, GLG1 and LRRN1 showed significantly increased levels of ectodomains released into the culture media (Fig. 4B) demonstrating enhanced cleavage by BACE1 and thereby confirming the validity of the initial proteomic analysis. For CACHD1 and LRRN1, such increase in ectodomain shedding was rescued by C3 treatment (Fig. 4B, last two lanes), indicating that the increase is dependent on proteolytic activity of BACE1. In the lysates, statistical analysis showed significant increase of the full length GLG1 when introducing BACE1 with inhibitor compared to both control and only BACE1 condition (Fig. 4C). In the conditioned media, there were significantly increased levels of the shed ectodomains when introducing BACE1: 2.8-fold for CACHD1, 2.9-fold for GLG1 and 7.1-fold for LRRN1 compared to control, and conversely, decrease with combined BACE1 and C3 inhibitor: 1.3-fold for both CACHD1 and LRRN1. GLG1 also showed reduction of 2.4-fold, but was not statistically significant (Fig. 4D). Two other analysed proteins, NTM and DNER had no apparent change between the conditions (Fig. 4E). This may be due to competition of BACE1 with other secretases that in HEK293T are dominant and therefore the two proteins might be more efficiently cleaved by a different secretase other than BACE1 in this cell line.

Taken together, BACE1 substrate candidates that were initially discovered in large unbiased proteomic studies, including SPECS, were validated with an independent biochemical method. Out of five proteins chosen according to the percentage of cleavage by BACE1 using the SPECS method, CACHD1, GLG1 and LRRN1 are confirmed to be substrates using the HEK293T overexpression model. On the other hand, NTM and DNER failed to show any response to both enzyme overexpression and inhibitor.

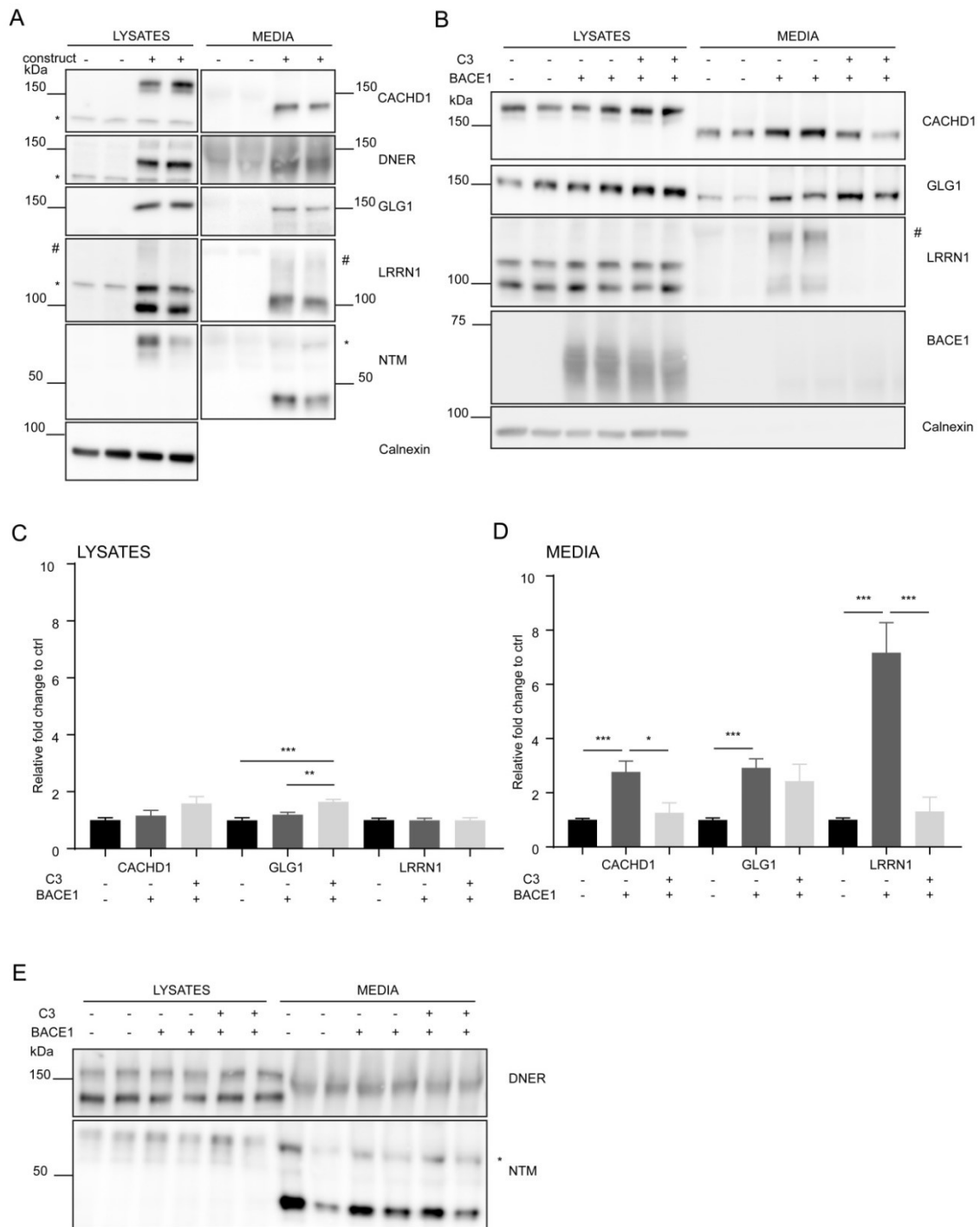


Figure 4. CACHD1, GLG1 and LRRN1 are BACE1 substrates in HEK293T overexpression model. (A) Establishment of the stable HEK293T cell lines with different BACE1 substrate candidates: CACHD1, DNER, GLG1, LRRN1 and NTM. Expression levels of the annotated protein compared to untransfected cells is shown in total cell lysates and conditioned media, analysed via Western blot. (B) Stable cell lines with BACE1 substrate candidates (CACHD1, GLG1 and LRRN1) were transiently transfected with BACE1 in the presence of C3 inhibitor or DMSO control. Western blot analysis showed significantly increased shedding upon BACE1 transfection and subsequent decrease with BACE1 inhibition of all three proteins. (C) Statistical analysis of CACHD1, GLG1 and LRRN1 in total lysates and (D) conditioned media done with n=8 replicates using Kruskal-Wallis test following by Mann-Whitney U test with the significance criteria of $p < 0.05$. Graphs are showing mean \pm SEM. (E) Stable cell lines with BACE1 substrate candidates (DNER and NTM) were transiently transfected with BACE1 in the presence of C3 inhibitor or solvent control. DNER and NTM did not show differences between the conditions. Unspecific bands are marked by asterisk, while the additional LRRN1 band with a hash.

4.1.2. SUSPECS method as a valuable tool to study cell surfaceomes

The SPECS study of primary mouse neurons revealed many previously unknown BACE1 substrates in the cell's secretome (Kuhn et al., 2012). However, BACE1 inhibition would as well alter other cell compartments that play important role in cell homeostasis like the cell surface. Membrane proteins that reside on the surface are integral part of cell-cell interaction and communication between the same but also different cell types (Yildirim et al., 2007). To target the effect of BACE1 on the surface, the next aim was to investigate changes occurring on the cell surface due to pharmacological inhibition of BACE1 and to compare the secretome with the surfaceome to see how the secreted form of the protein is correlating with the full length protein found on the cell surface.

For this purpose, surface labelling of glycosylated proteins was established in a complementary way to the SPECS method so that in one experiment both analyses could be done. The **SURface-Spanning Protein Enrichment with Click Sugars (SUSPECS)** method uses azido-modified sugar tetra-acetylated *N*-azidomannosamine (ManNAz) for labelling *N*- and *O*-linked glycans of the newly synthesised proteins in a cell culture system (Herber et al., 2018). After 48 h metabolically labelled glycoproteins that reside on the surface can then be biotinylated with membrane impermeable sulfo-dibenzylcyclooctyne (DBCO)-biotin. In a click reaction the azido group on labelled glycans forms a covalent bond with the added DBCO moiety. Following cell lysis, biotinylated proteins are enriched with streptavidin and further analysed (Fig. 5A).

To ensure that SUSPECS labels cell surface proteins and that the enrichment efficiency is adequately high, test experiments were performed using primary mouse cortical neurons and the resulting surface-enriched fraction was analysed via Western blot. The relative enrichment of the cell surfaceome as compared to the total lysates was assessed using previously known cell surface proteins: Neogenin (NEO1), Glutamate receptor 2 (GluR2), and GPI-anchored proteins Repulsive guidance molecule A (RGMa) and Membrane-type matrix metalloproteinase 4 (MT4MMP). All four proteins showed enrichment by using SUSPECS as measured with relative quantification of the surface levels compared to the total fraction of each protein: 4.4% increase for RGMa, 6% for MT4MMP, 67.2% for GluR2 and 91% for NEO1. Conversely, all other markers for intracellular organelles were barely detectable in the cell surface-enriched fraction (Fig. 5B and 5C).

In conclusion, the newly established SUSPECS method enriched glycosylated proteins at the cell surface. The efficiency of enrichment was evaluated in a semi-quantitative way, which demonstrated relative enrichment of the known cell surface proteins as compared to the total lysates. In contrast, proteins from other cellular compartments were largely absent from the enrichment, demonstrating the specificity of the labelling on surface proteins.

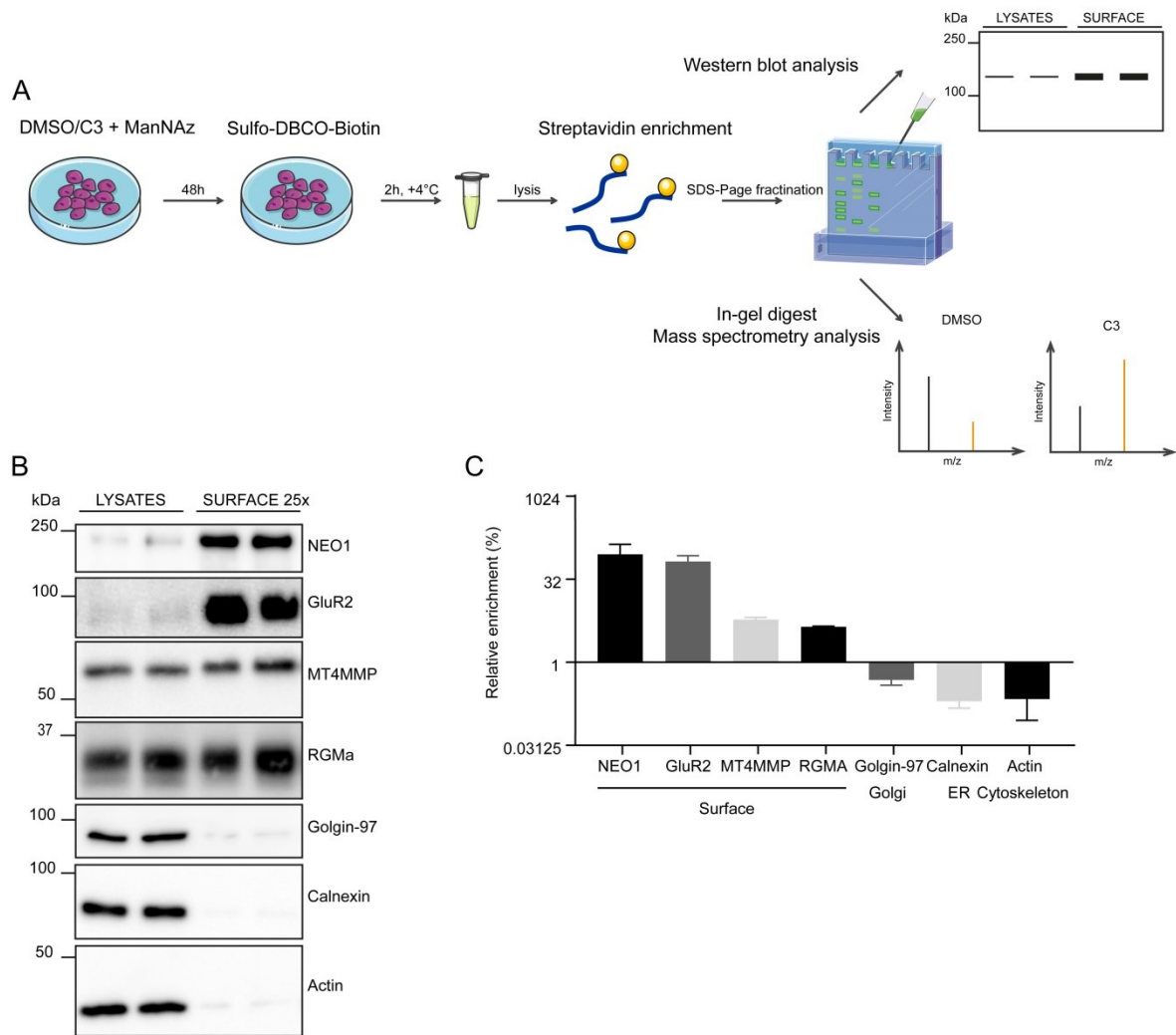


Figure 5. SUSPECS method enriches cell surface proteins. (A) Workflow of the SUSPECS method: Cells were cultured in the presence of the ManNAz sugar and labelled for 48 h. Afterwards, sulfo-DBCO-biotin was added to start the click reaction and biotinylate the surface proteins. Subsequently, cells were lysed and labelled glycoproteins were enriched by streptavidin for further analysis. (B) Western blot analysis of the total lysates compared to the cell surface-enriched fraction. Protein amounts used for enriching cell surface were 25× higher than those loaded in the total lysates. NEO1, GluR2, MT4MMP and RGMa showed enrichment in the surface fraction, while Golgin-97, Calnexin and Actin were barely detectable. (C) Relative enrichment in the surface fraction of the cell surface, golgi, ER and cytoskeleton markers compared to the total fraction. Graphs are showing mean \pm SEM in n=6 biological replicates. Modified from Herber and Njavro et al. (Herber et al., 2018).

4.1.3. Accumulation of BACE1 substrates on the neuronal surface

With SUSPECS method, the neuronal surfaceome upon BACE1 inhibition was analysed. Primary mouse cortical neurons were metabolically labelled with ManNAz in the presence of C3 inhibitor or DMSO for 48 h and afterwards clicked with sulfo-DBCO-biotin. Extracted biotinylated glycoproteins were enriched with streptavidin and analysed via mass spectrometry. Figure 6 shows a volcano plot representing neuronal surface proteins upon BACE1 inhibition compared to the solvent control (Herber et al., 2018). There were 471 transmembrane glycoproteins that were consistently quantified in at least three biological replicates and evaluated by statistical analysis. Additional correction for the multiple hypothesis test was applied using 5% false discovery rate (FDR) resulting in $q=0.0022$

(Herber et al., 2018). As expected, a number of proteins showed accumulation on the cell surface upon BACE1 inhibition, presumably due to decreased BACE1-mediated cleavage. Some of the proteins (e.g. APLP1, SEZ6 and SEZ6L) are known BACE1 substrates and were also identified in the SPECS analysis (Kuhn et al., 2012), confirming the concept of the method. Furthermore, SUSPECS analysis revealed enrichment of additional surface proteins other than previously known to be regulated by BACE1, suggesting the broad control of the surface levels of BACE1 substrate candidates.

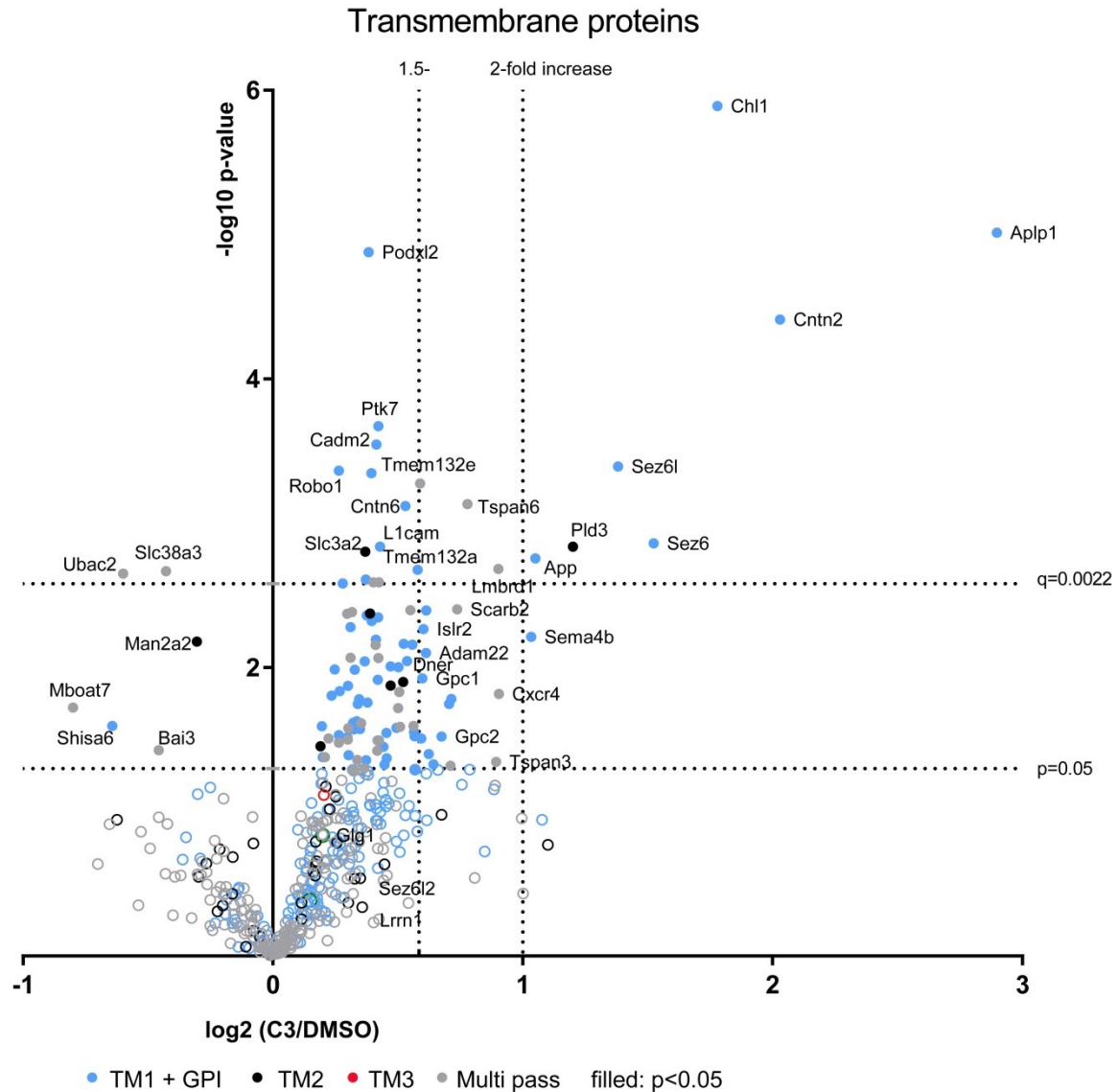


Figure 6. Volcano plot of BACE1 inhibited neurons. Mass spectrometry analysis represented in volcano plot and showing changes of glycosylated transmembrane proteins upon BACE1 inhibition. Proteins were quantified in at least 3 biological replicates and are depicted as closed circles (p-value more than 0.05) and opened circles (p-value less than 0.05). Transmembrane type I and GPI-anchored proteins (TM1 + GPI) are marked in blue, transmembrane type II proteins (TM2) are in black, transmembrane type III (TM3) are in red, and multi-pass proteins (Multi pass) are in gray. X-axis represents the log₂ fold change of BACE1 inhibition to the control (Log₂ C3/DMSO) and y-axis shows negative log₁₀ p-value according to one-sample t-test. Two dashed lines are applied statistical test: the lower one represents p-value of 0.05, while the upper one is the Benjamini-Hochberg correction to control for false discovery rate with 5% (q=0.0022). Vertical dashed lines annotate the fold change of 1.5- and 2-fold increase. Modified from Herber and Njavro et al. (Herber et al., 2018).

Proteomic results from SUSPECS analysis were further validated with Western blotting. Proteins with high, intermediate, mild or no accumulation upon BACE1 inhibition were chosen: Amyloid-like protein 1 (APLP1), Seizure protein 6 (SEZ6) and Seizure 6-like protein (SEZ6L); Tetraspanin-6 (TSPAN6); DNER; and Seizure 6-like protein 2 (SEZ6L2) and MT4MMP, respectively. Consistent with the proteomic data, Western blot analysis showed increase of surface levels of the proteins compared to the control: 7-fold for APLP1, 3.6-fold for SEZ6, 1.8-fold for SEZ6L, 3.5-fold for TSPAN6 and 1.8-fold for DNER (Fig. 7A and 7B). In the total lysates there were similar accumulations in the annotated proteins when comparing to the control: 5.4-fold for APLP1, 3.2-fold for SEZ6, 1.4-fold for SEZ6L2, 2.6-fold for TSPAN6 and 1.7-fold for DNER (Fig. 7C). Accordingly, SEZ6L2 and MT4MMP were changed neither on the surface nor in the total lysates.

From the HEK293T experiments, proteins that were followed-up according to the SPECS results, CACHD1, GLG1, LRRN1 and NTM showed no accumulation on the surface or were below the detection limit, demonstrating that BACE1 does not affect the surface levels of all its substrates in the same way.

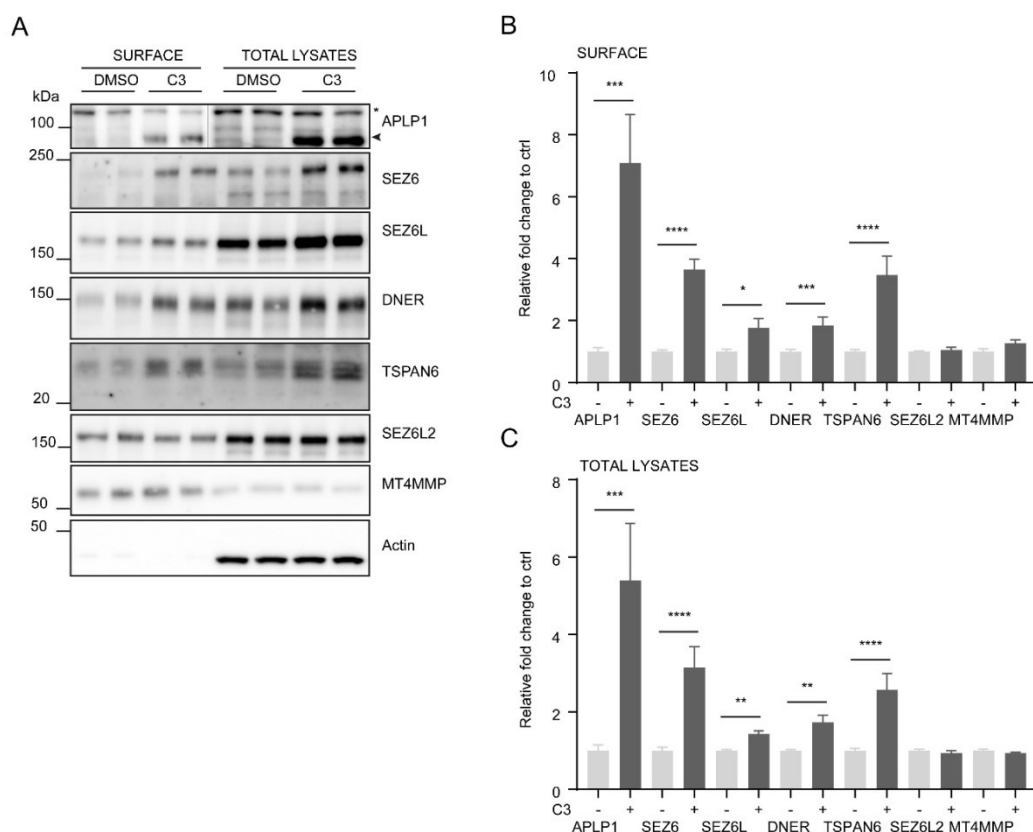


Figure 7. Accumulation of BACE1 substrates on the neuronal surface. (A) Western blot analysis of the surface levels and total lysates of selected proteins upon BACE1 inhibition. APLP1, SEZ6, SEZ6L, DNER and TSPAN6 showed accumulation in the presence of C3 inhibitor. SEZ6L2 and MT4MMP were used as a negative control of the treatment on the surface as they showed no change in the proteomic dataset. MT4MMP was used as a loading control on the surface, while Actin was a loading control in the total lysates and a negative control on the surface. (B) Statistical analysis of the accumulating surface levels of APLP1, SEZ6, SEZ6L, DNER, and TSPAN6 showed significance with Mann-Whitney U test. SEZ6L and MT4MMP levels were not changed. (C) Mann-Whitney U test of the total lysates compared to control. APLP1, SEZ6, SEZ6L, DNER and TSPAN6 were significantly increased with C3 inhibition, while SEZ6L2 and MT4MMP were not changed. Graphs are showing mean \pm SEM in n=6-10 biological replicates. Modified from Herber and Njavro et al. (Herber et al., 2018).

4.1.4. Validation of BACE1 substrates in BACE1^{-/-} brains

To further test whether the accumulation upon pharmacological inhibition of BACE1 is also seen *in vivo* Western blot analysis of the postnatal day 7 (P7) BACE1^{-/-} mice were used. The age of the mice was chosen according to the known peak of expression of the BACE1 in the postnatal development (Willem et al., 2006). Since the SPECS and SUSPECS methods are not suitable for *in vivo* experiments, but only in tissue culture, membrane fraction of BACE1^{-/-} and wild-type (WT) littermate control cortices were used (Fig 8A). Similarly to primary cortical neurons, in P7 cortices there was an increase of the full length protein by 2.3-fold for APLP1, 1.6-fold for SEZ6 and 1.2-fold for SEZ6L upon BACE1 deletion (Fig. 8B). On the other hand, DNER and TSPAN6 did not show any significant change between the two genotypes. This can be due to the expression pattern of BACE1, which is mostly neuronal, whereas DNER and TSPAN6 are also found in other cell types where other proteases may take over (Sharma et al., 2015).

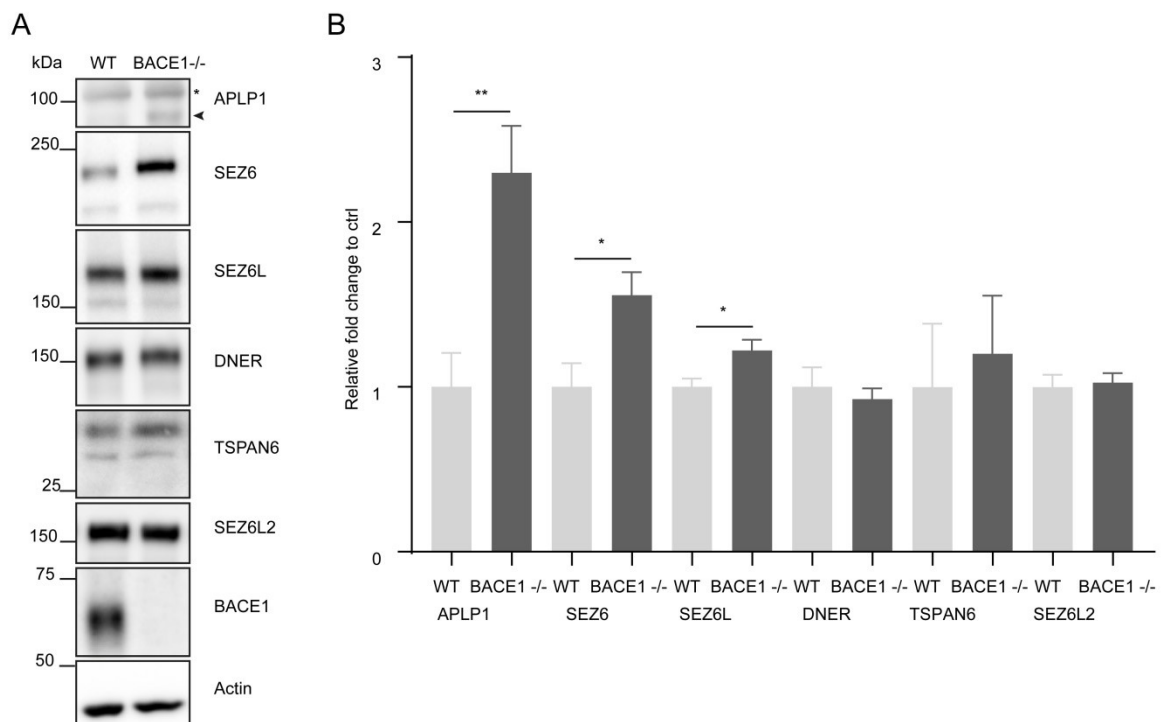


Figure 8. Accumulation of BACE1 substrates *in vivo*. (A) WT and BACE1^{-/-} membrane preparations of mouse cortices were analysed via Western blot for APLP1, SEZ6, SEZ6L, DNER and TSPAN6. SEZ6L2 was used as a negative control. Actin was used as a loading control. (B) Mann-Whitney U test with p-value less than 0.05 showed significant increases of APLP1, SEZ6 and SEZ6L. DNER and TSPAN6 remained unchanged. Graphs are showing mean \pm SEM in n=6 biological replicates. Unspecific bands are marked with asterisks (*). Modified from Herber and Njavro et al. (Herber et al., 2018).

In conclusion, BACE1 regulated cell surface proteins that were observed in SUSPECS were validated not only *in vitro* in primary cortical neurons, but also *in vivo* using a genetic approach of BACE1^{-/-} mouse brains.

4.2. Seizure 6-like protein (as one of the main BACE1 substrates)

As a major drug target in Alzheimer's disease, functions of BACE1 are still not completely understood and with all its substrates it remains a doubt of the possible side effects upon its inhibition. Seizure 6-like protein (SEZ6L) is one of the main confirmed BACE1 substrate and dominantly processed by BACE1 in murine brain (Pigoni et al., 2016). Therefore, it is plausible that BACE1 inhibition mediated SEZ6L accumulation on the surface or its subsequent reduction in the secretome may have possible impact on SEZ6L functions. To target the biological role of SEZ6L, an extensive behavioural and proteomic analysis of SEZ6L^{-/-} mice was performed.

4.2.1. Expression pattern of SEZ6L

SEZ6L is a transmembrane type I protein with a large extracellular part with protein-protein interaction domains: 3 CUB and 5 SCR domains (Fig. 9A). Two of the more N-terminal CUB domains are Ca²⁺-binding (Gaboriaud et al., 2011), while on the intracellular part of the protein, there is an NPxY and a putative PDZ binding motif (Pigoni et al., 2017). It is expressed throughout the brain together with the two other members of the family: SEZ6 and SEZ6L2. To investigate whether other members of the family could compensate the SEZ6L loss-of-function in SEZ6L^{-/-} brains, a Western blot analysis was performed. Indeed, there was a 1.8-fold increase of the SEZ6 protein in SEZ6L^{-/-} cerebrum as compared to the control. On the other hand, SEZ6L2 level was not altered in the cerebrum, or cerebellum (Fig. 9B, 9C and 9D).

The relative expression of SEZ6L in different brain regions were studied at the protein levels by immunohistochemistry using a monoclonal antibody that recognizes the ectodomain of SEZ6L (Pigoni et al., 2016). SEZ6L expression was observed throughout the brain, in particular in hippocampal dentel gyrus, CA3, cortex and cerebellum (Fig. 9E). The specificity of the antibody was confirmed with SEZ6L^{-/-} brains where no signal was detected. This results are in line with previous study using in situ hybridization with oligonucleotide probes specific for SEZ6L in the triple-knockout mice lacking all three family members and showed similar expression of SEZ6L in the gray matter of the brain with high levels in the olfactory bulb, anterior olfactory nuclei, hippocampus and cerebellar cortex and low levels in the white matter (Miyazaki et al., 2006). In the cerebellum intense expression was observed in Purkinje cells and granule cells with positive signals seen also in interneurons of the molecular layer (Miyazaki et al., 2006).

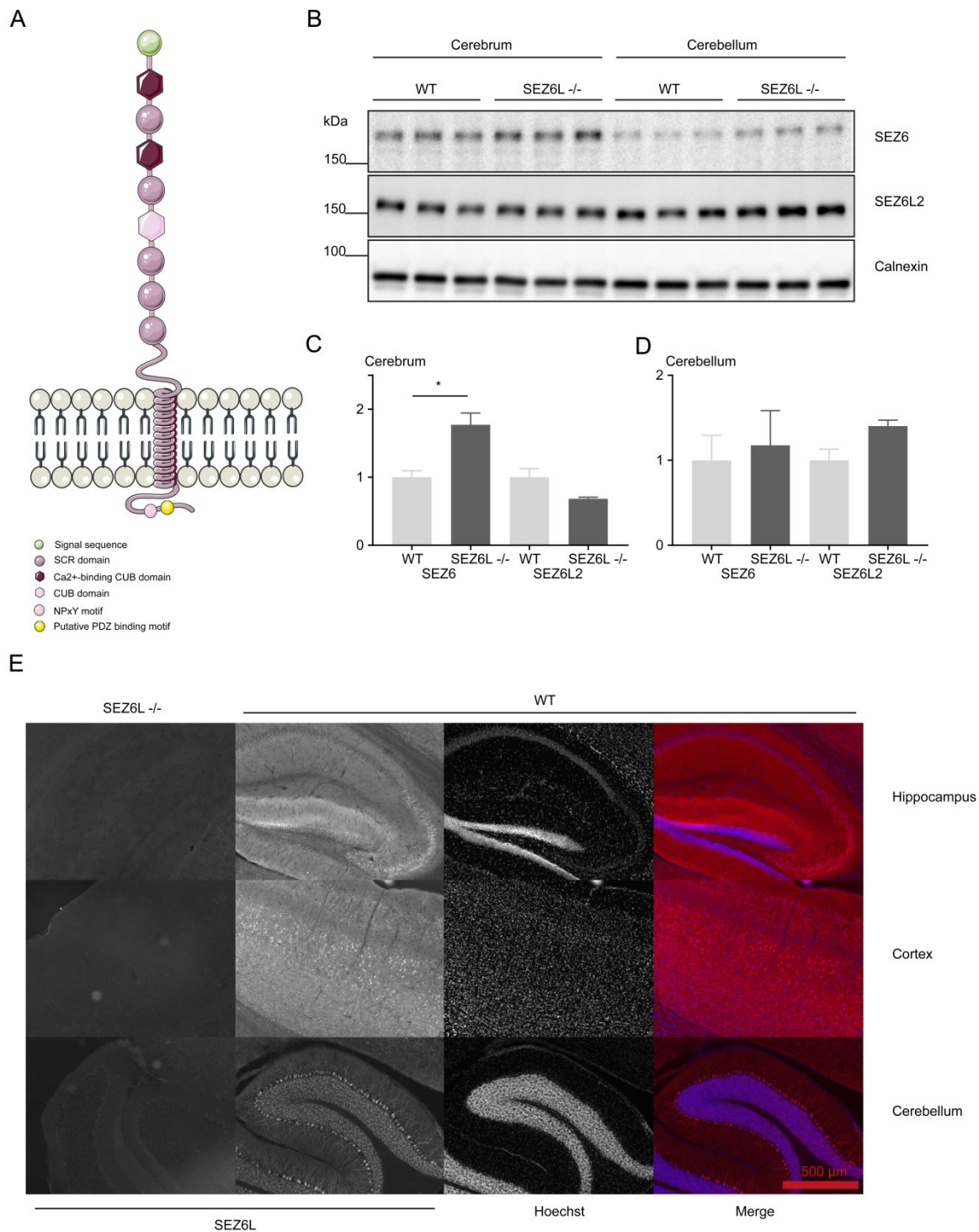


Figure 9. Expression of SEZ6L and its family members. (A) Schematic model of the SEZ6L protein showing 3 CUB and 5 SCR domains, signal sequence, NPxY and putative PDZ binding motif. (B) Expression levels of SEZ6 and SEZ6L2 in 8-month-old WT and SEZ6L^{-/-} mouse cerebrum and cerebellum. Calnexin is used as a loading control. (C) Unpaired t-test of the SEZ6 and SEZ6L2 in cerebrum showing significant increase of SEZ6 in the SEZ6L^{-/-} mouse. (D) Cerebellar extracts did not show any significant change of the two proteins. Graphs are showing mean \pm SEM in n=3 biological replicates. (E) Immunohistochemistry of WT and SEZ6L^{-/-} mouse brains in hippocampus, cortex and cerebellum using SEZ6L monoclonal antibody and Hoechst dye for nuclear staining. Scale bar: 500 μ m.

4.2.2. Behavioural analyses of SEZ6L^{-/-} mice

Upon combined deletion of SEZ6, SEZ6L and SEZ6L2, mice are experiencing motor discoordination in fixed bar when compared to their WT control, walking slowly by crawling on the bar with often stops and wounding their tail around the bar. Rotarod analysis also showed significant impairments of the TKO mice that failed to stay on the rotating device (Miyazaki et al., 2006). Since the expression of the SEZ6L is relatively high in the cerebellum and to test to which extent the phenotype come from SEZ6L, detailed behavioural analyses of the motor coordination were performed.

To assess the motor coordination of SEZ6L^{-/-} mice the following tests were used: ledge beam, forelimb grip strength, rotarod and DigiGait analyses. Adult mice, 4 to 6 month old were used, in total 92 for ledge beam, 77 for forelimb grip strength, 89 for rotarod and 78 for DigiGait analyses. Motor movement was first analysed through ledge beam and the results showed significant effect of gender on forepaws errors per step ($p=0.0351$) (Fig. 10A and 10E), hindpaw errors per step ($p=0.0017$) (Fig. 10B and 10E) and time to traverse the beam ($p=0.0450$) (Fig. 10C and 10E), but with no significant effect of genotype or interaction for any of these measures using 2-way ANOVA. There was, however, a non-significant trend ($p=0.0674$) (Fig. 10E) for genotype for variation in hindpaw errors per step, with a tendency for increased errors in particular for male SEZ6L^{-/-} mice. In the total number of steps taken to traverse the beam no difference was observed between genotypes or genders (Fig. 10D and 10E).

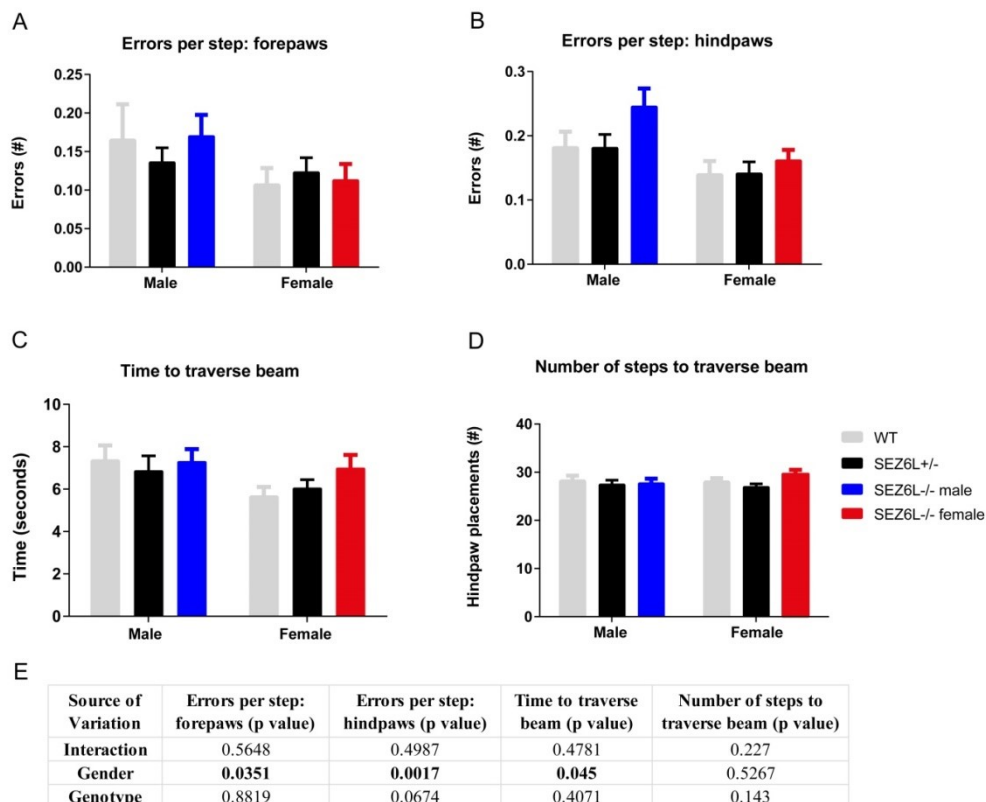


Figure 10. Ledge beam analysis of SEZ6L^{-/-} mice. (A) Ledge beam analysis showed no significant effect of the genotype of the forepaws errors per step, (B) hindpaws errors per step, (C) time to traverse the beam or (D) number of steps to traverse the beam using 2-way ANOVA. (E) Summary of 2-way ANOVA on interaction, gender and genotype. Graphs are showing mean ± SEM. Analysis included 13 WT, 16 SEZ6L^{+/-} and 16 SEZ6L^{-/-} male and 16 WT, 16 SEZ6L^{+/-} and 15 SEZ6L^{-/-} female mice.

Next, to test the neuromuscular strength of the mice, the forelimb grip strength analysis was performed. The mice showed no difference of the peak strength per body mass between genotypes of the same gender using 2-way ANOVA (Fig. 11). These results would suggest that SEZ6L^{-/-} mice do not experience a change in neuromuscular strength as compared to the WT mice.

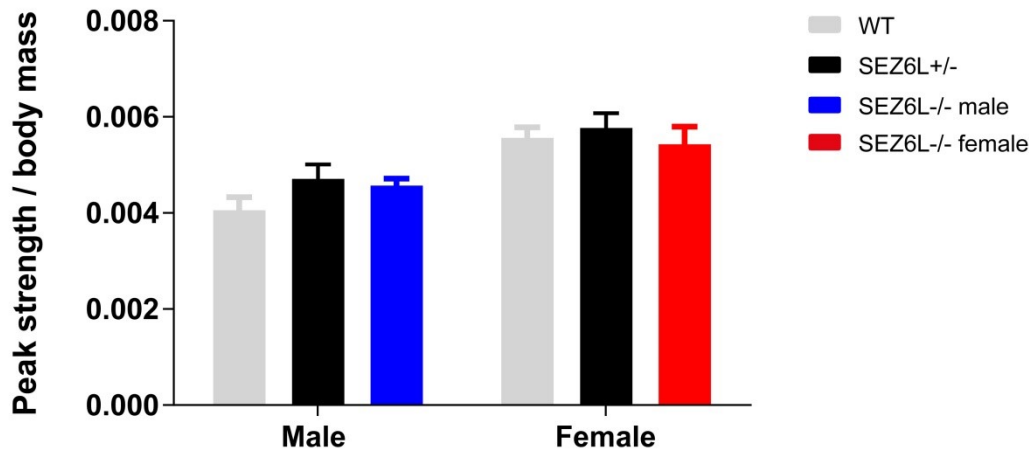


Figure 11. Forelimb grip strength analysis of SEZ6L^{-/-} mice. Forelimb grip strength analysis showed no difference of the peak strength per body mass between the genotypes of the same gender using 2-way ANOVA. Graphs are showing mean \pm SEM. Analysis included 9 WT, 15 SEZ6L^{+/-} and 15 SEZ6L^{-/-} male and 15 WT, 15 SEZ6L^{+/-} and 8 SEZ6L^{-/-} female mice.

To further evaluate motor capabilities of SEZ6L^{-/-} mice, rotarod analysis was performed and showed different results between male and female cohorts. In the male cohort all three genotypes were similar over the 15 trials (Fig. 12A). Using 2-way repeated measured ANOVA there was no significant effect of genotype ($p=0.0722$). Nevertheless, there were significant effects of trial ($p<0.0001$) and interaction between factors ($p=0.0156$). At individual trials, Tukey's multiple comparisons test indicated no differences between WT and SEZ6L^{-/-} males. SEZ6L^{+/-} and SEZ6L^{-/-} males however, showed differences from trials 9 to 11 and 13 to 14, while SEZ6L^{+/-} and WT males at trial 14. SEZ6L^{+/-} males had an increased latency to fall in all cases (Fig. 12A). On the other hand, in the female cohort there were significant effects of genotype ($p=0.0001$), trial ($p<0.0001$) and interaction between factors ($p=0.0001$) using 2-way repeated measured ANOVA. On the trials 7 and 10 to 15, Tukey's multiple comparisons test indicated differences between WT and SEZ6L^{-/-} females and additionally, from trials 4 to 15 differences between SEZ6L^{+/-} and SEZ6L^{-/-} females (Fig. 12B). Altogether, differences between male genotypes were subtle compared to striking deficit of female SEZ6L^{-/-} mice on the rotarod. The SEZ6L^{-/-} females were unable to improve at the same degree compared to the SEZ6L^{+/-} and WT mice over the course of the experiment, indicating motor deficits in these mice.

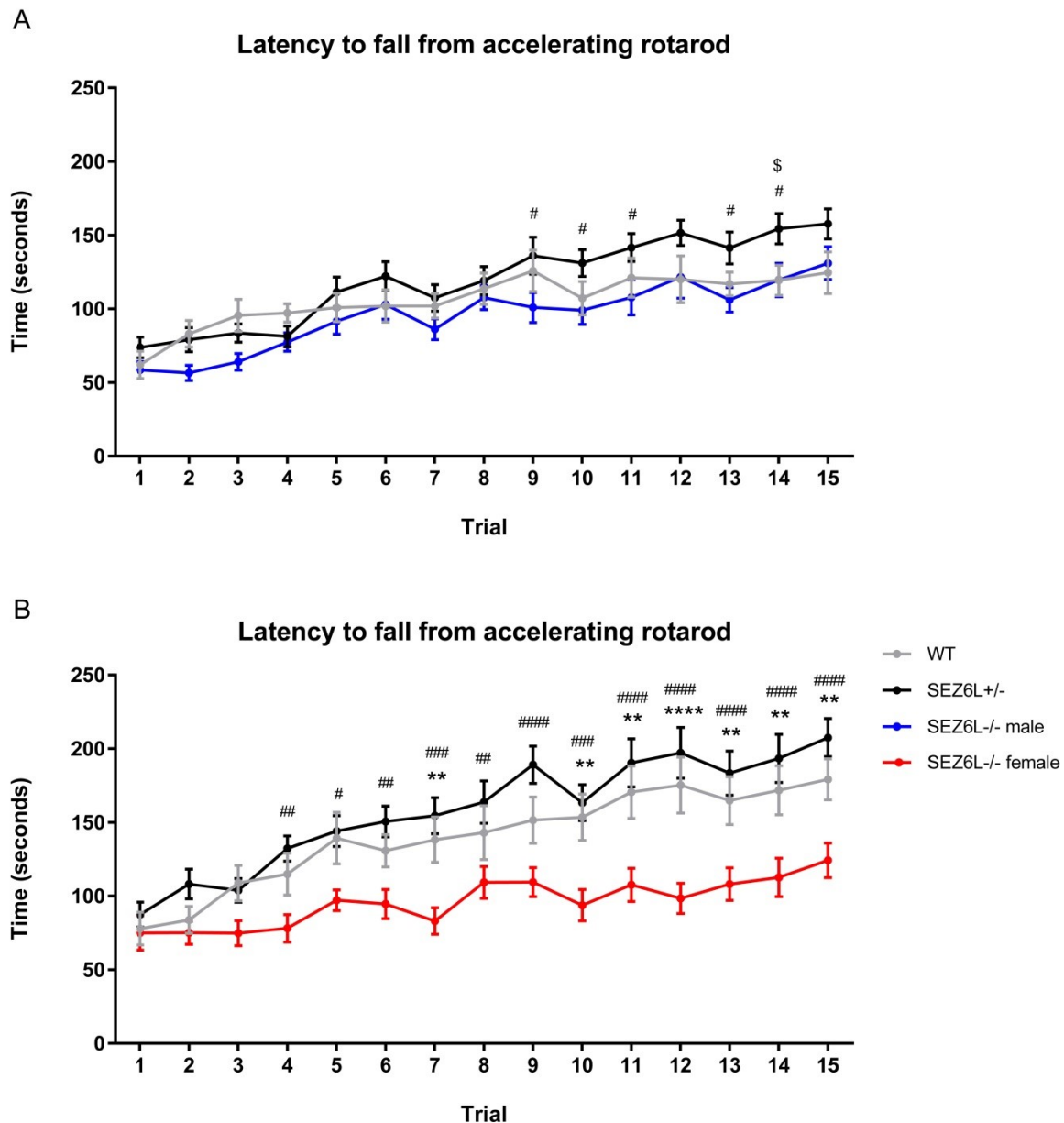


Figure 12. Rotarod analysis of SEZ6L^{-/-} mice. (A) Rotarod analysis of male and (B) female mice. Shown is the latency to fall from the accelerating rotarod (s) per trial. Effects of genotype, trial and interaction between factors was analysed using 2-way repeated ANOVA, while the differences between the trials was measured with Tukey's multiple comparison test. Analysis included 15 WT, 18 SEZ6L^{+/-} and 21 SEZ6L^{-/-} male and 14 WT, 16 SEZ6L^{+/-} and 15 SEZ6L^{-/-} female mice. Significant WT and SEZ6L^{-/-} differences are annotated with an asterisk (*), SEZ6L^{+/-} and SEZ6L^{-/-} with a hash (#) and WT and SEZ6L^{+/-} with \$. * p≤0.05; ** p≤0.01; *** p≤0.001; **** p≤0.0001 (or equivalent symbol). Data is shown as mean ± SEM.

Next, the gait analysis was performed using the DigiGait Imaging system to assess kinematics of the animals. This software generates a number of indices of posture and gait dynamics of an animal in a quantitative and robust way. The analysis of the SEZ6L mice revealed altered gait patterns of SEZ6L^{-/-} compared to the SEZ6L^{+/-} and WT mice (Table 25). Generally, both genders showed the same gait changes analysed by 2-way ANOVA (with gender and genotype as factors) and therefore the male and female data were pooled and analysed with 1-way ANOVA. Alteration in the SEZ6L^{-/-} mice was seen in the stride length, which is the length needed for a paw that traverses through a given stride, and is ~13-14% longer in the SEZ6L^{-/-} mice, as well as the time duration for one paw for one complete stride (stride time),

that is ~11% higher in SEZ6L^{-/-} mice. Consequently, the SEZ6L^{-/-} mice need fewer strides to cover a given distance (stride frequency) which showed ~10-12% decrease in the SEZ6L^{-/-} mice. This phenotype is more pronounced at the higher treadmill speed examined. Thus to maintain a given treadmill pace SEZ6L^{-/-} mice take longer and less frequent strides compared to the WT mice. Another gait displaying differences between the genotypes is swing time. The measured duration of the swing phase, the phase when the paw is in no contact with the belt, was higher in the SEZ6L^{-/-} hindlimbs at both measured speeds. In the forelimbs, there was the same trend of prolonging the time for needed for the swing, but the difference was not significant.

Table 25. DigiGait analysis of SEZ6L^{-/-} mice. Listed are significant and non-significant indices changing in the SEZ6L^{-/-} mice compared to the WT and SEZ6L^{+/-}. Data are analysed using 1-way ANOVA and represented with mean ± SEM. Male and female data are pooled. At the lower treadmill speed (15 cm/s) 24 WT (9 male, 15 female), 29 SEZ6L^{+/-} (14 male, 15 female) and 24 SEZ6L^{-/-} (15 male, 9 female) mice were analysed, while at the higher treadmill speed (25 cm/s) 19 WT (6 male, 13 female), 28 SEZ6L^{+/-} (13 male, 15 female) and 20 SEZ6L^{-/-} (13 male, 7 female). The same cohort was measured at both treadmill speeds (differences in number come from the mice that were unable to run at a given speed). Significant differences between WT and SEZ6L^{-/-} are marked with an asterisk (*), while SEZ6L^{+/-} and SEZ6L^{-/-} with a hash (#). * or # p≤0.05; ** or ## p≤0.01; *** or ### p≤0.001.

DigiGait indices	Treadmill speed	Data analysed	p-value	WT	SEZ6L ^{+/-}	SEZ6L ^{-/-}
Stride length (cm)	15 cm/s	Forelimb avg.	n.s.	5.13 ± 0.212	5.07 ± 0.072	5.43 ± 0.166
		Hindlimb avg.	n.s.	4.18 ± 0.381	4.27 ± 0.315	4.50 ± 0.406
	25 cm/s	Forelimb avg.	0.0013	5.87 ± 0.196	6.26 ± 0.083	6.65 ± 0.134 ***
		Hindlimb avg.	0.0006	5.88 ± 0.200	6.27 ± 0.075	6.72 ± 0.150 *** and #
Stride frequency (steps/s)	15 cm/s	Forelimb avg.	n.s.	3.11 ± 0.080	3.02 ± 0.044	2.87 ± 0.091
		Hindlimb avg.	0.0109	3.10 ± 0.073	3.04 ± 0.052	2.81 ± 0.080 * and #
	25 cm/s	Forelimb avg.	0.0024	4.31 ± 0.101	4.10 ± 0.054	3.88 ± 0.091 **
		Hindlimb avg.	0.0006	4.35 ± 0.101	4.11 ± 0.049	3.86 ± 0.097 ***
Stride time (s)	15 cm/s	Forelimb avg.	0.0399	0.332 ± 0.008	0.339 ± 0.005	0.361 ± 0.011 *
		Hindlimb avg.	0.0044	0.333 ± 0.008	0.339 ± 0.006	0.370 ± 0.010 ** and #
	25 cm/s	Forelimb avg.	0.0017	0.240 ± 0.005	0.251 ± 0.003	0.266 ± 0.005 **
		Hindlimb avg.	0.0005	0.239 ± 0.006	0.251 ± 0.003	0.269 ± 0.006 *** and #
Swing time (s)	15 cm/s	Forelimb avg.	n.s.	0.111 ± 0.004	0.110 ± 0.003	0.118 ± 0.004
		Hindlimb avg.	0.0036	0.092 ± 0.003	0.093 ± 0.003	0.107 ± 0.004 ** and ##
	25 cm/s	Forelimb avg.	n.s.	0.093 ± 0.004	0.095 ± 0.002	0.100 ± 0.003
		Hindlimb avg.	0.0044	0.083 ± 0.003	0.087 ± 0.002	0.098 ± 0.004 ** and #

Taken together, a detailed behavioural analysis of SEZ6L^{-/-} mice demonstrated motor discoordination as assessed by rotarod and DigiGait. Differences were observed both in

gender and genotype and the alterations are showing deficits in motor behaviour. The mice have no difference on the ledge beam nor are there changes in the neuromuscular strength as shown by forelimb grip strength analysis.

4.2.3. Proteomic analysis of the cerebellar membranes of adult SEZ6L^{-/-} mice

To further unravel the changes occurring in the SEZ6L^{-/-} mice and possibly connect them on the protein level with the observed behavioural phenotypes, a proteomic approach was used. Due to SEZ6L being a membrane protein, membrane preparation of the adult SEZ6L and WT cerebella was performed.

Mass spectrometry analysis identified 2760 proteins that were relatively quantified in at least 3 out of 6 biological replicates, of which 232 were significantly altered with the p-value less than 0.05. When correcting with a permutation based false discovery rate (FDR) of 5% with s_0 of 0.1, 14 proteins remain significant, 13 of which are downregulated and only 1 being upregulated as presented in the volcano plot (Fig. 13). Of all significant proteins, the highest downregulation was detected for: 83% for the Heterogeneous nuclear ribonucleoprotein A3 (hnRNP A3), followed by the 65% reduction for the Interleukin enhancer-binding factor 2 (ILF2) and 63% for the Beta-chimaerin (CHN2). The only upregulated protein was Histone H4 (Hist1h4a) with 2.1-fold increase in the SEZ6L^{-/-} cerebellum. Other changed proteins with p-value less than 0.05 are listed in the tables 26 and 27.

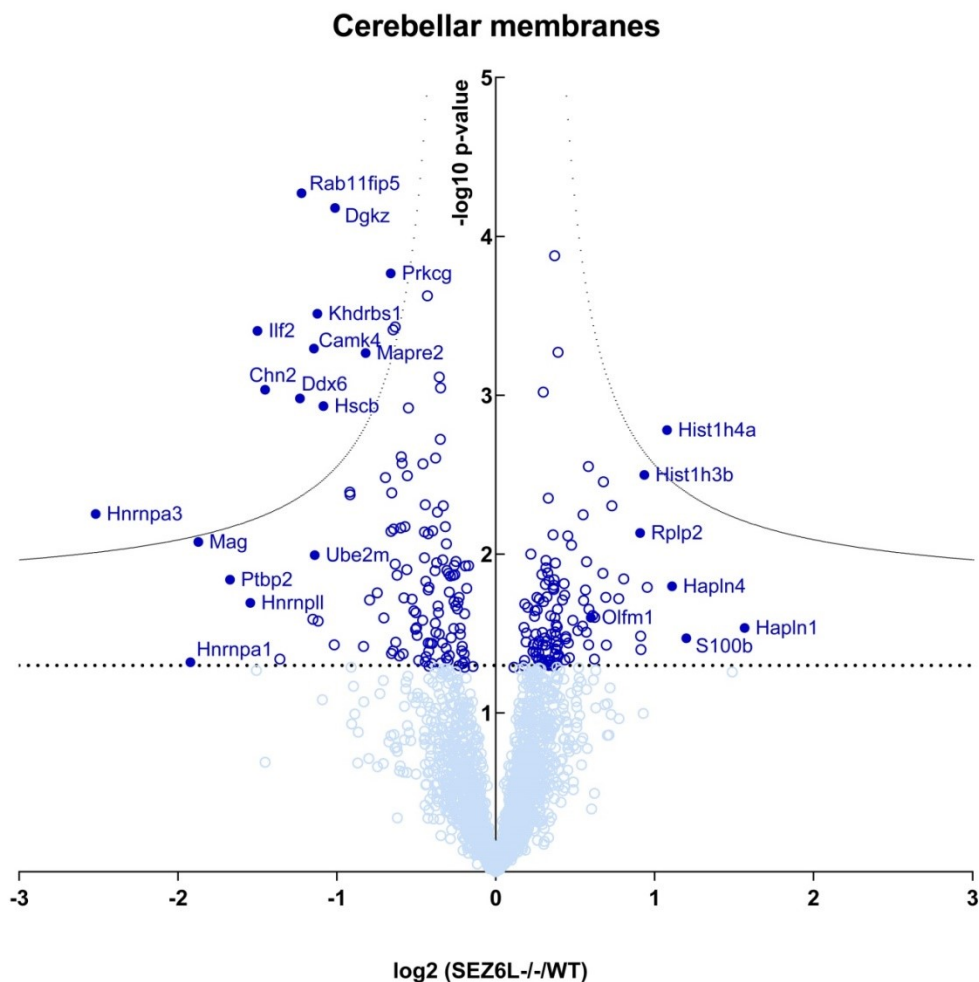


Figure 13. Proteomic analysis of SEZ6L^{-/-} cerebella. Volcano plot representing membrane preparation of SEZ6L^{-/-} cerebella compared to the WT. Dark blue opened and filled circles represent the 232 proteins that were significantly changed in at least 3 out of 6 biological replicates, while the unchanged proteins are annotated with light blue open circles. Y-axis depicts the negative log₁₀ transformation of the p-value, where 0.05 is 1.3 on the logarithmic scale (black dashed line). X-axis represents the log₂ transformation of the fold change of the SEZ6L^{-/-} cerebella compared to the control. 14 proteins remain significant after false discovery rate based multiple hypotheses testing (black dashed curve).

Table 26. Membrane preparation of adult SEZ6L^{-/-} cerebella. List of significantly downregulated proteins in SEZ6L^{-/-} cerebella with t-test less than 0.05 in at least 3 out of 6 biological replicates as shown in figure 13. Proteins are listed with their gene names that have at least 40% reduction when compared to the control (mean SEZ6L^{-/-}/CTR).

Protein name	Gene name	MEAN (SEZ6L ^{-/-} /CTR)	TTEST p-value
<i>Downregulated proteins</i>			
Heterogeneous nuclear ribonucleoprotein A3	Hnrnpa3	0.17	5.60E-03
Heterogeneous nuclear ribonucleoprotein A1	Hnrnpa1	0.26	4.79E-02
Myelin-associated glycoprotein	Mag	0.27	8.38E-03
Polypyrimidine tract-binding protein 2	Ptbp2	0.31	1.45E-02
Heterogeneous nuclear ribonucleoprotein L-like	Hnrnp11	0.34	2.03E-02
Interleukin enhancer-binding factor 2	Ilf2	0.35	3.93E-04
Beta-chimaerin	Chn2	0.37	9.25E-04
Cytochrome c oxidase subunit 7A-related protein, mitochondrial	Cox7a2l	0.39	4.57E-02
Probable ATP-dependent RNA helicase DDX6	Ddx6	0.43	1.05E-03
Rab11 family-interacting protein 5	Rab11fip5	0.43	5.34E-05
Protein phosphatase methylesterase 1	Ppme1	0.45	1.82E-03
Ribosomal protein S6 kinase alpha-5	Rps6ka5	0.45	2.57E-02
Calcium/calmodulin-dependent protein kinase type IV	Camk4	0.45	5.08E-04
NEDD8-conjugating enzyme Ubc12	Ube2m	0.45	1.01E-02
KH domain-containing, RNA-binding, signal transduction-associated protein 1	Khdrbs1	0.46	3.06E-04
Nucleophosmin	Npm1	0.46	2.64E-02
Iron-sulfur cluster co-chaperone protein HscB, mitochondrial	Hscb	0.47	1.17E-03
Ubiquitin-conjugating enzyme E2 N	Ube2n	0.49	3.73E-02
Diacylglycerol kinase zeta	Dgkz	0.50	6.61E-05
Cold shock domain-containing protein E1	Csde1	0.53	4.07E-03

Table 27. Membrane preparation of adult SEZ6L^{-/-} cerebella. Listed are significantly upregulated proteins in SEZ6L^{-/-} cerebella with t-test less than 0.05 in at least 3 out of 6 biological replicates (Fig. 13). Proteins are listed with their gene names that have at least 1.4-fold accumulation when compared to the control (mean SEZ6L^{-/-}/CTR).

Protein name	Gene name	Mean (SEZ6L ^{-/-} /CTR)	TTEST p-value
<i>Upregulated proteins</i>			
Hyaluronan and proteoglycan link protein 1	Hapln1	2.96	2.92E-02
Mitochondrial inner membrane protein COX18	Cox18	2.31	2.83E-02
Protein S100-B	S100b	2.30	3.38E-02
Hyaluronan and proteoglycan link protein 4	Hapln4	2.16	1.59E-02
Histone H4	Hist1h4a	2.11	1.66E-03
Histone H2A type 2-C;Histone H2A type 2-A	Hist2h2ac;Hist2h2aa1	1.94	1.62E-02
Histone H3.2	Hist1h3b	1.91	3.17E-03
NADH dehydrogenase [ubiquinone] complex I, assembly factor 7	Ndufaf7	1.88	3.98E-02
Histone H2B type 1-K;Histone H2B type 1-F/J/L;Histone H2B type 1-C/E/G;Histone H2B type 1-H;Histone H2B type 1-P;Histone H2B type 1-B;Histone H2B type 2-B;Histone H2B type 1-M;Histone H2B type 1-A	Hist1h2bk;Hist1h2bf;Hist1h2bc;Hist1h2bh;Hist1h2bp;Hist1h2bb;Hist2h2bb;Hist1h2bm;Hist1h2ba	1.88	3.28E-02
60S acidic ribosomal protein P2	Rplp2	1.88	7.36E-03
Uncharacterized protein C4orf19 homolog		1.75	1.43E-02
60S ribosomal protein L26	Rpl26	1.71	1.91E-02
Transmembrane protein 9B	Tmem9b	1.70	2.73E-02
Glypican-6;Secreted glypican-6	Gpc6	1.66	4.96E-03
Band 4.1-like protein 1	Epb41l1	1.62	3.74E-02
Ankyrin-2	Ank2	1.62	1.87E-02
Guanine nucleotide-binding protein G(I)/G(S)/G(O) subunit gamma-10	Gng10	1.60	3.51E-03
Potassium voltage-gated channel subfamily A member 2	Kcna2	1.60	1.32E-02
60S ribosomal protein L10a	Rpl10a	1.54	2.50E-02
HIG1 domain family member 1A, mitochondrial	Higd1a	1.54	4.58E-02
Lysophospholipid acyltransferase 2	Mboat2	1.53	2.44E-02
Noelin	Olfm1	1.51	2.52E-02

When taking into consideration statistical significance, the fold change and the availability of the antibodies, two proteins were selected for further validation via Western blot. Calcium/calmodulin-dependent protein kinase type IV (CaMKIV) was statistically significant also after the correction for the FDR with 55% downregulation in the SEZ6L^{-/-} membrane preparation of the cerebellum. Noelin (OLFM1) was among upregulated proteins and showed increase of 1.5-fold compared to the WT. Western blot analysis using membrane preparation of the WT and SEZ6L^{-/-} cerebellum showed statistical significance for both CaMKIV and OLFM1, with 50% decrease and 1.6-fold increase, respectively (Fig. 14A and 14B).

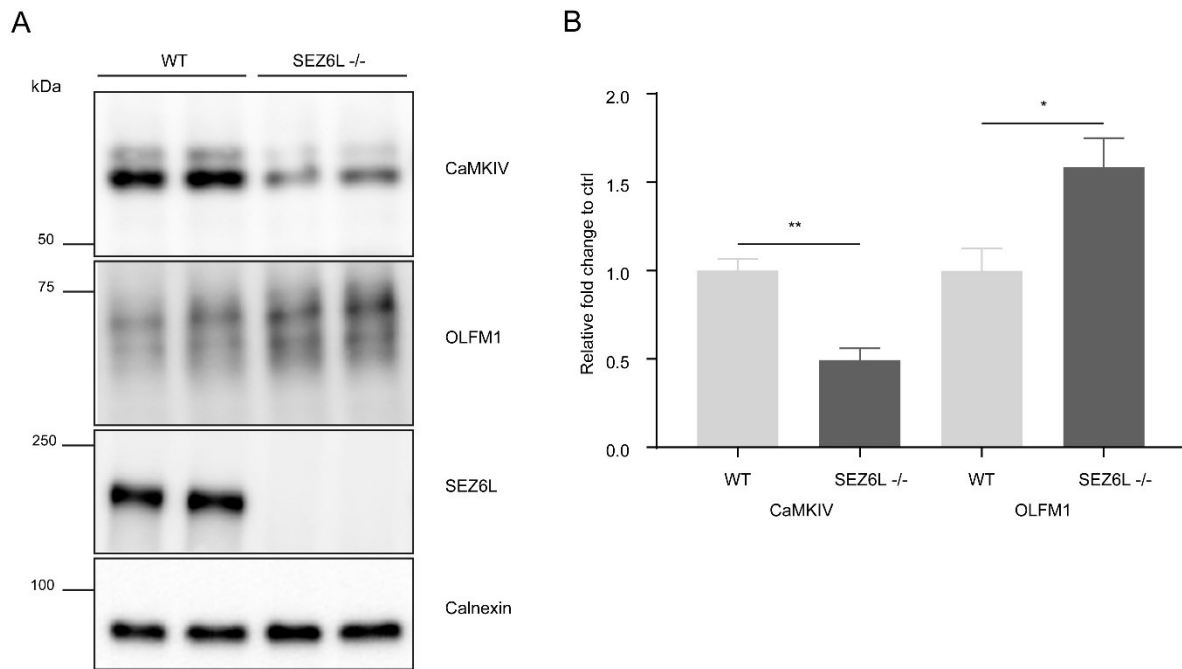


Figure 14. Validation of CaMKIV and OLFM1. (A) Membrane preparations of the WT and SEZ6L^{-/-} cerebella are blotted for CaMKIV and OLFM1. SEZ6L and Calnexin are used as a control. (B) Mann-Whitney U test showing significant downregulation of CaMKIV for 50%, and 1.5-fold increase for OLFM1. Graphs are represented with mean \pm SEM in n=6 biological replicates.

In conclusion, analysis of adult SEZ6L^{-/-} cerebellum revealed a number of downregulated proteins in the deficient cerebellum. Two of the proteins were further validated via Western blot showing similar significant downregulation in the case of CaMKIV, and upregulation for OLFM1.

4.2.4. Proteomic analysis of the cerebellar membranes of young SEZ6L^{-/-} mice

The expression of SEZ6L in the cerebellum is reaching its peak until the fourth week after which is going down by the eighth week (Miyazaki et al., 2006). To test whether there are developmental changes influenced by the SEZ6L, proteomic analysis was done using membrane preparation of the postnatal day 21 (P21) cerebella. In this way, comparison between changes of the young and above analysed adult mice can be done, thereby investigating the extent of change that is occurring due to age.

Proteomic analysis identified 3967 proteins in the membrane preparation of P21 cerebella, of which 2760 were quantified in at least 3 out of 5 for SEZ6L^{-/-} or 6 for WT biological replicates (Fig. 15). After applying unpaired two samples t-test using the p-value less than 0.05, 115 proteins were significantly altered. No protein remained significantly changed after correction for the multiple hypotheses tests for the FDR (p=0.05, s0=0.1). Top upregulated proteins with the p-value less than 0.05 included E3 SUMO-protein ligase RanBP2 (Ranbp2) with 4.9-fold, Ras/Rap GTPase-activating protein SynGAP (Syngap1) with 2.54-fold, Protein-S-isoprenylcysteine O-methyltransferase (Icmt) with 2.32-fold and Lipase maturation factor 1 (Lmf1) with 2.18-fold increase. On the other hand, downregulation was seen for Collagen alpha-2(I) chain (Col1a2) with 83%, Peroxisomal membrane protein PEX16 (Pex16) with 71%, 6.8 kDa mitochondrial proteolipid (Mp68) with 60% and Eukaryotic translation

initiation factor 5A-1 (Eif5a) with 56% reduction in the SEZ6L^{-/-} cerebella. The list of other altered protein is annotated in the tables 28 and 29.

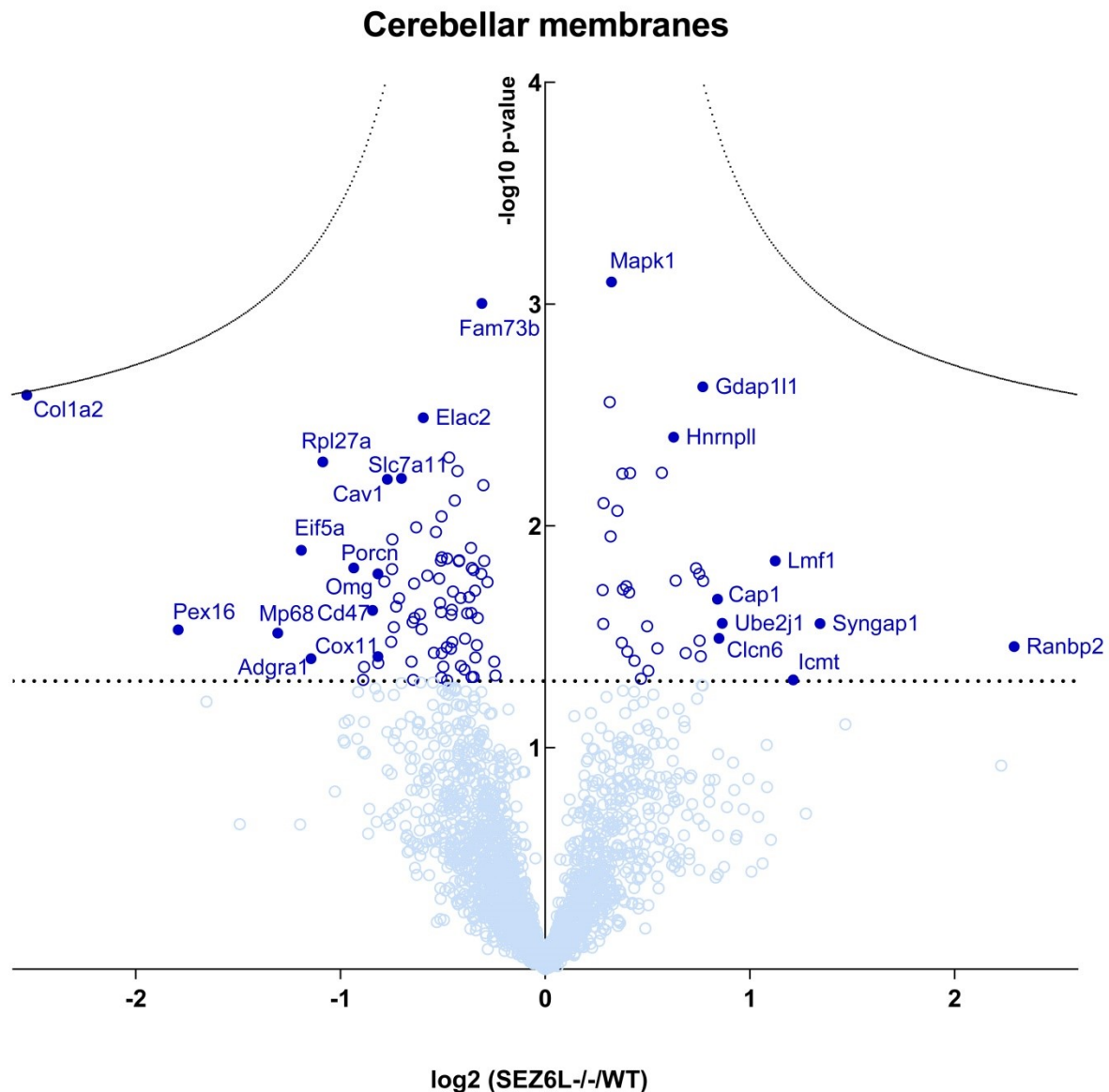


Figure 15. Proteomic analysis of membrane preparation of young SEZ6L^{-/-} cerebella. SEZ6L^{-/-} and WT littermates control cerebella of P21 mice were analysed via mass spectrometry and represented in the volcano plot. The significantly altered proteins are depicted with dark blue empty and filled dots, while non-significant with light blue empty dots. P-value is represented on the y-axis in negative log₁₀ transformation with the threshold of 0.05, or 1.3 at the logarithmic scale (dashed line). Fold change of the proteins in the SEZ6L^{-/-} cerebella compared to the WT control is log₂ transformed and represented on the x-axis. The dashed black curve represents the FDR threshold of 5% with s₀=0.1.

Table 28. Downregulated proteins in membrane preparation of young SEZ6L^{-/-} cerebella. List of significantly downregulated proteins in the membrane preparation of the SEZ6L^{-/-} cerebella compared to the WT littermate control (Fig. 15). Shown are proteins statistically significant with t-test less than 0.05 in at least 3 out of 5 or 6 biological replicates, with their protein name, gene name, p-value and mean (SEZ6L^{-/-}/CTR).

Protein name	Gene name	Mean (SEZ6L ^{-/-} /CTR)	TTEST p-value
<i>Downregulated proteins</i>			
Collagen alpha-2(I) chain	Colla2	0.17	2.57E-03
Peroxisomal membrane protein PEX16	Pex16	0.29	2.94E-02
6.8 kDa mitochondrial proteolipid	Mp68	0.40	3.05E-02
Eukaryotic translation initiation factor 5A-1	Eif5a	0.44	1.29E-02
Adhesion G protein-coupled receptor A1	Adgral	0.45	3.97E-02
60S ribosomal protein L27a	Rpl27a	0.47	5.15E-03
Protein-serine O-palmitoleoyltransferase porcupine	Porcn	0.52	1.55E-02
Probable cysteine--tRNA ligase, mitochondrial	Cars2	0.54	4.95E-02
Syntaxin-8	Stx8	0.54	4.33E-02
Leukocyte surface antigen CD47	Cd47	0.56	2.40E-02
Oligodendrocyte-myelin glycoprotein	Omg	0.57	1.65E-02
Cytochrome c oxidase assembly protein COX11, mitochondrial	Cox11	0.57	3.89E-02
Receptor activity-modifying protein 1	Ramp1	0.57	4.16E-02
Voltage-dependent calcium channel gamma-8 subunit	Cacng8	0.58	1.78E-02
Caveolin-1	Cav1	0.59	6.17E-03
Protein FAM131B	Fam131b	0.59	3.34E-02
2-aminoethanethiol dioxygenase	Ado	0.60	1.57E-02
Neuronal pentraxin receptor	Nptxr	0.60	1.15E-02
Immediate early response 3-interacting protein 1	Ier3ip1	0.60	2.86E-02
Receptor expression-enhancing protein 1	Reep1	0.60	2.31E-02

Table 29. Upregulated proteins in membrane preparation of young SEZ6L^{-/-} cerebella. List of significantly upregulated proteins in the membrane preparation of the SEZ6L^{-/-} cerebella compared to the WT littermate control as showed in figure 15. Shown are proteins statistically significant with t-test less than 0.05 in at least 3 out of 5 or 6 biological replicates, with their protein name, gene name, p-value and mean (SEZ6L^{-/-}/CTR).

Protein name	Gene name	Mean (SEZ6L ^{-/-} /CTR)	TTEST p-value
<i>Upregulated proteins</i>			
E3 SUMO-protein ligase RanBP2	Ranbp2	4.90	3.50E-02
Ras/Rap GTPase-activating protein SynGAP	Syngap1	2.54	2.76E-02
Protein-S-isoprenylcysteine O-methyltransferase	Icmt	2.32	4.95E-02
Lipase maturation factor 1	Lmf1	2.18	1.44E-02
Ubiquitin-conjugating enzyme E2 J1	Ube2j1	1.82	2.75E-02
Chloride transport protein 6	Cln6	1.80	3.22E-02
Adenylyl cyclase-associated protein 1	Cap1	1.79	2.14E-02
Coronin-1C	Coro1c	1.71	1.77E-02
Ganglioside-induced differentiation-associated protein 1-like 1	Gdap111	1.70	2.36E-03
Guanine nucleotide-binding protein subunit beta-5	Gnb5	1.69	3.87E-02
Endoplasmic reticulum lectin 1	Erlec1	1.69	3.30E-02
Acyl-CoA:lysophosphatidylglycerol acyltransferase 1	Lpgat1	1.69	1.65E-02
Rho GTPase-activating protein 21	Arhgap21	1.67	1.55E-02
Septin-8	Sept8	1.61	3.74E-02
Cytochrome b5	Cyb5a	1.56	1.77E-02
Heterogeneous nuclear ribonucleoprotein L-like	Hnrnp11	1.54	3.98E-03
Tail-anchored protein insertion receptor WRB	Wrb	1.48	5.77E-03
Tubulin alpha-4A chain	Tuba4a	1.46	3.57E-02
tRNA-splicing ligase RtcB homolog	Rtcb	1.42	4.51E-02
Small integral membrane protein 12	Smim12	1.41	2.84E-02

Additionally, there were a number of proteins that are not listed or annotated in the volcano plot since their relative quantification was measurable only in the SEZ6L^{-/-} (at least 4 out of 5) and in none of the WT biological replicates (Table 30). In other words, these proteins were below the detection limit in all WT, but accumulating in most or all SEZ6L^{-/-} samples. Having no value in the WT samples, no statistical analysis could be performed. Nevertheless, this information gives additional valuable insight on the changes occurring due to the loss of SEZ6L. Only 1 protein was found consistently in all WT, but in none of the SEZ6L^{-/-} replicates and is as expected, SEZ6L.

Table 30. Proteins detected in either SEZ6L^{-/-} or WT biological replicates. List of proteins found only in the SEZ6L^{-/-} or WT samples with at least 4 unique peptides, with annotated protein names, gene names, unique peptides and average log₂ transformed LFQ-intensities of 5 SEZ6L^{-/-} and 6 WT (CTR) biological replicates. Samples that were below detection limit are annotated as NaN.

Protein names	Gene names	Unique peptides	SEZ6L ^{-/-}	CTR
Seizure 6-like protein	Sez6l	11	NaN	26.91325167
Proteasome subunit beta type-5	Psmb5	4	24.7827525	NaN
Serine--tRNA ligase, cytoplasmic	Sars	4	24.37836	NaN
Mannosyl-oligosaccharide 1,2-alpha-mannosidase IB	Man1a2	6	24.78398	NaN
Leukemia inhibitory factor receptor	Lifr	5	21.4642775	NaN
Beta-1,4 N-acetylgalactosaminyltransferase 1	B4galnt1	4	22.7257075	NaN
Centrosomal protein of 76 kDa	Cep76	4	25.286702	NaN
CSC1-like protein 2	Tmem63b	5	25.2956575	NaN
Endothelin-converting enzyme 1	Ece1	4	23.698435	NaN
Girdin	Ccdc88a	8	24.4702475	NaN
KH domain-containing, RNA-binding, signal transduction-associated protein 1	Khdrbs1	4	24.468896	NaN
Brevican core protein	Bcan	9	24.843525	NaN
Calcineurin subunit B type 1	Ppp3r1	4	24.5542225	NaN
Serine/threonine-protein kinase DCLK2	Dclk2	5	24.2207725	NaN
Talin-2	Tln2	9	24.8046025	NaN
Protein VAC14 homolog	Vac14	5	23.839655	NaN
Transmembrane protein 127	Tmem127	4	23.064205	NaN
Protein unc-80 homolog	Unc80	5	23.70559	NaN
Abl interactor 1	Abi1	4	24.0520925	NaN
Solute carrier family 35 member E1	Slc35e1	5	24.4359575	NaN
Epsin-2	Epn2	4	23.70989	NaN
Hydroxymethylglutaryl-CoA synthase, cytoplasmic	Hmgcs1	6	24.956815	NaN
Rho guanine nucleotide exchange factor 12	Arhgef12	10	25.13166	NaN
EPM2A-interacting protein 1	Epm2aip1	5	23.8194675	NaN
DnaJ homolog subfamily C member 3	Dnajc3	4	24.5282025	NaN
UTP--glucose-1-phosphate uridylyltransferase	Ugp2	7	24.8137325	NaN
Mucolipin-1	Mcoln1	4	23.990095	NaN
Suppressor of tumorigenicity 7 protein	St7	4	23.5389375	NaN
Coactosin-like protein	Cotl1	4	24.588195	NaN
Calponin-3	Cnn3	5	23.5316875	NaN
6-phosphogluconate dehydrogenase, decarboxylating	Pgd	5	24.62735	NaN
Striatin-3	Strn3	4	24.460355	NaN
Rho guanine nucleotide exchange factor 7	Arhgef7	7	24.8879675	NaN
CAP-Gly domain-containing linker protein 2	Clip2	5	23.4092	NaN

Altogether, membrane preparation of the cerebellum of the young SEZ6L^{-/-} mice did not show many significant alterations. However, a number of additional proteins were identified that were accumulating only in the SEZ6L^{-/-} conditions suggesting a broader role of SEZ6L in the cerebellum.

4.2.5. Whole proteome analysis of the young SEZ6L^{-/-} cerebellum

Membrane preparation and proteomic analysis of SEZ6L^{-/-} and WT cerebellum give valuable insights. However, information on other cellular compartments and the general overview of the alteration in the mutant cerebellum might be missing. Therefore, total proteome of SEZ6L^{-/-} cerebella was analysed in P21 mice and compared to the gender balanced WT littermate control.

Using mass spectrometry approach, total cerebellar homogenates of WT and SEZ6L^{-/-} mice were analysed and 5359 proteins were identified, of which 3843 quantified in at least 3 out of 7 biological replicates (Fig. 16). When applying unpaired two samples t-test with the p-value less than 0.05, 199 proteins were significantly altered. None of the proteins remained significant after additional multiple hypotheses testing with the FDR correction with s_0 being 0.1. Generally, more proteins were found to be downregulated, with the highest downregulation observed for: 76% Histone H3.2 (Hist1h3b), 69% Histone H3.1 (Hist1h3a) and Uncharacterized family 31 glucosidase KIAA1161 (Kiaa1161), 63% Protein phosphatase 1 regulatory subunit 14A (Ppp1r14a), 57% Plastin-2 (Lcp1). The top upregulated proteins were 2.2-fold Nuclear-interacting partner of ALK (Zc3hc1), 2-fold DnaJ homolog subfamily B member 11 (Dnajb11), 1.8-fold ADP-ribosylation factor-like protein 8B (Arl8b), 1.7-fold Phosphatidylethanolamine-binding protein 1; Hippocampal cholinergic (Pebp1) and 1.6-fold Paralemmin-1 (Palm). Other altered proteins are listed in the tables 31 and 32.

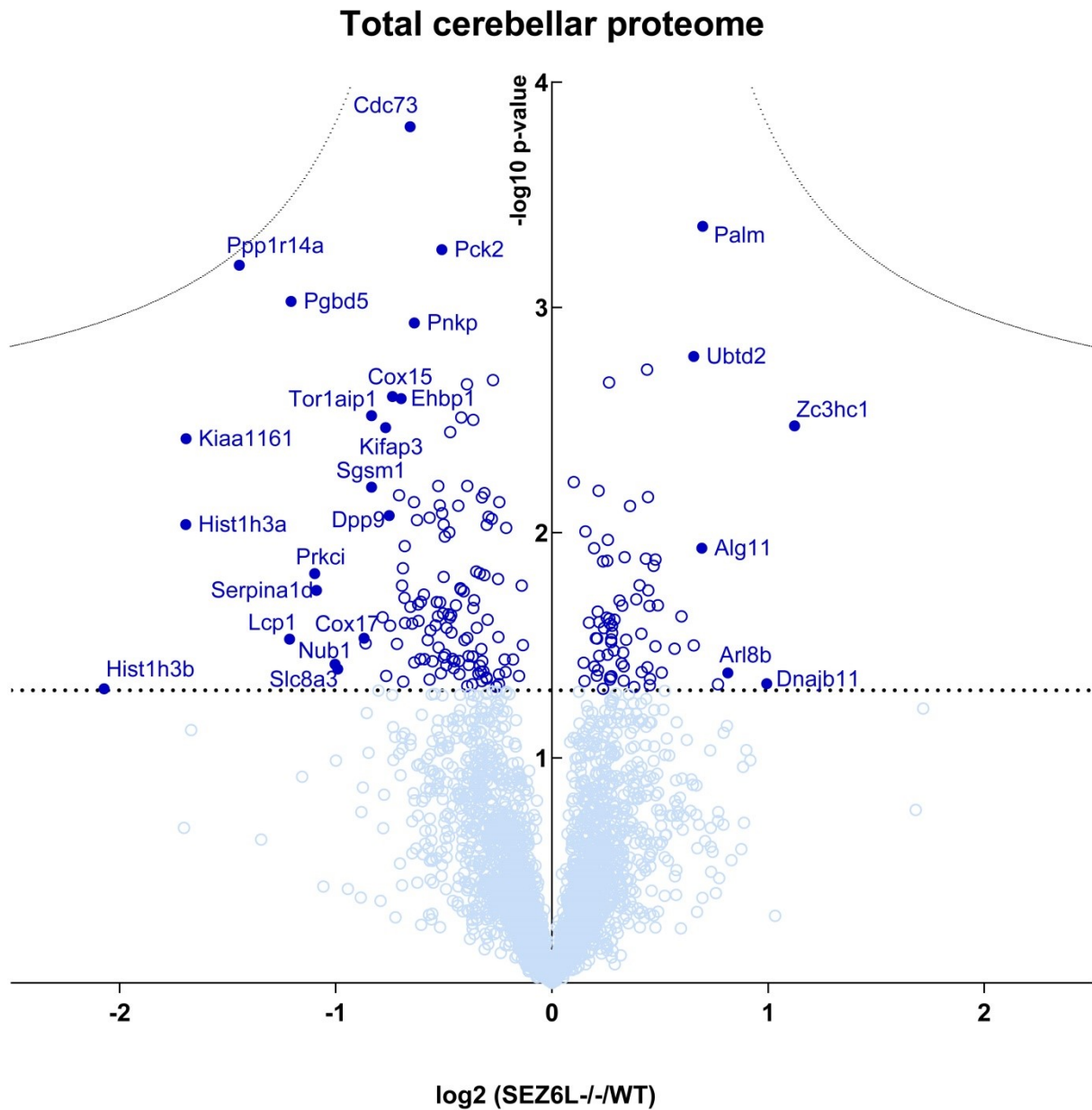


Figure 16. Total proteome of young SEZ6L^{-/-} cerebella. Volcano plot representation of total proteome analysis of SEZ6L^{-/-} cerebella compared to the WT littermates of P21 mice. 199 proteins were significantly altered in at least 3 out of 7 biological replicates and annotated with dark blue empty and filled dots. Proteins that were unchanged are depicted with the light blue empty dots. Y-axis represents the p-value in the negative log₁₀ transformation. On the logarithmic scale, 0.05 is 1.3 and annotated with the black dashed line. X-axis shows the fold change of the SEZ6L^{-/-} cerebella compared to the WT control, with log₂ transformation. The black dashed curve is the FDR threshold of 5% with $s_0=0.1$.

Table 31. Downregulated proteins in the total proteome of young SEZ6L^{-/-} cerebella. Shown are significantly downregulated proteins in the SEZ6L^{-/-} cerebella with t-test less than 0.05 in at least 3 out of 7 biological replicates, with their protein name, gene name, p-value and mean (SEZ6L^{-/-}/CTR).

Protein name	Gene name	Mean (SEZ6L ^{-/-} /CTR)	TTEST p-value
<i>Downregulated proteins</i>			
Histone H3.2	Hist1h3b	0.24	4.94E-02
Histone H3.1	Hist1h3a	0.31	9.21E-03
Uncharacterized family 31 glucosidase KIAA1161	Kiaa1161	0.31	3.82E-03
Protein phosphatase 1 regulatory subunit 14A	Ppp1r14a	0.37	6.49E-04
Plastin-2	Lcp1	0.43	2.97E-02
PiggyBac transposable element-derived protein 5	Pgbd5	0.43	9.39E-04
Protein kinase C iota type	Prkci	0.47	1.52E-02
Alpha-1-antitrypsin 1-4	Serpina1d	0.47	1.80E-02
NEDD8 ultimate buster 1	Nub1	0.50	3.84E-02
Sodium/calcium exchanger 3	Slc8a3	0.50	4.04E-02
Cytochrome c oxidase copper chaperone	Cox17	0.55	2.94E-02
Histone H3.3;Histone H3.3C	H3f3a;H3f3c	0.55	3.10E-02
Torsin-1A-interacting protein 1	Tor1aip1	0.56	3.02E-03
Small G protein signaling modulator 1	Sgsm1	0.56	6.28E-03
Protein FAM131B	Fam131b	0.58	2.37E-02
Kinesin-associated protein 3	Kifap3	0.59	3.41E-03
Paired box protein Pax-6	Pax6	0.59	4.34E-02
Dipeptidyl peptidase 9	Dpp9	0.59	8.40E-03
Mitogen-activated protein kinase 14	Mapk14	0.59	2.59E-02
Cytochrome c oxidase assembly protein COX15 homolog	Cox15	0.60	2.48E-03

Table 32. Upregulated proteins in the total proteome of young SEZ6L^{-/-} cerebella. List of significantly upregulated proteins in the SEZ6L^{-/-} cerebella with t-test less than 0.05 in at least 3 out of 7 biological replicates. Proteins are annotated with their protein name, gene name, p-value and mean (SEZ6L^{-/-}/CTR).

Protein name	Gene name	Mean (SEZ6L ^{-/-} /CTR)	TTEST p-value
<i>Upregulated proteins</i>			
Nuclear-interacting partner of ALK	Zc3hc1	2.18	3.36E-03
DnaJ homolog subfamily B member 11	Dnajb11	1.99	4.69E-02
ADP-ribosylation factor-like protein 8B	Arl8b	1.76	4.20E-02
Phosphatidylethanolamine-binding protein 1;Hippocampal cholinergic neurostimulating peptide	Pebp1	1.70	4.71E-02
Paralemmin-1	Palm	1.62	4.36E-04
GDP-Man:Man(3)GlcNAc(2)-PP-Dol alpha-1,2-mannosyltransferase	Alg11	1.62	1.17E-02
Ubiquitin domain-containing protein 2	Ubtd2	1.58	1.65E-03
Chromobox protein homolog 3	Cbx3	1.58	3.17E-02
Thioredoxin-like protein 1	Txnl1	1.52	2.35E-02
AP-2 complex subunit sigma	Ap2s1	1.48	3.28E-02
Vesicle-associated membrane protein 1	Vamp1	1.42	4.19E-02
Thioredoxin, mitochondrial	Txn2	1.40	2.10E-02
Kininogen-1;Kininogen-1 heavy chain;Bradykinin;Kininogen-1 light chain	Kng1	1.39	3.19E-02
Ras-related protein Rab-39B	Rab39b	1.39	1.32E-02
Small nuclear ribonucleoprotein-associated protein B;Small nuclear ribonucleoprotein-associated protein N	Snrpb;Snrpn	1.39	1.40E-02
Regulating synaptic membrane exocytosis protein 2	Rims2	1.37	4.46E-02
Guanine nucleotide-binding protein G(s) subunit alpha isoforms short;Guanine nucleotide-binding protein G(s) subunit alpha isoforms XLas	Gnas	1.37	4.76E-02
Y-box-binding protein 3	Ybx3	1.37	2.12E-02
RING finger protein 11	Rnf11	1.36	1.81E-02
Protein phosphatase 1H	Ppm1h	1.36	6.94E-03

In conclusion, total cerebellar proteome showed rather downregulation than upregulation of proteins dependent on the loss of SEZ6L. In general, not many alterations between the WT and SEZ6L^{-/-} mice was observed, which might be due to the sample complexity, since the total proteome of the whole cerebellum was analysed. If proteins with the highest abundance are not changed, but only the proteins with low abundance that are not detectable, then the results may be misleadingly negative. Alternatively, detected changes might be not as drastic, but anyway sufficient to trigger the observed behavioural phenotype.

4.2.6. Comparison of the adult and young SEZ6L proteome

Changes observed in the adult and young mice might be consistent throughout the investigated time span or alternatively, there could be age-specific changes that are more prominent either in development or in adulthood. To target this open point, changes between adult and young proteome were analysed in order to detect which proteins are overlapping. Statistically significant proteins were taken from adult (Adult MP) and young membrane preparation (Young MP) of the cerebellum, as well as the young total proteome of the cerebellum (Young TP). Results are depicted with Venn diagram, in the figure 17.

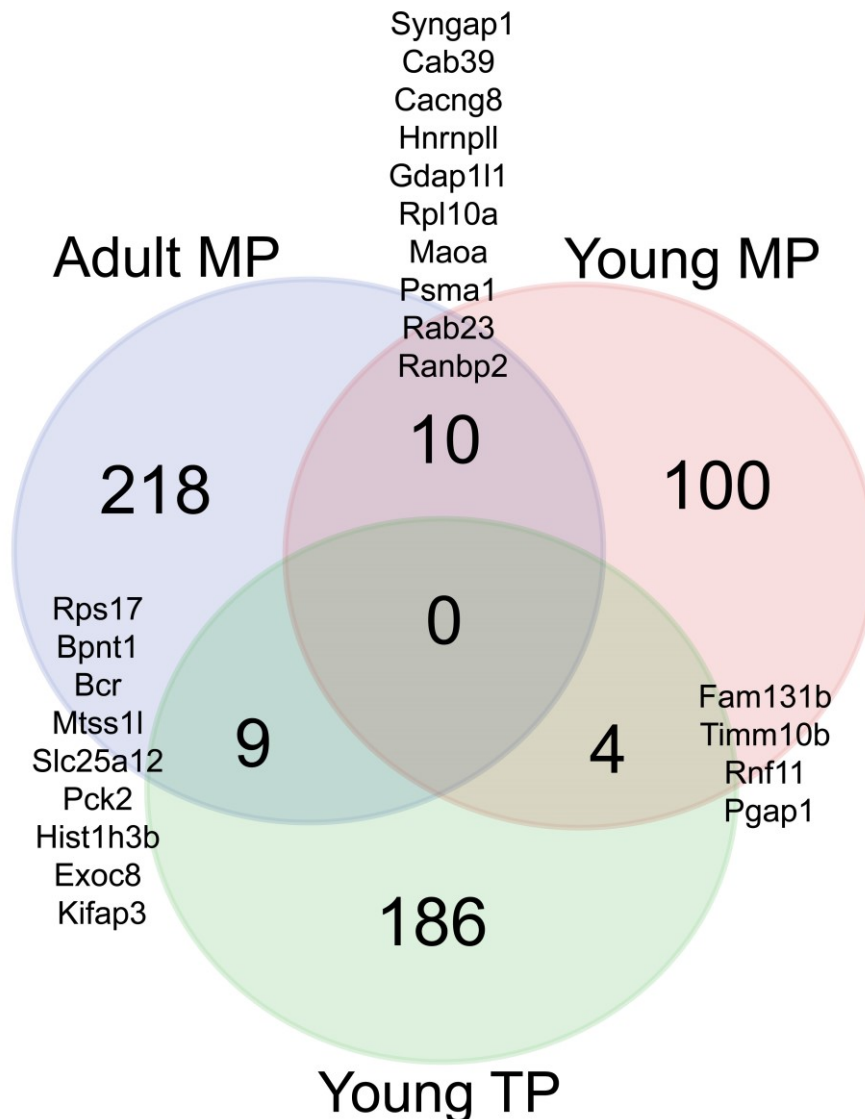


Figure 17. Comparison of the adult and young SEZ6L proteome. Proteins with the p-value less than 0.05 were taken from the above described proteomic analysis: adult (Adult MP) and young membrane preparation of the cerebellum (Young MP), and total cerebellar proteome (Young TP). 10 proteins were overlapping between adult and young MP, 9 between adult MP and young TP, and 4 between the young MP and TP and are annotated with their gene name. None of the proteins were found in all three datasets.

Adult membrane proteome had the highest amount of significantly changed proteins, 237, while young total proteome had 199, and young membrane proteome only 114. None of the proteins were found changed in all three proteomic analysis. On the other hand, there were 10 proteins found changed in both adult and young membrane proteome, 9 in adult membrane

proteome and young total proteome, and only 4 overlapping between young membrane and total proteome. Of the 10 proteins significantly altered in both adult and young membrane proteome, only two proteins had the same changes, Calcium-binding protein 39 (Cab39) and Proteasome subunit alpha type-1 (Psm1). In comparison with adult membrane and young total proteome, 3(2),5-bisphosphate nucleotidase 1 (Bpnt1), Breakpoint cluster region protein (Bcr), Calcium-binding mitochondrial carrier protein Aralar1 (Slc25a12), Exocyst complex component 8 (Exoc8) and Kinesin-associated protein 3 (Kifap3), while in young membrane and total proteome Protein FAM131B (Fam131b), RING finger protein 11 (Rnf11), and GPI inositol-deacylase (Pgap1) had similar changes between described proteomes. All other proteins that were overlapping between proteomes had opposite effect, accumulating in one and decreasing in other or vice versa.

Taken together, none of the proteins were found changed in all three proteomes: adult and young membrane proteomes, and young total proteome of SEZ6L cerebellum. However, some of them were changing in a similar manner at different age or compartment, while others had opposing changes between proteomes, indicating different spatial and temporal functions.

4.2.7. SEZ6L interaction partners

SEZ6L is a single-pass type I membrane protein with evolutionarily conserved CUB and SCR domains known to be involved in protein-protein interactions (Bork and Beckmann, 1993; Hourcade et al., 1989). To potentially infer the functions of SEZ6L through its interaction partners, co-immunoprecipitation followed by mass spec analysis was performed.

To circumvent the technical issue of leakage of capturing antibody of the immunoprecipitation assay in the eluate, the antibody was immobilized on protein G Sepharose beads followed by covalent crosslinkage. The amine-amine crosslinking was done with non-cleavable bis(sulfosuccinimidyl)suberate (BS3) forming a stable amide bond. After the coupling to the beads, SEZ6L was used as bait for its interacting partners in the total brain homogenates of adult SEZ6L^{-/-} and WT mouse brains and analysed via mass spectrometry (Fig. 18A).

The test experiment for evaluation of the leakage of the antibodies in the eluate was done comparing the eluate between the crosslinked and control beads using Western blot analysis (Fig. 18B). First, a known amount of immunoglobulin G (IgG) was loaded in decreasing quantity in order to estimate the amount of IgG in the eluate (Fig. 18B, first 5 lanes). To evaluate the amount of IgG that was coupled to the beads, hybridoma supernatants of the SEZ6 as a control and SEZ6L clones of the monoclonal antibodies (Pigoni et al., 2016) was compared before and after conjugation to the beads (Fig. 18B, sixth to ninth lane). There was an observable depletion of the IgG after conjugation indicating successful binding of the antibody to the beads and therefore decreased amounts in hybridoma supernatants. Elution of bound antibodies was then tested with and without crosslinkage and results demonstrated that crosslinked beads eluate contains considerably fewer amounts of immunoglobulins with its levels reduced to a minimum (Fig. 18B, tenth to thirteenth lane). Next, to prove that the crosslinking to the beads is not altering the binding properties of the antibody, a Western blot was used to analyse for the SEZ6L binding in the WT brain homogenates (Fig. 18C). SEZ6L could be detected in the immunoprecipitation fraction of the WT, but not in the SEZ6L^{-/-} homogenates.

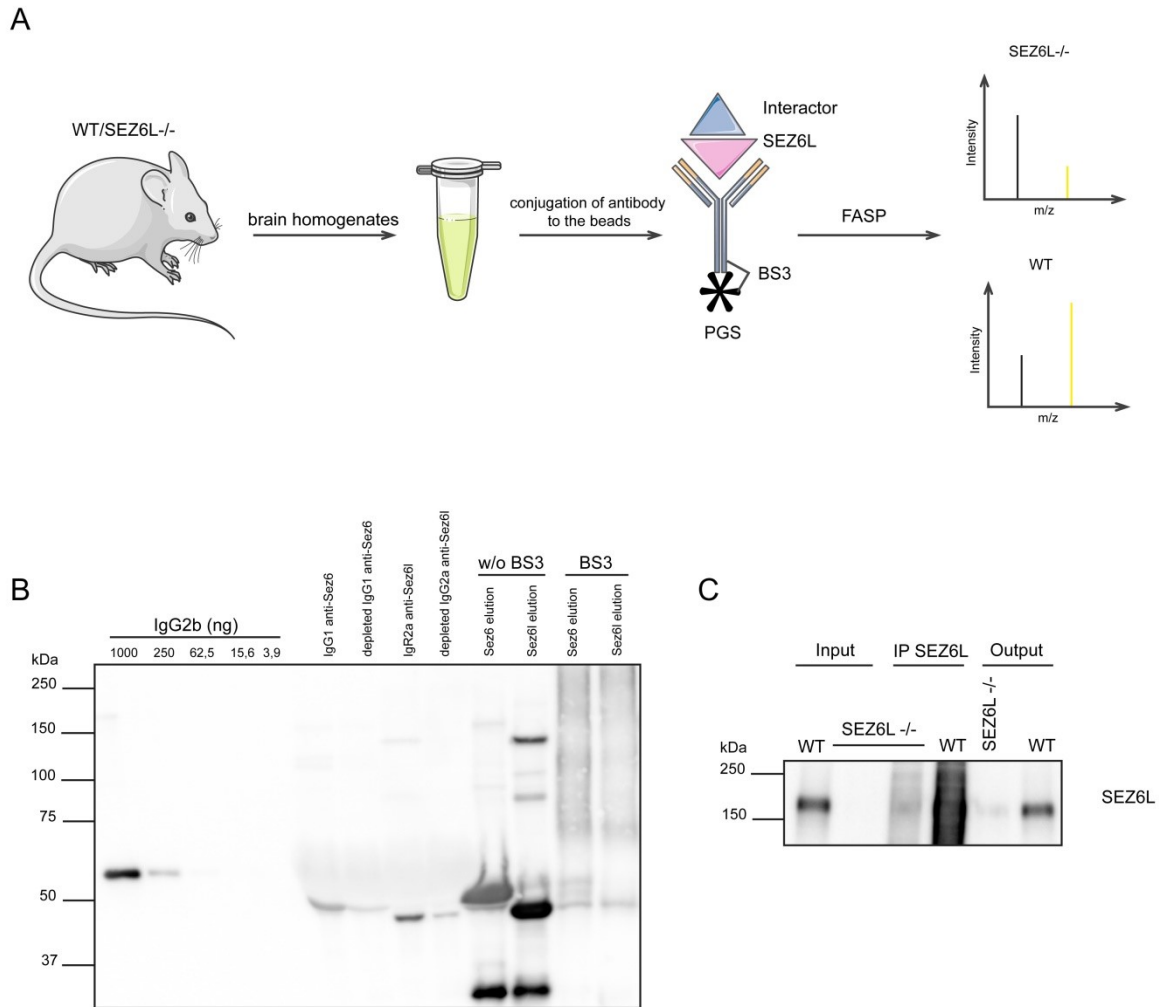


Figure 18. Crosslinking the capturing antibodies to the beads decreases the leakage of the immunoglobulins. (A) Workflow of the interactome analysis. WT and SEZ6L^{-/-} brains were homogenized and SEZ6L was immunoprecipitated from the sample by using conjugated capture monoclonal antibody. Samples were then processed by FASP and analysed via mass spectrometry. (B) Western blot detection of the leaking immunoglobulins from the conjugating beads. A known dose of IgG2b was detected to compare the amount of leakage. Hybridoma supernatant of the SEZ6L monoclonal rat IgG2a antibody was loaded before and after the binding to the protein G Sepharose beads. The elution was done in the presence or absence of BS3 crosslinker. The same control was done for the other member of the family, SEZ6. Membrane was blotted with anti-rat secondary antibody. (C) Immunoprecipitation of the SEZ6L from the WT and SEZ6L^{-/-} brain homogenates. The same amount of the input and output is loaded. SEZ6L was detected in the WT but not in the deficient brain.

Using the above described approach (Fig. 18A) adult WT and SEZ6L^{-/-} total brain homogenates were analysed via mass spectrometry. Proteomic analysis yielded a total of 477 proteins quantified in at least 3 out of 4 to 6 biological replicates with 71 having a p-value less than 0.05, as presented in the volcano plot (Fig. 19). After discarding the proteins that were found to be bound more in the SEZ6L^{-/-} brain rather than in the WT, as in this setup they are considered to be contaminants, 17 proteins were identified including SEZ6L itself. Of 16 proteins, 10 proteins were immunoglobulins that had significant increase of binding in the WT brains (Table 33). Six other proteins included Alpha-1B-glycoprotein (A1bg) and Protein 4.1 (Epb41).

SEZ6L Interactomics

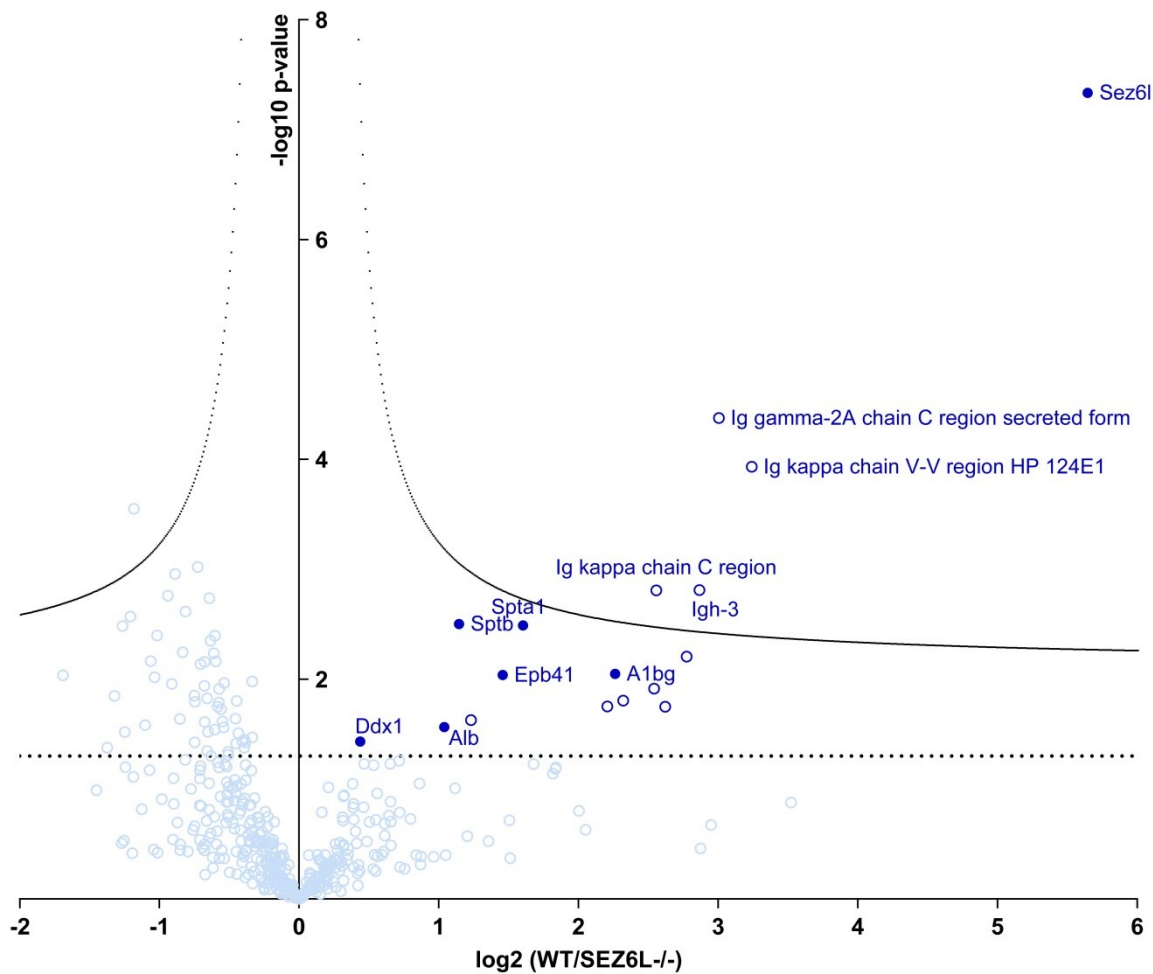


Figure 19. Proteomic analysis of the SEZ6L interacting partners. Volcano plot of the WT and SEZ6L^{-/-} brain homogenates immunoprecipitated with the SEZ6L antibody. Dark blue empty and filled dots represent the 17 proteins that were significantly enriched using SEZ6L antibody in WT samples. Empty dark blue dots are immunoglobulins. Empty light blue dots are not significant or proteins found to bind in the SEZ6L^{-/-} brain. On Y-axis, the negative log₁₀ transformation of the p-value is plotted, where black dashed line presents the statistical significance criteria of 0.05 (1.3 on the logarithmic scale). X-axis shows the fold change of the SEZ6L^{-/-} samples compared to the control in a log₂ transformation. 5 proteins remain significant after false discovery rate based multiple hypothesis testing (black dashed curve): immunoglobulins and the SEZ6L.

Table 33. List of interaction partner candidates of SEZ6L. Proteins are listed according to the fold change of binding in the WT brain homogenates with the t-test less than 0.05 in at least 3 out of 4 to 6 biological replicates.

Protein name	Gene name	Mean (CTR/SEZ6L-/-)	TTEST p-value
Seizure 6-like protein	Sez6l	50.11	4.63E-08
Ig kappa chain V-V region HP 124E1		9.46	1.17E-04
Ig gamma-2A chain C region secreted form		8.04	4.22E-05
Ig gamma-2B chain C region	Igh-3	7.29	1.55E-03
Ig lambda-1 chain C region		6.85	6.24E-03
Ig kappa chain V-III region PC 7210;Ig kappa chain V-III region PC 7183;Ig kappa chain V-III region PC 7043;Ig kappa chain V-III region CBPC 101		6.15	1.78E-02
Ig kappa chain C region		5.89	1.56E-03
Ig kappa chain V-III region PC 4050;Ig kappa chain V-III region ABPC 22/PC 9245		5.83	1.22E-02
Ig kappa chain V-V region HP 123E6		5.00	1.57E-02
Alpha-1B-glycoprotein	A1bg	4.80	8.98E-03
Ig heavy chain V region AC38 205.12;Ig heavy chain V region J558;Ig heavy chain V region MOPC 104E		4.61	1.77E-02
Spectrin alpha chain, erythrocytic 1	Spta1	3.04	3.25E-03
Protein 4.1	Epb41	2.75	9.14E-03
Ig lambda-3 chain C region	Iglc3	2.35	2.35E-02
Spectrin beta chain, erythrocytic	Sptb	2.21	3.15E-03
Serum albumin	Alb	2.05	2.72E-02
ATP-dependent RNA helicase DDX1	Ddx1	1.35	3.69E-02

Interestingly, two other proteins were detected before selecting for the significance criteria, Complement C3 (C3) and High affinity immunoglobulin gamma Fc receptor I (Fcgr1) (Table 34). Both proteins were quantified in at least 5 out of 6 WT and in 1 or none of the SEZ6L-/- samples, suggesting that the binding is indeed occurring mostly in the WT and probably not in the deficient brain. In other words, they would be excluded from the statistical analysis, but would in fact make ideal interactor partner candidates.

Table 34. Proteins detected in WT biological replicates. List of proteins found only in WT samples and in none or one SEZ6L-/- biological replicate with at least 4 unique peptides. Annotated are protein names, gene names, unique peptides and average log2 transformed LFQ-intensities of 4 SEZ6L-/- and 6 WT (CTR) biological replicates. Samples that were below detection limit are annotated as NaN.

Protein names	Gene names	Unique peptides	SEZ6L-/-	CTR
Complement C3	C3	6	NaN	23.55459
High affinity immunoglobulin gamma Fc receptor I	Fcgr1	7	22.51434*	24.34228

*Detected in only 1 SEZ6L-/- biological replicate

In conclusion, despite having the additional step of coupling antibodies to the beads and therefore drastically reducing the amount of immunoglobulin leakage in the eluate of the immunoprecipitation, the proteomic analysis demonstrated high amounts of potential binding of different immunoglobulins to the SEZ6L protein. Besides different immunoglobulin chains several other proteins were found as interaction partner candidates. Additionally, two other proteins, namely C3 and Fcgr1, were identified as the ideal candidates, as they were detected in only one or none of the SEZ6L-/-, but in most of the WT biological replicates therefore

excluding them from the statistical analysis. These interactions are pointing to potential role of SEZ6L in immunity.

5. DISCUSSION

BACE1 is the rate-limiting enzyme that catalyses the initial step of A β generation and therefore a key drug target for AD. Though initially considered to have fewer functions and presumably be well tolerated in patients, the discovery of multiple substrates of BACE1, particularly in the central nervous system, have continued to raise the concern about acute and chronic inhibition of BACE1. Numerous studies demonstrated a complex biology of BACE1 and are serving as a basis for understanding BACE1, guiding the development of the inhibitors.

In our recent SPECS method, the optimized workflow is able to assess the secretome of primary neurons without interference of serum proteins coming from culturing conditions. This method enabled the discovery of more than 30 substrate candidates that arose upon BACE1 pharmacological inhibition and gave insight of the extent of BACE1's sheddase properties (Kuhn et al., 2012). Evaluating the protease through its substrates gives the opportunity to gain more knowledge of BACE1 and to the end goal to better estimate its therapeutic potential.

In the first part of this thesis the focus was on BACE1 and on validation of the substrates coming from two complementary methods of SPECS and SUSPECS that were used to analyse the secretome and surfaceome of primary cortical neurons, respectively. The second part of the thesis went more in-depth on one of the main BACE1 substrate, the member of the seizure protein family, SEZ6L and to characterize the basic biology of this poorly understood protein.

5.1. BACE1 substrates from SPECS and SUSPECS

5.1.1. Validation of SPECS candidates reveals new BACE1 substrates

The long list of BACE1 substrates and substrate candidates identified with SPECS included proteins with different extents of abundance reduction in the secretome related to BACE1 inactivation (Kuhn et al., 2012). Out of five selected proteins with highest dependence of the BACE1 processing, three of them were validated in the overexpression system of HEK293T cells: CACHD1, GLG1 and LRRN1. When introducing BACE1 in the system, all three proteins showed increase shedding, an effect that for CACHD1 and LRRN1 was possible to block with the BACE inhibitor C3. Besides the SPECS study, CACHD1 and GLG1 were also found in another unbiased proteomic study with overexpression of BACE1 in HEK293 and HeLa cell lines, respectively (Hemming et al., 2009), where the secretion of these two proteins was dependent on BACE1 by more than 80%. Furthermore, SILAC based quantitative proteomics done on the membrane fraction of the BACE1-deficient mice demonstrated a significant increase of CACHD1 and GLG1 (Dislich, 2013). These findings are further confirming the validity of its processing via BACE1.

CACHD1 is a single-pass type I membrane protein that shares structural homology to the members of alpha-2/delta ($\alpha 2\delta$) voltage-gated Ca²⁺ channel auxiliary subunit family. It is widely expressed in the central nervous system, especially in the hippocampus, thalamus and cerebellum (Cottrell et al., 2018). CACHD1 increases the low-voltage-activated (Ca_v3, T-type) calcium channel currents and forms complexes on the cell surface thereby modulating Ca_v3 activity (Cottrell et al., 2018). Besides increasing Ca_v3, it also increases neuronal N-type (Ca_v2.2) channels on the cell surface by reducing endocytosis as well as competing and

inhibiting $\alpha 2\delta$ -1 responses (Dahimene et al., 2018). T-type calcium channels are known to be involved in the pathology of both acquired and genetic epilepsies, but also in acute, inflammatory and chronic pain conditions (Powell et al., 2014; Snutch and Zamponi, 2018). Other members of this family are also accessory subunits of voltage-gated calcium channel subunits influencing the calcium channel function, but are as well involved in other functions, like synaptogenesis. The $\alpha 2\delta$ -2 mutant or deficient mice exhibit spike-wave epilepsy and, in some mouse strains, tonic-clonic seizures (Dolphin, 2012). The link between $\alpha 2\delta$ -2 and epilepsy was identified with spontaneously arising mutant mouse strain Ducky, which shows cerebellar ataxia, absence of epilepsy, and demyelination of the hindbrain and spinal cord, together with the mutation in CACNA2D2. This mutation found in Ducky mice is predicted to express C-terminally truncated protein. Another spontaneous mutation in the same gene where the $\alpha 2\delta$ -2 protein has an intact C-terminus exhibit generalized epilepsy, as does a targeted knockout of CACNA2D2 (Canti et al.; Dolphin, 2013).

BACE1^{-/-} mice were also reported to have spontaneous epileptic seizures, but this phenotype was connected to different channels. In one study, the voltage-gated sodium channels Na_v1.2 subunits were significantly elevated in BACE1^{-/-} mice and suggested to play a role in seizure phenotype (Hu et al., 2010), whereas another study is drawing the attention to yet another culprit, a subtype of potassium channel, KCNQ (Kv7) that is giving rise to the M-current, a potassium current deficient in the BACE1^{-/-} hippocampal neurons (Hessler et al., 2015). On the other hand, increases of N- and T-type calcium channel currents by CACHD1 could potentially also influence seizure phenotype and the effect might be exacerbated upon BACE1 inhibition since CACHD1 would be no longer processed and therefore accumulated in cells. Future studies targeting this point could investigate the role of CACHD1 in relation to BACE1 seizure phenotype and elucidate whether it plays a role with above mentioned ion channels or with additional BACE1 substrates.

While the role of GLG1 is studied in immunity and hematopoietic stem cell proliferation (Leiva et al., 2016), its function in the central nervous system is unknown. Deficiency of GLG1 causes early embryonic lethality in mice (Luo et al., 2012), making it more difficult to study.

On the other hand, LRRN1 is known to be expressed in ventricular layer neuroepithelial cells and is responsible for formation of midbrain-hindbrain boundary in chick (Andreae et al., 2007; Tossell et al., 2011) as for the known roles in the central nervous system. In relation to BACE1, the two above mentioned proteins are unexplored, and it is unclear how the inhibition of the BACE1 and subsequent inhibition of their cleavage would be contributing to the BACE1 related phenotypes.

5.1.2. SUSPECS shows altered neuronal surfaceome upon BACE1 inhibition

The SPECS method enabled the discovery of potential BACE1 substrates in the secretome of primary cortical neurons and put the focus on BACE1 as a major protease, processing most likely more than 30 transmembrane or GPI-anchored proteins (Kuhn et al., 2012). Comparably, the SUSPECS method developed by a colleague and myself, that utilizes the same concept of enriching glycoproteins with metabolic labelling and subsequent click chemistry-mediated biotinylation, provided information how acute BACE1 inhibition is influencing the neuronal surface proteome (Herber et al., 2018). The SUSPECS method is specific for the surface proteins, as demonstrated using different cellular markers. When comparing the total fraction of neuronal lysates with the SUSPECS containing fraction, the

known surface proteins NEO1, GluR2, MT4MMP and RGMa were enriched in the SUSPECS fraction relative to the total lysates. Conversely, proteins originating from intracellular compartments were largely depleted and were found with higher abundance in total lysates. SUSPECS method is easy and fast to carry out and is compatible with SPECS method so that in the same experiment both secretome and surfaceome could be analysed, therefore providing valuable information of the differences between the two compartments. Furthermore, physiological culturing condition can be used with the presence of serum or supplement, since the high abundance proteins from serum are not interfering with the mass spectrometric analysis of SUSPECS. On the other hand, the main disadvantage of SUSPECS is that the specific labelling of glycosylated proteins excludes non-glycosylated ones which leads to a loss of additional information of status on the surface. Nevertheless, a large fraction of membrane proteins are glycosylated (Herber et al., 2018). Additionally, SUSPECS is not suitable for freshly prepared cells or tissues that are not cultured.

In this thesis, we analysed changes on the surface using SUSPECS upon pharmacological inhibition of BACE1 (Herber et al., 2018). We identified 106 proteins that significantly changed its abundance on the neuronal surface upon inhibition of BACE1 (Herber et al., 2018). Most of the altered proteins were accumulated (100 proteins), either mild, intermediate, or some of the proteins even showed strong accumulation, from 2-fold, up to more than 7-fold increase. Such large changes may affect cell-cell interactions and their communication via surface proteins and receptors. Among the proteins found to be altered upon inhibition are already known BACE1 substrates found with SPECS as well, like strongly accumulated APLP1, SEZ6 and SEZ6L, and therefore validating the method itself (Li and Sudhof, 2004; Pignoni et al., 2016). These changes were further confirmed in an independent set of experiments analysing SUSPECS enriched protein fractions of neurons via Western blot both *in vitro* and *in vivo*. These experiments validated the accumulation of APLP1, SEZ6 and SEZ6L on the cell surface and showed similar fold changes as already detected by mass spectrometry analysis.

Additionally, TSPAN6 and DNER were found enriched using the SUSPECS methods with intermediate or mild accumulation, respectively and further validated with immunoblotting. TSPAN6 was not identified as secreted protein using SPECS. It is a multi-pass protein which makes it less likely to be cleaved by BACE1. The protein DNER, was identified in the SPECS study, but could not be validated in overexpressing conditions. These results suggest that BACE1 inhibition does not only alter cell surface levels of some of its substrates, but also leads to secondary effects which affect the cell surface proteome of neurons. Therefore, BACE1 inhibition might have more consequences than expected.

Previously validated BACE1 substrates in the overexpression condition, CACHD1 and GLG1 were both identified in the SUSPECS mass spectrometry analysis with at least 2 unique peptides and quantified in at least 3 out of 12 experiments (6 inhibitor and 6 vehicle treated). While CACHD1 was not quantified in enough experiments to perform a statistical analysis, GLG1 was further analysed but did not show any significant change upon the treatment.

Some of the substrates such as APLP1, SEZ6 and SEZ6L showed high accumulation of the full-length protein on the surface upon BACE1 inhibition in the SUSPECS study and consequently, high reduction of the cleaved ectodomain in the media as observed in SPECS study. These results demonstrate high correlation of the above mentioned substrates in the two compartments of the two studies. However, not all proteins showed the same consequent correlation. CACHD1 and GLG1 that both had a strong decrease of the shed ectodomain in SPECS study did not show a change on the surface as seen with SUSPECS study. This

discrepancy in correlation might be due to different molecular mechanisms, e.g. if only a minor portion of the protein is processed, the complete blockage of the cleavage would affect levels in the secretome, but no significant change in the surfaceome. Alternatively, some substrates may not be transported when they are not shed and could be even degraded, again showing no change at the surface levels. Additionally, it can be arguable that proteins with a long half-life may show higher accumulation upon BACE1 inhibition than the proteins with shorter half-life. While this may be true for APLP1 due to its slower endocytosis rate (Schilling et al., 2017), in the case of APP that is known to be degraded in less than 45 minutes (Gersbacher et al., 2013; Weidemann et al., 1989) the continuous labelling with click sugars is efficiently detecting its accumulation.

Another phenotype observed in BACE1^{-/-} mice is the reduced spine density in hippocampal pyramidal neurons (Savonenko et al., 2008). Furthermore, an *in vivo* study using wild-type mice treated with BACE1 inhibitor caused reversible reduction of the total spine density in cortical layer V pyramidal neurons (Zhu et al., 2018b). The same study used SEZ6^{-/-} mice treated with the inhibitor and the total spine density was not affected. These results suggested that SEZ6 is involved in dendritic spine alterations through BACE1 inhibition, but is also needed for maintaining normal dendritic spine dynamics (Zhu et al., 2018b). Additionally, loss of APLP1 was as well found to cause reduced spine density in aged mice and was shown that APLP1 has strong trans-dimerization properties, more prominent cell surface localization and a slower endocytosis rate than its family members APP or APLP2 (Muller et al., 2017; Schilling et al., 2017). The slower internalization might affect its processing by BACE1 as BACE1 was shown to predominantly cleave in the pH optimal endosomes (Vassar et al., 1999). On the other hand, slow endocytosis rate might also influence the accumulation of APLP1 if other degradation related processes are not compensating for APLP1 clearance. Moreover, APLP1 together with the other APP family members has the capacity to induce presynaptic differentiation via trans-synaptic signalling (Muller et al., 2017; Schilling et al., 2017). Taken together, BACE1 inhibition and the subsequent increase in surface levels of SEZ6 and APLP1 or potentially other changed proteins may interfere with synapse formation and maintenance, like is observed in BACE1^{-/-} mice.

Conclusively, SPECS and SUSPECS are valuable methods for enriching glycoproteins both in the secretome and surfaceome. Both methods can be used within the same experiment and have the great advantage to be compatible with cells cultured in the presence of serum or other protein containing supplements. These two methods enabled the extensive analyses of the broad range of change related to BACE1 inhibition in primary neurons in the above mentioned compartments. Additionally, validation of these changes in different cells and tissue confirmed the method and revealed new BACE1 substrates and substrate candidates. The alterations that are happening as a consequence of BACE1 inhibition might also influence the extent of the unwanted mechanism based-side effects and should be taken into consideration when conducting clinical trials, but also to further unravel the basic biology of BACE1.

5.2. Seizure 6-like protein

Initially, SEZ6L was first revealed as one of the major BACE1 substrate in primary cortical neurons using the SPECS methods with its ectodomain largely abolished upon BACE1 inhibition (Kuhn et al., 2012). This finding was further confirmed in the BACE1^{-/-} mice. The SEZ6L ectodomain was also found to be strongly reduced in the CSF of BACE1^{-/-} mice, suggesting it might serve as a potential biomarker to monitor BACE1 activity (Pigoni et al.,

2016). Here, we found it to be upregulated on the surface upon BACE1 inhibition using SUSPECS method (Herber et al., 2018). Altogether, it is evident that this protein is processed by BACE1. However, to which extent its function is dependent on BACE1 and possibly contributing to known BACE1 phenotypes or whether its basic biology is pointing to other functions unrelated of BACE1 is to date unknown.

5.2.1. SEZ6L^{-/-} mice have a motor phenotype

Behavioural analyses of the SEZ6L^{-/-} mice showed locomotor deficits as determined in this thesis. In the rotarod tests, there were considerable differences between the genders. Over the course of the experiment, female SEZ6L^{-/-} mice performed poorly and failed to achieve the same degree of motor improvement compared to female WT and SEZ6L^{+/-} mice. On the other hand, the differences between male mice were not as striking. Only subtle changes were observed between SEZ6L^{-/-} and SEZ6L^{+/-} mice in later trials. Apart from one trial in males, no differences were seen between WT and SEZ6L^{+/-} mice.

Besides the SEZ6L^{-/-} females that had poor performance in the rotarod tests, female mice were able to stay on the accelerating rod for extended period of time and therefore were generally performing better than male ones. The enhanced performance of the female mice and their longer latency to fall was already seen in previous studies and not obviously correlating with weight differences (Ashworth et al., 2015; Bothe et al., 2004). The triple knockout of all members of the seizure family failed to remain on the rotating rod using fixed speed of 16 rpm with the single SEZ6L^{-/-} mice having a mild impairment (Miyazaki et al., 2006). However, the data for the single SEZ6L^{-/-} were not shown in this study as well as the distribution of genders.

The differences in gender observed in the SEZ6L^{-/-} mice may come from the lack of the SEZ6L itself. On the other hand, it may as well be due to overall higher performance of the female mice. If the rotarod parameters are more suitable to the female mice that showed good improvement by the end of the 15th trial, then it might be challenging to observe any subtle differences in the male mice as their general performance did not ameliorate greatly over the course of the experiment.

Further motor coordination analysis using DigiGait system showed altered gait patterns of the SEZ6L^{-/-} compared to WT and SEZ6L^{+/-} mice. Very few differences arose from the gender and therefore the analysis was done combining both genders. The stride length of the mice described as “the distance between successive footfalls of the same hindpaw” (Hannigan and Riley, 1988) is longer for the SEZ6L^{-/-} mice compared to WT and SEZ6L^{+/-} mice. In line with this result, the duration of one complete stride for the paw or stride time is longer and therefore the SEZ6L^{-/-} mice have lower stride frequency, meaning that they take fewer strides to cover a given distance. The observed phenotype is more pronounced at the higher speed of the treadmill. Another gait pattern was seen changing in the SEZ6L^{-/-} mice, swing time. It is defined as the duration of the swing phase when the paw is in no contact with the belt. At both measured speed settings, hindlimbs of the SEZ6L^{-/-} mice had significantly longer swing time.

The observed gait parameters that were changing in the SEZ6L^{-/-} mice are related to one another and could be interpreted as rather enhanced motor abilities. One possible explanation might be that the SEZ6L^{-/-} mice have a beneficial motor adaptation due to the lack of SEZ6L. This is supported with the observed gait differences, especially with the increased stride length of the SEZ6L^{-/-} mice that in the known mouse models with motor deficits is rather

decreased. This is true for the mice bearing different syndromes or diseases that affect coordination including Parkinson's disease mouse model (Amende et al., 2005), inflammatory murine arthritis (Williams et al., 1993), Rett syndrome (Gadalla et al., 2014) and aged 5xFAD mouse model of AD (O'Leary et al., 2018).

The data from the rotarod analysis suggest that the mice have cerebellar changes which affect coordination and would be detrimental for the animal. There are examples of different gene mutants that have altered stride distance just like the SEZ6L^{-/-} mice. One of them is the Niemann-Pick disease, type C1, an autosomal recessive lysosomal storage disorder caused by a loss-of-function in NPC1. These patients exhibit neurological and psychiatric symptoms, including loss of motor coordination and dementia (Vanier, 2010). The disease has a lot of similarities to AD and therefore is often termed as "juvenile Alzheimer's disease" (Nixon, 2004). The NPC1^{-/-} model for this disease die between 10-14 weeks of age and have many abnormalities including locomotor dysfunctions. Behavioral analyses of NPC1^{-/-} mice demonstrated poorer rotarod performance that worsened with age and mice could not perform the DigiGait analysis. Gait patterns of the heterozygous mice on the other hand showed longer stride length and duration with followed decrease in the stride frequency, similarly to the SEZ6L^{-/-}. Since the NPC1 phenotype includes ataxia, results were quite surprising and opposite of expected. The proposed explanation was that mice failed to adjust their gait to the forced locomotion imposed by the treadmill, unlike the WT that shortened their stride length as an adaptation to the given speed (Hung et al., 2016). Another example of increased stride length and enhanced motor phenotype is seen in the 6-month-old 3×Tg AD mouse model that has a complex behavior showing both enhanced and worsened performance between different behavioral tests (Stover et al., 2015). Anatomy is also playing a role in gait analyses, mice with longer limbs – Longshanks mice – take also longer and fewer strides (Sparrow et al., 2017). Additional example of elongated strides is a protein highly expressed in Purkinje cells, Nedd4. Heterozygous Nedd4 showed increased stride time and decreased stride frequency, and explanation for the observed gait alterations might come from the increased activity of inhibitory Purkinje neurons in mutant cerebellum (Camera et al., 2014).

Likewise, detailed behavioral tests have been performed on BACE1^{-/-} mice as well as the BACE inhibitor treated WT mice (Cheret et al., 2013). Both mutant and inhibitor treated mice had disrupted motor coordination. The mice were unable to hang to an inverted grid, unlike SEZ6L^{-/-} that performed the same as WT mice. Furthermore, gait analysis was assessed using different setup – Treadscan system – that showed severely affected homolateral coupling of both mutant and inhibitor treated mice. The mice had swaying walking pattern reflected with a lack of forelimb/hindlimb coordination. Homologue coupling was slightly disturbed in mutant mice and the results were in line with inhibitor treated mice. This phenotype of motor coordination was connected to the muscle spindle formation that is reduced due to the lack of processing of another BACE1 substrate, Neuregulin-1 (Cheret et al., 2013). SEZ6L^{-/-} mice on the other hand, show alterations in different gait indices that are not comparable to BACE1^{-/-} mice and do not exhibit the same neuromuscular deficits, suggesting that the phenotype might not come from the lack of processing of SEZ6L and thus reduction of cleaved ectodomain. Alternatively, if the function of SEZ6L is exerted through the full-length SEZ6L rather than its ectodomain, then the SEZ6L^{-/-} mice would not necessarily phenocopy the function.

The phenotype observed in the SEZ6L^{-/-} mice might be not as pronounced if the other members of the family are compensating and sharing the functions, therefore ameliorating the effect that would otherwise be more detrimental for the animal. The described TKO mice lacking all three members of the family, were shown to have rotarod and fixed bar deficits (Miyazaki et al., 2006), but more detailed behavioural analyses was to date not carried out. It

was previously shown that other multiple knockouts from the same family members are performing worse than the respective single knockouts. This is true for the example of the APP family members, where single knockout subtle phenotypes are exacerbated in the multiple knockouts, where the double knockout mice carrying APLP2/APLP1 and APLP2/APP-deficiencies or even the triple knockout of APP/APLP1/APLP2 proved lethal shortly after birth (Muller and Zheng, 2012).

In conclusion, SEZ6L^{-/-} mice exhibit abnormalities in the motor coordination assessed through rotarod and DigiGait analyses. Female SEZ6L^{-/-} mice are unable to improve on the rotating rod, while changes in the male SEZ6L^{-/-} mice are just a few. Gait analysis revealed enhanced motor phenotype, since the mice show longer strides and lower stride frequency. Combined, these changes might come from the alterations in the proteome that is misbalanced due to the lack of SEZ6L. These phenotypes are suggesting a role of SEZ6L in cerebellum related motor coordination of mice and are presumably independent of BACE1 activity.

5.2.2. SEZ6L^{-/-} cerebellum has an altered proteome

To assess the underlying alterations in proteome of SEZ6L^{-/-} mice an extensive analysis of the deficient cerebella was performed. Different age was used according to the expression of the SEZ6L that is increasing postnatally, reaching its peak at fourth week and afterwards declining by the eighth week of age (Miyazaki et al., 2006). Although the increase in postnatal expression may point towards developmental function of SEZ6L in the cerebellum, proteomic analysis of both total and membrane proteome of young mice did not show major changes. Additional analyses of membrane proteome of young mice revealed more than 30 proteins accumulating only in the SEZ6L^{-/-} conditions, being below detection limit in the WT conditions and therefore not subjected to statistical analysis. On the other hand, adult membrane preparation gave more significant changes related to the loss of SEZ6L, mostly observing downregulation of proteins. The most prominent one was hnRNPA3, showing 83% reduction in the cerebellum of SEZ6L^{-/-} mice. Two other members of the family were also reduced, but to a lesser extent and did not reach significance after multiple hypothesis correction: hnRNPA1, with 74% and hnRNPLL with 66% reduction. These RNA-binding proteins are known to be involved in amyotrophic lateral sclerosis (ALS) and related diseases such as frontotemporal dementia (FTD) (Purice and Taylor, 2018). Additionally, they are regulating differentiation of lymphocytes and metastasis of colorectal cancer cells as in the case of hnRNPLL (Oberdoerffer et al., 2008; Sakuma et al., 2018). However, their function in cerebellum is still largely unexplored and is unclear how SEZ6L would influence the reduction of their abundance in the cerebellum.

Among other downregulated proteins, CaMKIV was more than 50% reduced. This Ca²⁺-dependent protein kinase is abundant in the nucleus where it phosphorylates the transcription factor cAMP response element binding protein (CREB) during synaptic stimulation and activating memory-related transcriptional activity of many downstream genes (Takemoto-Kimura et al., 2017). Lack of CaMKIV in mice impaired CREB phosphorylation, long-term potentiation in hippocampal CA1 neurons and a late phase of long-term depression in cerebellar Purkinje neurons (Ho et al., 2000). Furthermore, the null mice had locomotor defects and immature development of Purkinje neurons, suggesting its role in the function and development of the cerebellum (Ribar et al., 2000). SEZ6L locomotor phenotype might at least partial come from the downregulated CaMKIV and thus have a role in the function of the cerebellum. Being identified as a substrate of γ -secretase as well (Stutzer et al., 2013) SEZ6L's intracellular domain might enter nucleus and thus alter nuclear signalling by

affecting CaMKIV. However, to date is not known whether the SEZ6L mice have also immature development of Purkinje cells, or impaired CREB phosphorylation as seen in the CaMKIV^{-/-} mice.

Additional downregulated protein emerging from the adult proteomic analysis is the KH domain-containing, RNA-binding, signal transduction-associated protein 1 (KHDRBS1), and is another RNA-binding protein whose null mice have motor coordination defects as assessed by beam walking and rotarod performance (Lukong and Richard, 2008). This protein was found as well in the young cerebellar proteome. However, the effect was opposite, being accumulated only in the SEZ6L conditions, and below the detection limit in the WT. This discrepancy in results between different ages makes unclear whether the motor discoordination that we observe in the SEZ6L^{-/-} mice could come from the downregulated KHDRBS1 in the adult mice. Alternatively, the protein might have different function during development or the mechanism might be more general including combination of alteration of different proteins, including CaMKIV and is subject for further research.

Intracellular Ca²⁺ levels are needed for complex signalling roles in the brain and are regulating neuronal plasticity involved in learning, memory and neuronal survival. It is regulated among others by Ca²⁺-binding proteins and its dysregulation is central to the neurodegenerative process (Zundorf and Reiser, 2011). It was previously shown that knockdown of members of the seizure-related gene 6 family, including SEZ6L, is decreasing Ca²⁺ signals and altering neuronal network activity (Anderson et al., 2012). In SEZ6L cerebellar proteomic analysis there were other Ca²⁺-binding or dependent proteins besides CaMKIV altered, such as downregulated CaMKII β and Cab39, or upregulated S100B. Therefore, altered Ca²⁺-binding proteins in SEZ6L^{-/-} cerebellum may contribute to the explanation of the behavioural analyses and additional reported altered neuronal network activity in the SEZ6L knocked-down cortical neurons may point to other phenotypes of SEZ6L. Furthermore, it was reported that AD and frontotemporal lobe dementia patients have significantly increased S100B levels. Noteworthy, there is a connection between S100B and A β expression as well as the inflammation in the brain which affects S100B expression (Yardan et al., 2011). However, S100B-deficient mice have normal cerebellar development (Bluhm et al., 2015). Additionally, there is no indication that SEZ6L^{-/-} mice show increased inflammation making it unclear whether the two proteins have a common mechanism of action.

Another protein that emerged from the study being upregulated in the adult deficient brain was Noelin (OLFM1). OLFM1 is a secreted glycoprotein involved in the generation of the neural crest (Barembaum et al., 2000), promotes neurogenesis in *Xenopus* (Moreno and Bronner-Fraser, 2001), modulates Wnt signalling, plays a role in optic nerve extension, and retinal ganglion axon branching (Nakaya et al., 2008), and interacts with Nogo A receptor complex regulating axonal growth (Nakaya et al., 2012). OLFM1 mutant mice show reduced brain size, deficits in behavioural tests, olfactory activity and functions associated with Ca²⁺ signalling. The mice exhibit abnormal anxiety behaviour and social activity, but also motor activity as shown by reduced latency on balance beam tests (Nakaya et al., 2013). OLFM1 was also shown to modulate cortical cell migration and effect cleavage of endogenous APP, more specifically to reduce the level of sAPP β , while having no effect on sAPP α (Rice et al., 2012; Rice et al., 2013). Moreover, in zebrafish with null mutation in *olfm1a* and *olfm1b* genes, OLFM1 is interacting with AMPA receptors (AMPA) and pre-synaptic soluble NSF attachment protein receptor (SNARE) complex proteins. Knocking-down both OLFM1 genes in zebrafish modified internalization of GluR2 in cultured neurons as well as the composition of lipid raft proteins (Nakaya et al., 2017). Furthermore, OLFM1 is affecting synaptic

AMPA mobility and the reduction in AMPAR lateral mobility is limiting synaptic plasticity (Pandya et al., 2018). OLFM1 functions in the cerebellum are not well studied, its high affinity to AMPAR complex and its effect on AMPAR mobility points towards a general function and role in synaptic plasticity. Increased levels of OLFM1 in the SEZ6L^{-/-} brains might influence this interaction and mobility and possibly have an effect on other important functions of AMPAR in the central nervous system, such as excitatory neurotransmission, synaptic plasticity or development (Henley and Wilkinson, 2016). Furthermore, SEZ6L shares 30% of its sequence identity with its family members, SEZ6 and SEZ6L2, as well as the protein-protein interaction domains, making it possible that the functions of this family are overlapping. Recently proposed function of SEZ6L2 as a critical modulator of AMPAR function through its interactions with adducin and glutamate receptor 1 (Yaguchi et al., 2017) could suggest the possible involvement of SEZ6L in AMPAR function as well, perhaps through exactly OLFM1.

One of the most upregulated proteins in the young cerebellum was the neurodevelopmental disorder risk factor gene *Syngap1* (+2.54-fold, Fig. 15) (Kilinc et al., 2018). *Syngap1* is a protein involved in regulation of the synaptic plasticity and neuronal homeostasis through negative regulation of Ras, Rap and AMPAR trafficking to the postsynaptic membrane. It was established as a major signaling protein by playing an important role in dendritic spine morphology. Heterozygous mice (*Syngap1*^{+/-}) show a lack of inhibition of Ras-GTPase, increase in mushroom-shaped dendritic spines and more AMPAR transport to the postsynaptic membrane. Moreover, those mice show a disruption of neuronal growth and maturation leading to neurodevelopmental disorders (Jeyabalan and Clement, 2016). Young SEZ6L^{-/-} mice might as well have neurodevelopmental changes that involve increased *Syngap1* among other proteins. However, no abundance changes were detected in cerebella of the adult mice.

Nevertheless, differences observed in young and adult mice might come from the different temporal and spatial expression of proteins that exert different functions in the development of the mice compared to adult ones. *hnRNPLL* for example is upregulated in the young SEZ6L^{-/-} mice, while it is downregulated by the adulthood. It was reported that different members of the heterogeneous nuclear ribonucleoproteins family are partially up- and downregulated at P90 in rats, compared to P7 and is even further changing in later stages (P637) (Wille et al., 2015). The same could be true for other distinctly altered proteins in SEZ6L cerebellum. Thus, the differences that we observe in SEZ6L^{-/-} mice at different stages might come from the function of specific proteins that are influenced by SEZ6L, and which are more prominent in adulthood compared to young mice.

In conclusion, cerebellum proteomics reveals changes occurring in the absence of the SEZ6L protein, with different proteins being up- or down-regulated that are involved in calcium signalling, neurodegeneration, development of the cerebellum and synaptic plasticity.

5.2.3. SEZ6L interaction partners reveal potential role in immunity

To better understand the role of SEZ6L in the brain an interactome analysis was performed revealing a dozen of proteins as SEZ6L interactor candidates, with most of them being different immunoglobulin chains, pointing to the possible contamination. However, additional two proteins, Complement C3 (C3) and High affinity immunoglobulin gamma Fc receptor I (Fcgr1), were identified being quantified in one or none of the SEZ6L^{-/-} biological replicates suggesting its specific interaction only in the WT conditions.

Complement is important part of innate immunity and functions to protect against infections and disposal of the tissue waste in the periphery, while it also contributes to maintenance and homeostasis of synapses in the brain (Morgan, 2018). In the healthy brain during development, C3 is activated by another complement protein, C1q that leads to opsonisation of synapses causing its elimination. This process is however, downregulated in the mature brain (Schafer et al., 2012; Stevens et al., 2007). Genome-wide association studies have revealed mutations in microglia-specific and immune-related genes as risk factors of AD, which also includes the component protein C3 (Hong et al., 2016b). Furthermore, the temporal cortex of AD brains contains 3-fold more C3 expression than the controls implying the importance of the complements in AD (Walker and McGeer, 1992). Moreover, studies with complement and microglia showed that complement-dependent pathways are mediating synaptic loss early in AD (Hong et al., 2016a). Additional studies in mice showed discrepancies between different AD models, in APP/PS1 mice, C3^{-/-} was shown to be neuroprotective, while in other APP transgenic AD mouse models neurodegenerative. C3^{-/-} was also associated with increased amyloid burden (Nizami et al., 2019).

Although the interaction between C3 and SEZ6L could not be validated with an additional method, SEZ6L contains in its extracellular part 1 CUB and 2 Ca²⁺-binding CUB domain, known to be involved in protein-protein interaction and thereby exerting a wide range of functions including complement activation (Gaboriaud et al., 2011; Major et al., 2010). Proteins with CUB or SCR domains frequently appear in components of the complement system, regulating neurotransmitter receptors and many of them are involved in the development and function of neural circuits (Nakayama and Hama, 2011). It has been suggested that some of the CUB and SCR domain-containing proteins because of their complement-related motifs may have been evolutionary conserved and first employed during neural differentiation, since there is no complement system found in protostomes (Nakayama and Hama, 2011). SEZ6L interaction with C3 may happen through the CUB and SCR domain, however, whether is stable or transient and if the complement-dependending pathway can be altered via SEZ6L or perhaps if SEZ6L is involved in function of neural circuits through its domains, and thus connected to AD, is yet subject for further research.

The protein Fcgr1 is also important in immunity and involved in antibody-dependent cellular cytotoxicity and clearance of immune complexes via internalization. It binds with high affinity the monomeric IgG making it a target for development of therapeutics for antibody-mediated autoimmune diseases (Akinrinmade et al., 2017). In a recent study, AD brain microglia was immunophenotyped revealing that Fcgr1 expression is positively correlated with the presence of dementia (Minett et al., 2016).

In conclusion, these two promising SEZ6L interactor candidates play a role in immunity and are involved or associated with AD, therefore suggesting an additional role of SEZ6L in AD besides being a substrate of BACE1. Together with the other results, SEZ6L presumably have a role in the function of the cerebellum through altering calcium signalling, and by affecting proteins involved in synaptic plasticity and the development of the cerebellum.

6. CONCLUSION

BACE1 is one of the most important drug targets in Alzheimer's disease. It is the central enzyme in the molecular pathology of the disease as it cleaves APP and together with γ -secretase produces A β peptides. Many efforts are being made to inhibit BACE1 and limit the production of A β in order to ameliorate the course of the disease. Recent failures in drug development that ended some of the clinical trials revealed worsening of cognitive symptoms (Das and Yan, 2019), putting even more importance on research of underlying mechanism-based side effects and the value of this thesis.

This thesis focus was on identifying, validating and investigating the function of BACE1 substrates and substrate candidates. In the first part of the thesis three additional BACE1 substrates were confirmed *in vitro* and further analysis were done on the neuronal surface. Using newly established SUSPECS method of enriching the surface proteins BACE1 inhibition in neurons demonstrated major changes, pointing again to the on-target effects as well as the secondary effects that the drug might have in patients. Additionally, this thesis contributed to the basic biology of SEZ6L, protein that is mainly cleaved by BACE1.

1. Validation of novel substrate candidates of BACE1

Three different BACE1 substrate candidates were identified previously in proteomic screenings: CACHD1, LRRN1 and GLG1. CACHD1 and GLG1 were identified in large proteomic screening with BACE1 overexpression in non-neuronal cell lines. However, the more physiological approach using BACE1 inhibition of primary neurons and analysing the secretome using the SPECS methods also identified these two proteins as potential BACE1 substrates. Additionally, LRRN1 was found to be significantly reduced in SPECS study, rendering this protein a potential BACE1 substrate. Here, these three BACE1 substrate candidates were validated with an independent method, using the overexpression system of HEK293T cells. These experiments provide further evidence that CACHD1, LRRN1 and GLG1 are indeed substrates of BACE1.

2. Pharmacological inhibition of BACE1 on the neuronal surface

Complementary to the SPECS method, a Surface Spanning Protein Enrichment with Click Sugars (SUSPECS) method was established by enriching the glycoproteome of the cell surface via click-chemistry mediated biotinylation. N-azido modified sugars were added to cells, incorporated in the newly synthesized glycoproteins and subsequently the click reaction was performed on the living cell thereby specifically labelling only the cell surface compartment enabling streptavidin enrichment. This approach was used to investigate the neuronal surface proteome composition in response to pharmacological BACE1 inhibition. The major changes were validated utilizing an independent set of biological samples both *in vitro* and *in vivo*. Overall, mostly accumulations of proteins were observed, with a strong enrichment of previously established BACE1 substrates, including APLP1, SEZ6 and SEZ6L. Validation of abundance changes of these proteins confirmed not only the results of this novel proteomic method, but also showed very similar fold changes on the surface as a consequence of BACE1 inhibition. Therefore, SUSPECS is a suitable method to investigate the cell surface proteome. Noteworthy, BACE1 does not control the cell surface levels of all of its substrates as previously assumed, but rather regulated only a subset of them, including SEZ6, SEZ6L and APLP1. Moreover, secondary effects of BACE1 inhibition leading to accumulation of proteins such as TSPAN6 and DNER could be demonstrated.

3. Analyses of SEZ6L^{-/-} mice

SEZ6L was initially discovered as a BACE1 substrate in the SPECS study showing that the shed ectodomain is greatly abolished in the secretome upon BACE1 inhibition. Here, we additionally showed with SUSPECS that SEZ6L accumulates on the neuronal surface. As a substrate that is cleaved mostly only by BACE1, this protein was studied more in-depth to investigate its functions and possibly connect the phenotype back to BACE1. To investigate its function, an extensive behavioural analysis was performed showing motor discoordination in the SEZ6L^{-/-} mice. Mice displayed poor performance on the rotarod and abnormalities in DigiGait analysis due to loss of SEZ6L. Furthermore, proteomic analyses of the cerebella deficient for SEZ6L revealed downregulation of proteins involved in neurodegeneration, cerebellar development and synaptic plasticity. Moreover, interactomic study identified novel interaction partner candidates, Complement C3 and Fcgr1. These two proteins play a role in immunity and are involved or associated with AD. None of the observed phenotypes could be directly linked to BACE1. However, interaction with C3 may point to different roles of SEZ6L related to AD, besides being processed by BACE1, as it was suggested that the complement-dependent pathway together with microglia have improper activation and are mediating early synapse loss in AD before the plaque formation occurs (Hong et al., 2016a). Follow-up studies on SEZ6L and C3 could deepen our understanding of this interaction and conclude whether it may have implications in AD.

Taken together, this study represents the first analysis of the SEZ6L^{-/-} mice. Additionally, it provides important insights on the extent of changes in surface protein levels upon BACE1 inhibition. The altered substrates of BACE1 may exert functions that would potentially interfere with the homeostasis of the brain when patients are treated with inhibitors. These implications should be carefully considered for BACE inhibitor treatment strategies. Instead of a complete BACE1 inhibition, a safe therapeutic window should be evaluated to efficiently reduce A β generation, but also minimize side effects. In this context, investigating the functions of BACE1 substrates also leads to better understanding of this enzyme and evaluates its therapeutic potential.

7. LITERATURE

- Abramov, E., Dolev, I., Fogel, H., Ciccotosto, G.D., Ruff, E., and Slutsky, I. (2009). Amyloid-beta as a positive endogenous regulator of release probability at hippocampal synapses. *Nat Neurosci* *12*, 1567-1576.
- Akinrinmade, O.A., Chetty, S., Daramola, A.K., Islam, M.U., Thepen, T., and Barth, S. (2017). CD64: An Attractive Immunotherapeutic Target for M1-type Macrophage Mediated Chronic Inflammatory Diseases. *Biomedicines* *5*.
- Alzheimer, A. (1907). Über eine eigenartige Erkrankung der Hirnrinde. *Allgemeine Zeitschrift für Psychiatrie und Psychisch-gerichtliche Medizin* *Jan*, 146-148.
- Alzheimer, A., Stelzmann, R.A., Schnitzlein, H.N., and Murtagh, F.R. (1995). An English translation of Alzheimer's 1907 paper, "Über eine eigenartige Erkrankung der Hirnrinde". *Clinical anatomy* (New York, NY) *8*, 429-431.
- Alzheimer's Association (2016). 2016 Alzheimer's disease facts and figures. *Alzheimer's & dementia : the journal of the Alzheimer's Association* *12*, 459-509.
- Ambalavanan, A., Girard, S.L., Ahn, K., Zhou, S., Dionne-Laporte, A., Spiegelman, D., Bourassa, C.V., Gauthier, J., Hamdan, F.F., Xiong, L., *et al.* (2016). De novo variants in sporadic cases of childhood onset schizophrenia. *Eur J Hum Genet* *24*, 944-948.
- Amende, I., Kale, A., McCue, S., Glazier, S., Morgan, J.P., and Hampton, T.G. (2005). Gait dynamics in mouse models of Parkinson's disease and Huntington's disease. *Journal of neuroengineering and rehabilitation* *2*, 20.
- Anderson, G.R., Galfin, T., Xu, W., Aoto, J., Malenka, R.C., and Sudhof, T.C. (2012). Candidate autism gene screen identifies critical role for cell-adhesion molecule CASPR2 in dendritic arborization and spine development. *Proc Natl Acad Sci U S A* *109*, 18120-18125.
- Andrae, L.C., Peukert, D., Lumsden, A., and Gilthorpe, J.D. (2007). Analysis of *Lrrn1* expression and its relationship to neuromeric boundaries during chick neural development. *Neural Dev* *22*, 22.
- Andrechek, E.R., Hardy, W.R., Girgis-Gabardo, A.A., Perry, R.L., Butler, R., Graham, F.L., Kahn, R.C., Rudnicki, M.A., and Muller, W.J. (2002). ErbB2 is required for muscle spindle and myoblast cell survival. *Mol Cell Biol* *22*, 4714-4722.
- Arndt, J.W., Qian, F., Smith, B.A., Quan, C., Kilambi, K.P., Bush, M.W., Walz, T., Pepinsky, R.B., Bussiere, T., Hamann, S., *et al.* (2018). Structural and kinetic basis for the selectivity of aducanumab for aggregated forms of amyloid-beta. *Sci Rep* *8*, 6412.
- Ashworth, A., Bardgett, M.E., Fowler, J., Garber, H., Griffith, M., and Curran, C.P. (2015). Comparison of Neurological Function in Males and Females from Two Substrains of C57BL/6 Mice. *Toxics* *3*, 1-17.
- Bang, M.L., and Owczarek, S. (2013). A matter of balance: role of neurexin and neuroligin at the synapse. *Neurochemical research* *38*, 1174-1189.
- Barembaum, M., Moreno, T.A., LaBonne, C., Sechrist, J., and Bronner-Fraser, M. (2000). Noelin-1 is a secreted glycoprotein involved in generation of the neural crest. *Nat Cell Biol* *2*, 219-225.
- Basi, G., Frigon, N., Barbour, R., Doan, T., Gordon, G., McConlogue, L., Sinha, S., and Zeller, M. (2003). Antagonistic effects of beta-site amyloid precursor protein-cleaving enzymes 1 and 2 on beta-amyloid peptide production in cells. *J Biol Chem* *278*, 31512-31520.
- Bateman, R.J., Xiong, C., Benzinger, T.L., Fagan, A.M., Goate, A., Fox, N.C., Marcus, D.S., Cairns, N.J., Xie, X., Blazey, T.M., *et al.* (2012). Clinical and biomarker changes in dominantly inherited Alzheimer's disease. *N Engl J Med* *367*, 795-804.
- Benjannet, S., Elagoz, A., Wickham, L., Mamarbachi, M., Munzer, J.S., Basak, A., Lazure, C., Cromlish, J.A., Sisodia, S., Checler, F., *et al.* (2001). Post-translational processing of beta-secretase (beta-amyloid-converting enzyme) and its ectodomain shedding. The pro- and transmembrane/cytosolic domains affect its cellular activity and amyloid-beta production. *J Biol Chem* *276*, 10879-10887.

- Bennett, B.D., Babu-Khan, S., Loeloff, R., Louis, J.C., Curran, E., Citron, M., and Vassar, R. (2000a). Expression analysis of BACE2 in brain and peripheral tissues. *J Biol Chem* 275, 20647-20651.
- Bennett, B.D., Denis, P., Haniu, M., Teplow, D.B., Kahn, S., Louis, J.C., Citron, M., and Vassar, R. (2000b). A furin-like convertase mediates propeptide cleavage of BACE, the Alzheimer's beta -secretase. *J Biol Chem* 275, 37712-37717.
- Beyreuther, K., and Masters, C.L. (1991). Amyloid precursor protein (APP) and beta A4 amyloid in the etiology of Alzheimer's disease: precursor-product relationships in the derangement of neuronal function. *Brain pathology (Zurich, Switzerland)* 1, 241-251.
- Blattmann, P., Schuberth, C., Pepperkok, R., and Runz, H. (2013). RNAi-based functional profiling of loci from blood lipid genome-wide association studies identifies genes with cholesterol-regulatory function. *PLoS Genet* 9, e1003338.
- Blennow, K., Hampel, H., Weiner, M., and Zetterberg, H. (2010). Cerebrospinal fluid and plasma biomarkers in Alzheimer disease. *Nature reviews Neurology* 6, 131-144.
- Blessed, G., Tomlinson, B.E., and Roth, M. (1968). The association between quantitative measures of dementia and of senile change in the cerebral grey matter of elderly subjects. *The British journal of psychiatry : the journal of mental science* 114, 797-811.
- Bluhm, B., Laffer, B., Hirnet, D., Rothermundt, M., Ambree, O., and Lohr, C. (2015). Normal cerebellar development in S100B-deficient mice. *Cerebellum* 14, 119-127.
- Bolduc, D.M., Montagna, D.R., Seghers, M.C., Wolfe, M.S., and Selkoe, D.J. (2016). The amyloid-beta forming tripeptide cleavage mechanism of gamma-secretase. *Elife* 5.
- Boonen, M., Staudt, C., Gilis, F., Oorschot, V., Klumperman, J., and Jadot, M. (2016). Cathepsin D and its newly identified transport receptor SEZ6L2 can modulate neurite outgrowth. *Journal of cell science* 129, 557-568.
- Bork, P., and Beckmann, G. (1993). The CUB domain. A widespread module in developmentally regulated proteins. *J Mol Biol* 231, 539-545.
- Bornstein, S., Schmidt, M., Choonoo, G., Levin, T., Gray, J., Thomas, C.R., Jr., Wong, M., and McWeeney, S. (2016). IL-10 and integrin signaling pathways are associated with head and neck cancer progression. *BMC Genomics* 17, 38.
- Bothe, G.W., Bolivar, V.J., Vedder, M.J., and Geistfeld, J.G. (2004). Genetic and behavioral differences among five inbred mouse strains commonly used in the production of transgenic and knockout mice. *Genes, brain, and behavior* 3, 149-157.
- Boucard, A.A., Ko, J., and Sudhof, T.C. (2012). High affinity neurexin binding to cell adhesion G-protein-coupled receptor C1RL1/latrophilin-1 produces an intercellular adhesion complex. *J Biol Chem* 287, 9399-9413.
- Braak, H., and Braak, E. (1991). Neuropathological staging of Alzheimer-related changes. *Acta Neuropathol* 82, 239-259.
- Braak, H., and Braak, E. (1997). Frequency of stages of Alzheimer-related lesions in different age categories. *Neurobiology of aging* 18, 351-357.
- Buggia-Prevot, V., Fernandez, C.G., Udayar, V., Vetrivel, K.S., Elie, A., Roseman, J., Sasse, V.A., Lefkow, M., Meckler, X., Bhattacharyya, S., *et al.* (2013). A function for EHD family proteins in unidirectional retrograde dendritic transport of BACE1 and Alzheimer's disease Abeta production. *Cell Rep* 5, 1552-1563.
- Cai, H., Wang, Y., McCarthy, D., Wen, H., Borchelt, D.R., Price, D.L., and Wong, P.C. (2001). BACE1 is the major beta-secretase for generation of Abeta peptides by neurons. *Nat Neurosci* 4, 233-234.
- Cai, J., Qi, X., Kociok, N., Skosyrski, S., Emilio, A., Ruan, Q., Han, S., Liu, L., Chen, Z., Bowes Rickman, C., *et al.* (2012). beta-Secretase (BACE1) inhibition causes retinal pathology by vascular dysregulation and accumulation of age pigment. *EMBO Mol Med* 4, 980-991.

- Camera, D., Boase, N.A., Kumar, S., Pow, D.V., and Poronnik, P. (2014). Subtle gait abnormalities in Nedd4 heterozygous mice. *Behavioural brain research* 260, 15-24.
- Campion, D., Dumanchin, C., Hannequin, D., Dubois, B., Belliard, S., Puel, M., Thomas-Anterion, C., Michon, A., Martin, C., Charbonnier, F., *et al.* (1999). Early-onset autosomal dominant Alzheimer disease: prevalence, genetic heterogeneity, and mutation spectrum. *American journal of human genetics* 65, 664-670.
- Canti, C., Davies, A., and Dolphin, A.C. Calcium Channel $\alpha 2\delta$ Subunits: Structure, Functions and Target Site for Drugs. *Current Neuropharmacology* 1, 209-217.
- Cao, L., Rickenbacher, G.T., Rodriguez, S., Moulia, T.W., and Albers, M.W. (2012). The precision of axon targeting of mouse olfactory sensory neurons requires the BACE1 protease. *Sci Rep* 2, 231.
- Capell, A., Steiner, H., Willem, M., Kaiser, H., Meyer, C., Walter, J., Lammich, S., Multhaup, G., and Haass, C. (2000). Maturation and pro-peptide cleavage of beta-secretase. *J Biol Chem* 275, 30849-30854.
- Casey, D.A., Antimisiaris, D., and O'Brien, J. (2010). Drugs for Alzheimer's disease: are they effective? *P & T : a peer-reviewed journal for formulary management* 35, 208-211.
- Castellano, J.M., Kim, J., Stewart, F.R., Jiang, H., DeMattos, R.B., Patterson, B.W., Fagan, A.M., Morris, J.C., Mawuenyega, K.G., Cruchaga, C., *et al.* (2011). Human apoE isoforms differentially regulate brain amyloid-beta peptide clearance. *Sci Transl Med* 3, 89ra57.
- Chapman, N.H., Nato, A.Q., Jr., Bernier, R., Ankenman, K., Sohi, H., Munson, J., Patowary, A., Archer, M., Blue, E.M., Webb, S.J., *et al.* (2015). Whole exome sequencing in extended families with autism spectrum disorder implicates four candidate genes. *Hum Genet* 134, 1055-1068.
- Chen, W.J., Goldstein, J.L., and Brown, M.S. (1990). NPXY, a sequence often found in cytoplasmic tails, is required for coated pit-mediated internalization of the low density lipoprotein receptor. *J Biol Chem* 265, 3116-3123.
- Cheret, C., Willem, M., Fricker, F.R., Wende, H., Wulf-Goldenberg, A., Tahirovic, S., Nave, K.A., Saftig, P., Haass, C., Garratt, A.N., *et al.* (2013). Bace1 and Neuregulin-1 cooperate to control formation and maintenance of muscle spindles. *Embo j* 32, 2015-2028.
- Clark, C.M., Pontecorvo, M.J., Beach, T.G., Bedell, B.J., Coleman, R.E., Doraiswamy, P.M., Fleisher, A.S., Reiman, E.M., Sabbagh, M.N., Sadowsky, C.H., *et al.* (2012). Cerebral PET with florbetapir compared with neuropathology at autopsy for detection of neuritic amyloid-beta plaques: a prospective cohort study. *The Lancet Neurology* 11, 669-678.
- Corder, E.H., Saunders, A.M., Strittmatter, W.J., Schmechel, D.E., Gaskell, P.C., Small, G.W., Roses, A.D., Haines, J.L., and Pericak-Vance, M.A. (1993). Gene dose of apolipoprotein E type 4 allele and the risk of Alzheimer's disease in late onset families. *Science* 261, 921-923.
- Cottrell, G.S., Soubrane, C.H., Hounshell, J.A., Lin, H., Owenson, V., Rigby, M., Cox, P.J., Barker, B.S., Ottolini, M., Ince, S., *et al.* (2018). CACHD1 is an alpha2delta-like protein that modulates CaV3 voltage-gated calcium channel activity. *J Neurosci*.
- Cox, J., Hein, M.Y., Lubner, C.A., Paron, I., Nagaraj, N., and Mann, M. (2014). Accurate proteome-wide label-free quantification by delayed normalization and maximal peptide ratio extraction, termed MaxLFQ. *Mol Cell Proteomics* 13, 2513-2526.
- Cummings, J.L., Cohen, S., van Dyck, C.H., Brody, M., Curtis, C., Cho, W., Ward, M., Friesenhahn, M., Rabe, C., Brunstein, F., *et al.* (2018). ABBY: A phase 2 randomized trial of crenezumab in mild to moderate Alzheimer disease. *Neurology* 90, e1889-e1897.
- Dahimene, S., Page, K.M., Kadurin, I., Ferron, L., Ho, D.Y., Powell, G.T., Pratt, W.S., Wilson, S.W., and Dolphin, A.C. (2018). The alpha2delta-like Protein Cachd1 Increases N-type Calcium Currents and Cell Surface Expression and Competes with alpha2delta-1. *Cell Rep* 25, 1610-1621.e1615.
- Das, B., and Yan, R. (2019). A Close Look at BACE1 Inhibitors for Alzheimer's Disease Treatment. *CNS drugs*.

- De Strooper, B. (2003). Aph-1, Pen-2, and Nicastrin with Presenilin generate an active gamma-Secretase complex. *Neuron* 38, 9-12.
- Dislich, B., Wohlrab, F., Bachhuber, T., Muller, S.A., Kuhn, P.H., Hogl, S., Meyer-Luehmann, M., and Lichtenthaler, S.F. (2015). Label-free Quantitative Proteomics of Mouse Cerebrospinal Fluid Detects beta-Site APP Cleaving Enzyme (BACE1) Protease Substrates In Vivo. *Mol Cell Proteomics* 14, 2550-2563.
- Dislich, B. (2013). The global proteomic profiling of the BACE1 knockout mouse brain allows identification of novel BACE1 substrates in vivo. (Dissertation). Technical University Munich.
- Dolphin, A.C. (2012). Calcium channel alpha2delta subunits in epilepsy and as targets for antiepileptic drugs. In Jasper's Basic Mechanisms of the Epilepsies, th, J.L. Noebels, M. Avoli, M.A. Rogawski, R.W. Olsen, and A.V. Delgado-Escueta, eds. (Bethesda (MD): National Center for Biotechnology Information (US)
- Michael A Rogawski, Antonio V Delgado-Escueta, Jeffrey L Noebels, Massimo Avoli and Richard W Olsen.).
- Dolphin, A.C. (2013). The alpha2delta subunits of voltage-gated calcium channels. *Biochim Biophys Acta* 1828, 1541-1549.
- Dominguez, D., Tournoy, J., Hartmann, D., Huth, T., Cryns, K., Deforce, S., Serneels, L., Camacho, I.E., Marjaux, E., Craessaerts, K., *et al.* (2005). Phenotypic and biochemical analyses of BACE1- and BACE2-deficient mice. *J Biol Chem* 280, 30797-30806.
- Eckman, C.B., Mehta, N.D., Crook, R., Perez-tur, J., Prihar, G., Pfeiffer, E., Graff-Radford, N., Hinder, P., Yager, D., Zenk, B., *et al.* (1997). A new pathogenic mutation in the APP gene (I716V) increases the relative proportion of A beta 42(43). *Human molecular genetics* 6, 2087-2089.
- Etherton, M.R., Blaiss, C.A., Powell, C.M., and Sudhof, T.C. (2009). Mouse neurexin-1alpha deletion causes correlated electrophysiological and behavioral changes consistent with cognitive impairments. *Proc Natl Acad Sci U S A* 106, 17998-18003.
- Farrer, L.A., Cupples, L.A., Haines, J.L., Hyman, B., Kukull, W.A., Mayeux, R., Myers, R.H., Pericak-Vance, M.A., Risch, N., and van Duijn, C.M. (1997). Effects of age, sex, and ethnicity on the association between apolipoprotein E genotype and Alzheimer disease. A meta-analysis. APOE and Alzheimer Disease Meta Analysis Consortium. *Jama* 278, 1349-1356.
- Farzan, M., Schnitzler, C.E., Vasilieva, N., Leung, D., and Choe, H. (2000). BACE2, a beta -secretase homolog, cleaves at the beta site and within the amyloid-beta region of the amyloid-beta precursor protein. *Proc Natl Acad Sci U S A* 97, 9712-9717.
- Fleck, D., Garratt, A.N., Haass, C., and Willem, M. (2012). BACE1 dependent neuregulin processing: review. *Current Alzheimer research* 9, 178-183.
- Fluhrer, R., Capell, A., Westmeyer, G., Willem, M., Hartung, B., Condrón, M.M., Teplow, D.B., Haass, C., and Walter, J. (2002). A non-amyloidogenic function of BACE-2 in the secretory pathway. *J Neurochem* 81, 1011-1020.
- Gaboriaud, C., Gregory-Pauron, L., Teillet, F., Thielens, N.M., Bally, I., and Arlaud, G.J. (2011). Structure and properties of the Ca(2+)-binding CUB domain, a widespread ligand-recognition unit involved in major biological functions. *Biochem J* 439, 185-193.
- Gadalla, K.K., Ross, P.D., Riddell, J.S., Bailey, M.E., and Cobb, S.R. (2014). Gait analysis in a Mecp2 knockout mouse model of Rett syndrome reveals early-onset and progressive motor deficits. *PLoS One* 9, e112889.
- Gersbacher, M.T., Goodger, Z.V., Trutzel, A., Bundschuh, D., Nitsch, R.M., and Konietzko, U. (2013). Turnover of amyloid precursor protein family members determines their nuclear signaling capability. *PLoS One* 8, e69363.
- Giannakis, E., Male, D.A., Ormsby, R.J., Mold, C., Jokiranta, T.S., Ranganathan, S., and Gordon, D.L. (2001). Multiple ligand binding sites on domain seven of human complement factor H. *International immunopharmacology* 1, 433-443.

- Glennner, G.G., and Wong, C.W. (1984). Alzheimer's disease: initial report of the purification and characterization of a novel cerebrovascular amyloid protein. *Biochem Biophys Res Commun* *120*, 885-890.
- Goate, A., Chartier-Harlin, M.C., Mullan, M., Brown, J., Crawford, F., Fidani, L., Giuffra, L., Haynes, A., Irving, N., James, L., *et al.* (1991). Segregation of a missense mutation in the amyloid precursor protein gene with familial Alzheimer's disease. *Nature* *349*, 704-706.
- Gorlov, I.P., Meyer, P., Liloglou, T., Myles, J., Boettger, M.B., Cassidy, A., Girard, L., Minna, J.D., Fischer, R., Duffy, S., *et al.* (2007). Seizure 6-like (SEZ6L) gene and risk for lung cancer. *Cancer Res* *67*, 8406-8411.
- Grundke-Iqbal, I., Iqbal, K., Tung, Y.C., Quinlan, M., Wisniewski, H.M., and Binder, L.I. (1986). Abnormal phosphorylation of the microtubule-associated protein tau (tau) in Alzheimer cytoskeletal pathology. *Proc Natl Acad Sci U S A* *83*, 4913-4917.
- Gunnarsen, J.M., Kim, M.H., Fuller, S.J., De Silva, M., Britto, J.M., Hammond, V.E., Davies, P.J., Petrou, S., Faber, E.S., Sah, P., *et al.* (2007). Sez-6 proteins affect dendritic arborization patterns and excitability of cortical pyramidal neurons. *Neuron* *56*, 621-639.
- Hald, J., Galbo, T., Rescan, C., Radzikowski, L., Sprinkel, A.E., Heimberg, H., Ahnfelt-Ronne, J., Jensen, J., Scharfmann, R., Gradwohl, G., *et al.* (2012). Pancreatic islet and progenitor cell surface markers with cell sorting potential. *Diabetologia* *55*, 154-165.
- Haniu, M., Denis, P., Young, Y., Mendiaz, E.A., Fuller, J., Hui, J.O., Bennett, B.D., Kahn, S., Ross, S., Burgess, T., *et al.* (2000). Characterization of Alzheimer's beta -secretase protein BACE. A pepsin family member with unusual properties. *J Biol Chem* *275*, 21099-21106.
- Hannigan, J.H., and Riley, E.P. (1988). Prenatal ethanol alters gait in rats. *Alcohol (Fayetteville, NY)* *5*, 451-454.
- Hardy, J., and Allsop, D. (1991). Amyloid deposition as the central event in the aetiology of Alzheimer's disease. *Trends in pharmacological sciences* *12*, 383-388.
- Hardy, J., and Selkoe, D.J. (2002). The amyloid hypothesis of Alzheimer's disease: progress and problems on the road to therapeutics. *Science* *297*, 353-356.
- Harrison, S.M., Harper, A.J., Hawkins, J., Duddy, G., Grau, E., Pugh, P.L., Winter, P.H., Shilliam, C.S., Hughes, Z.A., Dawson, L.A., *et al.* (2003). BACE1 (beta-secretase) transgenic and knockout mice: identification of neurochemical deficits and behavioral changes. *Mol Cell Neurosci* *24*, 646-655.
- He, X., Li, F., Chang, W.P., and Tang, J. (2005). GGA proteins mediate the recycling pathway of memapsin 2 (BACE). *J Biol Chem* *280*, 11696-11703.
- Heber, S., Herms, J., Gajic, V., Hainfellner, J., Aguzzi, A., Rulicke, T., von Kretschmar, H., von Koch, C., Sisodia, S., Tremml, P., *et al.* (2000). Mice with combined gene knock-outs reveal essential and partially redundant functions of amyloid precursor protein family members. *J Neurosci* *20*, 7951-7963.
- Hemming, M.L., Elias, J.E., Gygi, S.P., and Selkoe, D.J. (2009). Identification of beta-secretase (BACE1) substrates using quantitative proteomics. *PLoS One* *4*, e8477.
- Henley, J.M., and Wilkinson, K.A. (2016). Synaptic AMPA receptor composition in development, plasticity and disease. *Nature reviews Neuroscience* *17*, 337-350.
- Herber, J., Njavro, J., Feederle, R., Schepers, U., Muller, U.C., Brase, S., Muller, S.A., and Lichtenthaler, S.F. (2018). Click Chemistry-mediated Biotinylation Reveals a Function for the Protease BACE1 in Modulating the Neuronal Surface Glycoproteome. *Molecular & Cellular Proteomics*.
- Herholz, K., and Ebmeier, K. (2011). Clinical amyloid imaging in Alzheimer's disease. *The Lancet Neurology* *10*, 667-670.
- Herms, J., Anliker, B., Heber, S., Ring, S., Fuhrmann, M., Kretschmar, H., Sisodia, S., and Muller, U. (2004). Cortical dysplasia resembling human type 2 lissencephaly in mice lacking all three APP family members. *Embo j* *23*, 4106-4115.

- Hessler, S., Zheng, F., Hartmann, S., Rittger, A., Lehnert, S., Volkel, M., Nissen, M., Edelmann, E., Saftig, P., Schwake, M., *et al.* (2015). beta-Secretase BACE1 regulates hippocampal and reconstituted M-currents in a beta-subunit-like fashion. *J Neurosci* 35, 3298-3311.
- Heyden, A., Angenstein, F., Sallaz, M., Seidenbecher, C., and Montag, D. (2008). Abnormal axonal guidance and brain anatomy in mouse mutants for the cell recognition molecules close homolog of L1 and NgCAM-related cell adhesion molecule. *Neuroscience* 155, 221-233.
- Hippenmeyer, S., Shneider, N.A., Birchmeier, C., Burden, S.J., Jessell, T.M., and Arber, S. (2002). A role for neuregulin1 signaling in muscle spindle differentiation. *Neuron* 36, 1035-1049.
- Hitt, B., Riordan, S.M., Kukreja, L., Eimer, W.A., Rajapaksha, T.W., and Vassar, R. (2012). beta-Site amyloid precursor protein (APP)-cleaving enzyme 1 (BACE1)-deficient mice exhibit a close homolog of L1 (CHL1) loss-of-function phenotype involving axon guidance defects. *J Biol Chem* 287, 38408-38425.
- Hitt, B.D., Jaramillo, T.C., Chetkovich, D.M., and Vassar, R. (2010). BACE1^{-/-} mice exhibit seizure activity that does not correlate with sodium channel level or axonal localization. *Molecular neurodegeneration* 5, 31.
- Ho, N., Liauw, J.A., Blaeser, F., Wei, F., Hanissian, S., Muglia, L.M., Wozniak, D.F., Nardi, A., Arvin, K.L., Holtzman, D.M., *et al.* (2000). Impaired synaptic plasticity and cAMP response element-binding protein activation in Ca²⁺/calmodulin-dependent protein kinase type IV/Gr-deficient mice. *J Neurosci* 20, 6459-6472.
- Hong, S., Beja-Glasser, V.F., Nfonoyim, B.M., Frouin, A., Li, S., Ramakrishnan, S., Merry, K.M., Shi, Q., Rosenthal, A., Barres, B.A., *et al.* (2016a). Complement and microglia mediate early synapse loss in Alzheimer mouse models. *Science* 352, 712-716.
- Hong, S., Dissing-Olesen, L., and Stevens, B. (2016b). New insights on the role of microglia in synaptic pruning in health and disease. *Current opinion in neurobiology* 36, 128-134.
- Hourcade, D., Holers, V.M., and Atkinson, J.P. (1989). The regulators of complement activation (RCA) gene cluster. *Advances in immunology* 45, 381-416.
- Hu, X., He, W., Diaconu, C., Tang, X., Kidd, G.J., Macklin, W.B., Trapp, B.D., and Yan, R. (2008). Genetic deletion of BACE1 in mice affects remyelination of sciatic nerves. *FASEB journal : official publication of the Federation of American Societies for Experimental Biology* 22, 2970-2980.
- Hu, X., He, W., Luo, X., Tsubota, K.E., and Yan, R. (2013). BACE1 regulates hippocampal astrogenesis via the Jagged1-Notch pathway. *Cell Rep* 4, 40-49.
- Hu, X., Hicks, C.W., He, W., Wong, P., Macklin, W.B., Trapp, B.D., and Yan, R. (2006). Bace1 modulates myelination in the central and peripheral nervous system. *Nat Neurosci* 9, 1520-1525.
- Hu, X., Zhou, X., He, W., Yang, J., Xiong, W., Wong, P., Wilson, C.G., and Yan, R. (2010). BACE1 deficiency causes altered neuronal activity and neurodegeneration. *J Neurosci* 30, 8819-8829.
- Huang, Y., and Mucke, L. (2012). Alzheimer mechanisms and therapeutic strategies. *Cell* 148, 1204-1222.
- Hung, Y.H., Walterfang, M., Churilov, L., Bray, L., Jacobson, L.H., Barnham, K.J., Jones, N.C., O'Brien, T.J., Velakoulis, D., and Bush, A.I. (2016). Neurological Dysfunction in Early Maturity of a Model for Niemann-Pick C1 Carrier Status. *Neurotherapeutics : the journal of the American Society for Experimental NeuroTherapeutics* 13, 614-622.
- Hussain, I., Powell, D., Howlett, D.R., Tew, D.G., Meek, T.D., Chapman, C., Gloger, I.S., Murphy, K.E., Southan, C.D., Ryan, D.M., *et al.* (1999). Identification of a novel aspartic protease (Asp 2) as beta-secretase. *Mol Cell Neurosci* 14, 419-427.
- Ishikawa, N., Daigo, Y., Takano, A., Taniwaki, M., Kato, T., Tanaka, S., Yasui, W., Takeshima, Y., Inai, K., Nishimura, H., *et al.* (2006). Characterization of SEZ6L2 cell-surface protein as a novel prognostic marker for lung cancer. *Cancer science* 97, 737-745.

- Jack, C.R., Jr., Vemuri, P., Wiste, H.J., Weigand, S.D., Lesnick, T.G., Lowe, V., Kantarci, K., Bernstein, M.A., Senjem, M.L., Gunter, J.L., *et al.* (2012). Shapes of the trajectories of 5 major biomarkers of Alzheimer disease. *Archives of neurology* *69*, 856-867.
- Jefferson, T., Causevic, M., auf dem Keller, U., Schilling, O., Isbert, S., Geyer, R., Maier, W., Tschickardt, S., Jumpertz, T., Weggen, S., *et al.* (2011). Metalloprotease meprin beta generates nontoxic N-terminal amyloid precursor protein fragments in vivo. *J Biol Chem* *286*, 27741-27750.
- Jeyabalan, N., and Clement, J.P. (2016). SYNGAP1: Mind the Gap. *Front Cell Neurosci* *10*, 32.
- Jonsson, T., Atwal, J.K., Steinberg, S., Snaedal, J., Jonsson, P.V., Bjornsson, S., Stefansson, H., Sulem, P., Gudbjartsson, D., Maloney, J., *et al.* (2012). A mutation in APP protects against Alzheimer's disease and age-related cognitive decline. *Nature* *488*, 96-99.
- Kalvodova, L., Kahya, N., Schwille, P., Eehalt, R., Verkade, P., Drechsel, D., and Simons, K. (2005). Lipids as modulators of proteolytic activity of BACE: involvement of cholesterol, glycosphingolipids, and anionic phospholipids in vitro. *J Biol Chem* *280*, 36815-36823.
- Kamada, Y., Sakata-Yanagimoto, M., Sanada, M., Sato-Otsubo, A., Enami, T., Suzukawa, K., Kurita, N., Nishikii, H., Yokoyama, Y., Okoshi, Y., *et al.* (2012). Identification of unbalanced genome copy number abnormalities in patients with multiple myeloma by single-nucleotide polymorphism genotyping microarray analysis. *International journal of hematology* *96*, 492-500.
- Kamenetz, F., Tomita, T., Hsieh, H., Seabrook, G., Borchelt, D., Iwatsubo, T., Sisodia, S., and Malinow, R. (2003). APP processing and synaptic function. *Neuron* *37*, 925-937.
- Kang, E.L., Biscaro, B., Piazza, F., and Tesco, G. (2012). BACE1 protein endocytosis and trafficking are differentially regulated by ubiquitination at lysine 501 and the Di-leucine motif in the carboxyl terminus. *J Biol Chem* *287*, 42867-42880.
- Kang, G.H., Lee, S., Cho, N.Y., Gandamihardja, T., Long, T.I., Weisenberger, D.J., Campan, M., and Laird, P.W. (2008). DNA methylation profiles of gastric carcinoma characterized by quantitative DNA methylation analysis. *Lab Invest* *88*, 161-170.
- Kang, J., Lemaire, H.G., Unterbeck, A., Salbaum, J.M., Masters, C.L., Grzeschik, K.H., Multhaup, G., Beyreuther, K., and Muller-Hill, B. (1987). The precursor of Alzheimer's disease amyloid A4 protein resembles a cell-surface receptor. *Nature* *325*, 733-736.
- Karch, C.M., and Goate, A.M. (2015). Alzheimer's disease risk genes and mechanisms of disease pathogenesis. *Biol Psychiatry* *77*, 43-51.
- Khoonsari, P.E., Haggmark, A., Lonnberg, M., Mikus, M., Kilander, L., Lannfelt, L., Bergquist, J., Ingelsson, M., Nilsson, P., Kultima, K., *et al.* (2016). Analysis of the Cerebrospinal Fluid Proteome in Alzheimer's Disease. *PLoS One* *11*, e0150672.
- Kilinc, M., Creson, T., Rojas, C., Aceti, M., Ellegood, J., Vaissiere, T., Lerch, J.P., and Rumbaugh, G. (2018). Species-conserved SYNGAP1 phenotypes associated with neurodevelopmental disorders. *Mol Cell Neurosci* *91*, 140-150.
- Kim, D.Y., Gersbacher, M.T., Inquimbert, P., and Kovacs, D.M. (2011). Reduced sodium channel Na(v)1.1 levels in BACE1-null mice. *J Biol Chem* *286*, 8106-8116.
- Kim, J., Onstead, L., Randle, S., Price, R., Smithson, L., Zwizinski, C., Dickson, D.W., Golde, T., and McGowan, E. (2007). Abeta40 inhibits amyloid deposition in vivo. *J Neurosci* *27*, 627-633.
- Kim, M.H., Gunnarsen, J.M., and Tan, S.S. (2002). Localized expression of the seizure-related gene SEZ-6 in developing and adult forebrains. *Mechanisms of development* *118*, 171-174.
- Kinoshita, A., Fukumoto, H., Shah, T., Whelan, C.M., Irizarry, M.C., and Hyman, B.T. (2003). Demonstration by FRET of BACE interaction with the amyloid precursor protein at the cell surface and in early endosomes. *Journal of cell science* *116*, 3339-3346.
- Ko, M.H., and Puglielli, L. (2009). Two endoplasmic reticulum (ER)/ER Golgi intermediate compartment-based lysine acetyltransferases post-translationally regulate BACE1 levels. *J Biol Chem* *284*, 2482-2492.

- Kobayashi, D., Zeller, M., Cole, T., Buttini, M., McConlogue, L., Sinha, S., Freedman, S., Morris, R.G., and Chen, K.S. (2008). BACE1 gene deletion: impact on behavioral function in a model of Alzheimer's disease. *Neurobiology of aging* 29, 861-873.
- Koh, Y.H., von Arnim, C.A., Hyman, B.T., Tanzi, R.E., and Tesco, G. (2005). BACE is degraded via the lysosomal pathway. *J Biol Chem* 280, 32499-32504.
- Kuhn, P.H., Koroniak, K., Hogg, S., Colombo, A., Zeitschel, U., Willem, M., Volbracht, C., Schepers, U., Imhof, A., Hoffmeister, A., *et al.* (2012). Secretome protein enrichment identifies physiological BACE1 protease substrates in neurons. *EMBO J* 31, 3157-3168.
- Kuhn, P.H., Wang, H., Dislich, B., Colombo, A., Zeitschel, U., Ellwart, J.W., Kremmer, E., Rossner, S., and Lichtenthaler, S.F. (2010). ADAM10 is the physiologically relevant, constitutive alpha-secretase of the amyloid precursor protein in primary neurons. *EMBO J* 29, 3020-3032.
- Kumar, R.A., Marshall, C.R., Badner, J.A., Babatz, T.D., Mukamel, Z., Aldinger, K.A., Sudi, J., Brune, C.W., Goh, G., Karamohamed, S., *et al.* (2009). Association and mutation analyses of 16p11.2 autism candidate genes. *PLoS One* 4, e4582.
- Laird, F.M., Cai, H., Savonenko, A.V., Farah, M.H., He, K., Melnikova, T., Wen, H., Chiang, H.C., Xu, G., Koliatsos, V.E., *et al.* (2005). BACE1, a major determinant of selective vulnerability of the brain to amyloid-beta amyloidogenesis, is essential for cognitive, emotional, and synaptic functions. *J Neurosci* 25, 11693-11709.
- Lammich, S., Kojro, E., Postina, R., Gilbert, S., Pfeiffer, R., Jasionowski, M., Haass, C., and Fahrenholz, F. (1999). Constitutive and regulated alpha-secretase cleavage of Alzheimer's amyloid precursor protein by a disintegrin metalloprotease. *Proc Natl Acad Sci U S A* 96, 3922-3927.
- Leiva, M., Quintana, J.A., Ligos, J.M., and Hidalgo, A. (2016). Haematopoietic ESL-1 enables stem cell proliferation in the bone marrow by limiting TGFbeta availability. *Nat Commun* 7, 10222.
- Leu, M., Bellmunt, E., Schwander, M., Farinas, I., Brenner, H.R., and Muller, U. (2003). Erbb2 regulates neuromuscular synapse formation and is essential for muscle spindle development. *Development* 130, 2291-2301.
- Li, Q., and Sudhof, T.C. (2004). Cleavage of amyloid-beta precursor protein and amyloid-beta precursor-like protein by BACE 1. *J Biol Chem* 279, 10542-10550.
- Lin, X., Koelsch, G., Wu, S., Downs, D., Dashti, A., and Tang, J. (2000). Human aspartic protease memapsin 2 cleaves the beta-secretase site of beta-amyloid precursor protein. *Proc Natl Acad Sci U S A* 97, 1456-1460.
- Lukong, K.E., and Richard, S. (2008). Motor coordination defects in mice deficient for the Sam68 RNA-binding protein. *Behavioural brain research* 189, 357-363.
- Luo, W., Wang, H., Guo, C., Wang, J., Kwak, J., Bahrou, K.L., and Eitzman, D.T. (2012). Haploinsufficiency of E-selectin ligand-1 is associated with reduced atherosclerotic plaque macrophage content while complete deficiency leads to early embryonic lethality in mice. *Atherosclerosis* 224, 363-367.
- Luo, Y., Bolon, B., Damore, M.A., Fitzpatrick, D., Liu, H., Zhang, J., Yan, Q., Vassar, R., and Citron, M. (2003). BACE1 (beta-secretase) knockout mice do not acquire compensatory gene expression changes or develop neural lesions over time. *Neurobiol Dis* 14, 81-88.
- Luo, Y., Bolon, B., Kahn, S., Bennett, B.D., Babu-Khan, S., Denis, P., Fan, W., Kha, H., Zhang, J., Gong, Y., *et al.* (2001). Mice deficient in BACE1, the Alzheimer's beta-secretase, have normal phenotype and abolished beta-amyloid generation. *Nat Neurosci* 4, 231-232.
- Maccarrone, G., Ditzen, C., Yassouridis, A., Rewerts, C., Uhr, M., Uhlen, M., Holsboer, F., and Turck, C.W. (2013). Psychiatric patient stratification using biosignatures based on cerebrospinal fluid protein expression clusters. *J Psychiatr Res* 47, 1572-1580.
- Major, B., Kardos, J., Kekesi, K.A., Lorincz, Z., Zavodszky, P., and Gal, P. (2010). Calcium-dependent conformational flexibility of a CUB domain controls activation of the complement serine protease C1r. *J Biol Chem* 285, 11863-11869.

- Mayeux, R., and Stern, Y. (2012). Epidemiology of Alzheimer disease. *Cold Spring Harbor perspectives in medicine* 2.
- McConlogue, L., Buttini, M., Anderson, J.P., Brigham, E.F., Chen, K.S., Freedman, S.B., Games, D., Johnson-Wood, K., Lee, M., Zeller, M., *et al.* (2007). Partial reduction of BACE1 has dramatic effects on Alzheimer plaque and synaptic pathology in APP Transgenic Mice. *J Biol Chem* 282, 26326-26334.
- Mena, R., Edwards, P.C., Harrington, C.R., Mukaetova-Ladinska, E.B., and Wischik, C.M. (1996). Staging the pathological assembly of truncated tau protein into paired helical filaments in Alzheimer's disease. *Acta Neuropathol* 91, 633-641.
- Meziane, H., Dodart, J.C., Mathis, C., Little, S., Clemens, J., Paul, S.M., and Ungerer, A. (1998). Memory-enhancing effects of secreted forms of the beta-amyloid precursor protein in normal and amnesic mice. *Proc Natl Acad Sci U S A* 95, 12683-12688.
- Min, S.W., Cho, S.H., Zhou, Y., Schroeder, S., Haroutunian, V., Seeley, W.W., Huang, E.J., Shen, Y., Masliah, E., Mukherjee, C., *et al.* (2010). Acetylation of tau inhibits its degradation and contributes to tauopathy. *Neuron* 67, 953-966.
- Minett, T., Classey, J., Matthews, F.E., Fahrenhold, M., Taga, M., Brayne, C., Ince, P.G., Nicoll, J.A., and Boche, D. (2016). Microglial immunophenotype in dementia with Alzheimer's pathology. *Journal of neuroinflammation* 13, 135.
- Miyazaki, T., Hashimoto, K., Uda, A., Sakagami, H., Nakamura, Y., Saito, S.Y., Nishi, M., Kume, H., Tohgo, A., Kaneko, I., *et al.* (2006). Disturbance of cerebellar synaptic maturation in mutant mice lacking BSRPs, a novel brain-specific receptor-like protein family. *FEBS Lett* 580, 4057-4064.
- Montag-Sallaz, M., Schachner, M., and Montag, D. (2002). Misguided axonal projections, neural cell adhesion molecule 180 mRNA upregulation, and altered behavior in mice deficient for the close homolog of L1. *Mol Cell Biol* 22, 7967-7981.
- Moreno, T.A., and Bronner-Fraser, M. (2001). The secreted glycoprotein Noelin-1 promotes neurogenesis in *Xenopus*. *Dev Biol* 240, 340-360.
- Morgan, B.P. (2018). Complement in the pathogenesis of Alzheimer's disease. *Seminars in immunopathology* 40, 113-124.
- Mullan, M., Crawford, F., Axelman, K., Houlden, H., Lilius, L., Winblad, B., and Lannfelt, L. (1992). A pathogenic mutation for probable Alzheimer's disease in the APP gene at the N-terminus of beta-amyloid. *Nature genetics* 1, 345-347.
- Muller, U.C., Deller, T., and Korte, M. (2017). Not just amyloid: physiological functions of the amyloid precursor protein family. *Nature reviews Neuroscience* 18, 281-298.
- Muller, U.C., and Zheng, H. (2012). Physiological functions of APP family proteins. *Cold Spring Harbor perspectives in medicine* 2, a006288.
- Mulley, J.C., Iona, X., Hodgson, B., Heron, S.E., Berkovic, S.F., Scheffer, I.E., and Dibbens, L.M. (2011). The Role of Seizure-Related SEZ6 as a Susceptibility Gene in Febrile Seizures. *Neurol Res Int* 2011, 917565.
- Murrell, J., Farlow, M., Ghetti, B., and Benson, M.D. (1991). A mutation in the amyloid precursor protein associated with hereditary Alzheimer's disease. *Science* 254, 97-99.
- Nakaya, N., Lee, H.S., Takada, Y., Tzchori, I., and Tomarev, S.I. (2008). Zebrafish olfactomedin 1 regulates retinal axon elongation in vivo and is a modulator of Wnt signaling pathway. *J Neurosci* 28, 7900-7910.
- Nakaya, N., Sultana, A., Lee, H.S., and Tomarev, S.I. (2012). Olfactomedin 1 interacts with the Nogo A receptor complex to regulate axon growth. *J Biol Chem* 287, 37171-37184.
- Nakaya, N., Sultana, A., Munasinghe, J., Cheng, A., Mattson, M.P., and Tomarev, S.I. (2013). Deletion in the N-terminal half of olfactomedin 1 modifies its interaction with synaptic proteins and causes brain dystrophy and abnormal behavior in mice. *Exp Neurol* 250, 205-218.

- Nakaya, N., Sultana, A., and Tomarev, S.I. (2017). Impaired AMPA receptor trafficking by a double knockout of zebrafish olfactomedin1a/b. *J Neurochem* *143*, 635-644.
- Nakayama, M., and Hama, C. (2011). Modulation of neurotransmitter receptors and synaptic differentiation by proteins containing complement-related domains. *Neuroscience research* *69*, 87-92.
- Nishioka, M., Kohno, T., Takahashi, M., Niki, T., Yamada, T., Sone, S., and Yokota, J. (2000). Identification of a 428-kb homozygously deleted region disrupting the SEZ6L gene at 22q12.1 in a lung cancer cell line. *Oncogene* *19*, 6251-6260.
- Nixon, R.A. (2004). Niemann-Pick Type C disease and Alzheimer's disease: the APP-endosome connection fattens up. *The American journal of pathology* *164*, 757-761.
- Nizami, S., Hall-Roberts, H., Warriar, S., Cowley, S.A., and Di Daniel, E. (2019). Microglial inflammation and phagocytosis in Alzheimer's disease: potential therapeutic targets. *British journal of pharmacology*.
- Norton, S., Matthews, F.E., Barnes, D.E., Yaffe, K., and Brayne, C. (2014). Potential for primary prevention of Alzheimer's disease: an analysis of population-based data. *The Lancet Neurology* *13*, 788-794.
- O'Brien, R.J., and Wong, P.C. (2011). Amyloid precursor protein processing and Alzheimer's disease. *Annu Rev Neurosci* *34*, 185-204.
- O'Leary, T.P., Robertson, A., Chipman, P.H., Rafuse, V.F., and Brown, R.E. (2018). Motor function deficits in the 12 month-old female 5xFAD mouse model of Alzheimer's disease. *Behavioural brain research* *337*, 256-263.
- Oberdoerffer, S., Moita, L.F., Neems, D., Freitas, R.P., Hacohen, N., and Rao, A. (2008). Regulation of CD45 alternative splicing by heterogeneous ribonucleoprotein, hnRNPLL. *Science* *321*, 686-691.
- Ohno, M. (2016). Alzheimer's therapy targeting the beta-secretase enzyme BACE1: Benefits and potential limitations from the perspective of animal model studies. *Brain Res Bull* *126*, 183-198.
- Ohno, M., Chang, L., Tseng, W., Oakley, H., Citron, M., Klein, W.L., Vassar, R., and Disterhoft, J.F. (2006). Temporal memory deficits in Alzheimer's mouse models: rescue by genetic deletion of BACE1. *The European journal of neuroscience* *23*, 251-260.
- Ohno, M., Cole, S.L., Yasvoina, M., Zhao, J., Citron, M., Berry, R., Disterhoft, J.F., and Vassar, R. (2007). BACE1 gene deletion prevents neuron loss and memory deficits in 5XFAD APP/PS1 transgenic mice. *Neurobiol Dis* *26*, 134-145.
- Ohno, M., Sametsky, E.A., Younkin, L.H., Oakley, H., Younkin, S.G., Citron, M., Vassar, R., and Disterhoft, J.F. (2004). BACE1 deficiency rescues memory deficits and cholinergic dysfunction in a mouse model of Alzheimer's disease. *Neuron* *41*, 27-33.
- Osaki, G., Mitsui, S., and Yuri, K. (2011). The distribution of the seizure-related gene 6 (Sez-6) protein during postnatal development of the mouse forebrain suggests multiple functions for this protein: an analysis using a new antibody. *Brain Res* *1386*, 58-69.
- Ostrowitzki, S., Lasser, R.A., Dorflinger, E., Scheltens, P., Barkhof, F., Nikolcheva, T., Ashford, E., Retout, S., Hofmann, C., Delmar, P., *et al.* (2017). A phase III randomized trial of gantenerumab in prodromal Alzheimer's disease. *Alzheimers Res Ther* *9*, 95.
- Ou-Yang, M.H., Kurz, J.E., Nomura, T., Popovic, J., Rajapaksha, T.W., Dong, H., Contractor, A., Chetkovich, D.M., Tourtellotte, W.G., and Vassar, R. (2018). Axonal organization defects in the hippocampus of adult conditional BACE1 knockout mice. *Sci Transl Med* *10*.
- Pandya, N.J., Seeger, C., Babai, N., Gonzalez-Lozano, M.A., Mack, V., Lodder, J.C., Gouwenberg, Y., Mansvelder, H.D., Danielson, U.H., Li, K.W., *et al.* (2018). Noelin1 Affects Lateral Mobility of Synaptic AMPA Receptors. *Cell Rep* *24*, 1218-1230.
- Paracchini, L., Beltrame, L., Boeri, L., Fusco, F., Caffarra, P., Marchini, S., Albani, D., and Forloni, G. (2018). Exome sequencing in an Italian family with Alzheimer's disease points to a role for seizure-related gene 6 (SEZ6) rare variant R615H. *Alzheimers Res Ther* *10*, 106.

- Pastorino, L., Ikin, A.F., Nairn, A.C., Pursnani, A., and Buxbaum, J.D. (2002). The carboxyl-terminus of BACE contains a sorting signal that regulates BACE trafficking but not the formation of total A(beta). *Mol Cell Neurosci* *19*, 175-185.
- Perez, R.G., Soriano, S., Hayes, J.D., Ostaszewski, B., Xia, W., Selkoe, D.J., Chen, X., Stokin, G.B., and Koo, E.H. (1999). Mutagenesis identifies new signals for beta-amyloid precursor protein endocytosis, turnover, and the generation of secreted fragments, including Abeta42. *J Biol Chem* *274*, 18851-18856.
- Pigoni, M., Gunnensen, J.M., and Lichtenthaler, S.F. (2017). Seizure-6 proteins highlight BACE1 functions in neurobiology. *Oncotarget* *8*, 7214-7215.
- Pigoni, M., Wanngren, J., Kuhn, P.H., Munro, K.M., Gunnensen, J.M., Takeshima, H., Feederle, R., Voytyuk, I., De Strooper, B., Levasseur, M.D., *et al.* (2016). Seizure protein 6 and its homolog seizure 6-like protein are physiological substrates of BACE1 in neurons. *Molecular neurodegeneration* *11*, 67.
- Poliak, S., Salomon, D., Elhanany, H., Sabanay, H., Kiernan, B., Pevny, L., Stewart, C.L., Xu, X., Chiu, S.Y., Shrager, P., *et al.* (2003). Juxtaparanodal clustering of Shaker-like K⁺ channels in myelinated axons depends on Caspr2 and TAG-1. *J Cell Biol* *162*, 1149-1160.
- Powell, K.L., Cain, S.M., Snutch, T.P., and O'Brien, T.J. (2014). Low threshold T-type calcium channels as targets for novel epilepsy treatments. *British journal of clinical pharmacology* *77*, 729-739.
- Prabhu, Y., Burgos, P.V., Schindler, C., Farias, G.G., Magadan, J.G., and Bonifacino, J.S. (2012). Adaptor protein 2-mediated endocytosis of the beta-secretase BACE1 is dispensable for amyloid precursor protein processing. *Molecular biology of the cell* *23*, 2339-2351.
- Prasher, V.P., Farrer, M.J., Kessling, A.M., Fisher, E.M., West, R.J., Barber, P.C., and Butler, A.C. (1998). Molecular mapping of Alzheimer-type dementia in Down's syndrome. *Annals of neurology* *43*, 380-383.
- Prince, M., Bryce, R., Albanese, E., Wimo, A., Ribeiro, W., and Ferri, C.P. (2013). The global prevalence of dementia: a systematic review and metaanalysis. *Alzheimer's & dementia : the journal of the Alzheimer's Association* *9*, 63-75.e62.
- Purice, M.D., and Taylor, J.P. (2018). Linking hnRNP Function to ALS and FTD Pathology. *Frontiers in neuroscience* *12*, 326.
- Qi-Takahara, Y., Morishima-Kawashima, M., Tanimura, Y., Dolios, G., Hirotsu, N., Horikoshi, Y., Kametani, F., Maeda, M., Saïdo, T.C., Wang, R., *et al.* (2005). Longer forms of amyloid beta protein: implications for the mechanism of intramembrane cleavage by gamma-secretase. *J Neurosci* *25*, 436-445.
- Rajapaksha, T.W., Eimer, W.A., Bozza, T.C., and Vassar, R. (2011). The Alzheimer's beta-secretase enzyme BACE1 is required for accurate axon guidance of olfactory sensory neurons and normal glomerulus formation in the olfactory bulb. *Molecular neurodegeneration* *6*, 88.
- Rajendran, L., Honsho, M., Zahn, T.R., Keller, P., Geiger, K.D., Verkade, P., and Simons, K. (2006). Alzheimer's disease beta-amyloid peptides are released in association with exosomes. *Proc Natl Acad Sci U S A* *103*, 11172-11177.
- Raji, O.Y., Agbaje, O.F., Duffy, S.W., Cassidy, A., and Field, J.K. (2010). Incorporation of a genetic factor into an epidemiologic model for prediction of individual risk of lung cancer: the Liverpool Lung Project. *Cancer prevention research (Philadelphia, Pa)* *3*, 664-669.
- Ribar, T.J., Rodriguiz, R.M., Khiroug, L., Wetsel, W.C., Augustine, G.J., and Means, A.R. (2000). Cerebellar defects in Ca²⁺/calmodulin kinase IV-deficient mice. *J Neurosci* *20*, Rc107.
- Rice, H.C., Townsend, M., Bai, J., Suth, S., Cavanaugh, W., Selkoe, D.J., and Young-Pearse, T.L. (2012). Pancortins interact with amyloid precursor protein and modulate cortical cell migration. *Development* *139*, 3986-3996.
- Rice, H.C., Young-Pearse, T.L., and Selkoe, D.J. (2013). Systematic evaluation of candidate ligands regulating ectodomain shedding of amyloid precursor protein. *Biochemistry* *52*, 3264-3277.

Roberds, S.L., Anderson, J., Basi, G., Bienkowski, M.J., Branstetter, D.G., Chen, K.S., Freedman, S.B., Frigon, N.L., Games, D., Hu, K., *et al.* (2001). BACE knockout mice are healthy despite lacking the primary beta-secretase activity in brain: implications for Alzheimer's disease therapeutics. *Human molecular genetics* *10*, 1317-1324.

Roch, J.M., Masliah, E., Roch-Levecq, A.C., Sundsmo, M.P., Otero, D.A., Veinbergs, I., and Saitoh, T. (1994). Increase of synaptic density and memory retention by a peptide representing the trophic domain of the amyloid beta/A4 protein precursor. *Proc Natl Acad Sci U S A* *91*, 7450-7454.

Sakuma, K., Sasaki, E., Kimura, K., Komori, K., Shimizu, Y., Yatabe, Y., and Aoki, M. (2018). HNRNPLL stabilizes mRNA for DNA replication proteins and promotes cell cycle progression in colorectal cancer cells. *Cancer science*.

Sannerud, R., Declerck, I., Peric, A., Raemaekers, T., Menendez, G., Zhou, L., Veerle, B., Coen, K., Munck, S., De Strooper, B., *et al.* (2011). ADP ribosylation factor 6 (ARF6) controls amyloid precursor protein (APP) processing by mediating the endosomal sorting of BACE1. *Proc Natl Acad Sci U S A* *108*, E559-568.

Savonenko, A.V., Melnikova, T., Laird, F.M., Stewart, K.A., Price, D.L., and Wong, P.C. (2008). Alteration of BACE1-dependent NRG1/ErbB4 signaling and schizophrenia-like phenotypes in BACE1-null mice. *Proc Natl Acad Sci U S A* *105*, 5585-5590.

Savvaki, M., Panagiotaropoulos, T., Stamatakis, A., Sargiannidou, I., Karatzioula, P., Watanabe, K., Stylianopoulou, F., Karagogeos, D., and Kleopa, K.A. (2008). Impairment of learning and memory in TAG-1 deficient mice associated with shorter CNS internodes and disrupted juxtapanodes. *Mol Cell Neurosci* *39*, 478-490.

Schafer, D.P., Lehrman, E.K., Kautzman, A.G., Koyama, R., Mardinly, A.R., Yamasaki, R., Ransohoff, R.M., Greenberg, M.E., Barres, B.A., and Stevens, B. (2012). Microglia sculpt postnatal neural circuits in an activity and complement-dependent manner. *Neuron* *74*, 691-705.

Scheltens, P., Blennow, K., Breteler, M.M.B., de Strooper, B., Frisoni, G.B., Salloway, S., and Van der Flier, W.M. (2016). Alzheimer's disease. *The Lancet* *388*, 505-517.

Scheuner, D., Eckman, C., Jensen, M., Song, X., Citron, M., Suzuki, N., Bird, T.D., Hardy, J., Hutton, M., Kukull, W., *et al.* (1996). Secreted amyloid beta-protein similar to that in the senile plaques of Alzheimer's disease is increased in vivo by the presenilin 1 and 2 and APP mutations linked to familial Alzheimer's disease. *Nat Med* *2*, 864-870.

Schilling, S., Mehr, A., Ludewig, S., Stephan, J., Zimmermann, M., August, A., Strecker, P., Korte, M., Koo, E.H., Muller, U.C., *et al.* (2017). APLP1 Is a Synaptic Cell Adhesion Molecule, Supporting Maintenance of Dendritic Spines and Basal Synaptic Transmission. *J Neurosci* *37*, 5345-5365.

Schneider, A., Rajendran, L., Honsho, M., Gralle, M., Donnert, G., Wouters, F., Hell, S.W., and Simons, M. (2008). Flotillin-dependent clustering of the amyloid precursor protein regulates its endocytosis and amyloidogenic processing in neurons. *J Neurosci* *28*, 2874-2882.

Schroeter, M.L., Stein, T., Maslowski, N., and Neumann, J. (2009). Neural correlates of Alzheimer's disease and mild cognitive impairment: a systematic and quantitative meta-analysis involving 1351 patients. *NeuroImage* *47*, 1196-1206.

Selkoe, D.J. (1991). The molecular pathology of Alzheimer's disease. *Neuron* *6*, 487-498.

Selkoe, D.J., and Hardy, J. (2016). The amyloid hypothesis of Alzheimer's disease at 25 years. *EMBO Mol Med* *8*, 595-608.

Sepulveda, J.L., Gutierrez-Pajares, J.L., Luna, A., Yao, Y., Tobias, J.W., Thomas, S., Woo, Y., Giorgi, F., Komissarova, E.V., Califano, A., *et al.* (2016). High-definition CpG methylation of novel genes in gastric carcinogenesis identified by next-generation sequencing. *Modern pathology : an official journal of the United States and Canadian Academy of Pathology, Inc* *29*, 182-193.

Shah, T., Zabaneh, D., Gaunt, T., Swerdlow, D.I., Shah, S., Talmud, P.J., Day, I.N., Whittaker, J., Holmes, M.V., Sofat, R., *et al.* (2013). Gene-centric analysis identifies variants associated with interleukin-6 levels and shared pathways with other inflammation markers. *Circulation Cardiovascular genetics* *6*, 163-170.

- Sharma, K., Schmitt, S., Bergner, C.G., Tyanova, S., Kannaiyan, N., Manrique-Hoyos, N., Kongi, K., Cantuti, L., Hanisch, U.K., Philips, M.A., *et al.* (2015). Cell type- and brain region-resolved mouse brain proteome. *Nat Neurosci* *18*, 1819-1831.
- Shimizu-Nishikawa, K., Kajiwara, K., Kimura, M., Katsuki, M., and Sugaya, E. (1995). Cloning and expression of SEZ-6, a brain-specific and seizure-related cDNA. *Brain research Molecular brain research* *28*, 201-210.
- Sinha, S., Anderson, J.P., Barbour, R., Basi, G.S., Caccavello, R., Davis, D., Doan, M., Dovey, H.F., Frigon, N., Hong, J., *et al.* (1999). Purification and cloning of amyloid precursor protein beta-secretase from human brain. *Nature* *402*, 537-540.
- Snutch, T.P., and Zamponi, G.W. (2018). Recent advances in the development of T-type calcium channel blockers for pain intervention. *British journal of pharmacology* *175*, 2375-2383.
- Sparrow, L.M., Pellatt, E., Yu, S.S., Raichlen, D.A., Pontzer, H., and Rolian, C. (2017). Gait changes in a line of mice artificially selected for longer limbs. *PeerJ* *5*, e3008.
- Stevens, B., Allen, N.J., Vazquez, L.E., Howell, G.R., Christopherson, K.S., Nouri, N., Micheva, K.D., Mehalow, A.K., Huberman, A.D., Stafford, B., *et al.* (2007). The classical complement cascade mediates CNS synapse elimination. *Cell* *131*, 1164-1178.
- Stover, K.R., Campbell, M.A., Van Winssen, C.M., and Brown, R.E. (2015). Analysis of motor function in 6-month-old male and female 3xTg-AD mice. *Behavioural brain research* *281*, 16-23.
- Stutzer, I., Selevsek, N., Esterhazy, D., Schmidt, A., Aebersold, R., and Stoffel, M. (2013). Systematic proteomic analysis identifies beta-site amyloid precursor protein cleaving enzyme 2 and 1 (BACE2 and BACE1) substrates in pancreatic beta-cells. *J Biol Chem* *288*, 10536-10547.
- Takemoto-Kimura, S., Suzuki, K., Horigane, S.I., Kamijo, S., Inoue, M., Sakamoto, M., Fujii, H., and Bito, H. (2017). Calmodulin kinases: essential regulators in health and disease. *J Neurochem* *141*, 808-818.
- Tesco, G., Koh, Y.H., Kang, E.L., Cameron, A.N., Das, S., Sena-Estevés, M., Hiltunen, M., Yang, S.H., Zhong, Z., Shen, Y., *et al.* (2007). Depletion of GGA3 stabilizes BACE and enhances beta-secretase activity. *Neuron* *54*, 721-737.
- Tossell, K., Andrae, L.C., Cudmore, C., Lang, E., Muthukrishnan, U., Lumsden, A., Gilthorpe, J.D., and Irving, C. (2011). *Lrrn1* is required for formation of the midbrain-hindbrain boundary and organiser through regulation of affinity differences between midbrain and hindbrain cells in chick. *Dev Biol* *352*, 341-352.
- Traka, M., Goutebroze, L., Denisenko, N., Bessa, M., Nifli, A., Havaki, S., Iwakura, Y., Fukamauchi, F., Watanabe, K., Soliven, B., *et al.* (2003). Association of TAG-1 with Caspr2 is essential for the molecular organization of juxtaparanodal regions of myelinated fibers. *J Cell Biol* *162*, 1161-1172.
- Tusher, V.G., Tibshirani, R., and Chu, G. (2001). Significance analysis of microarrays applied to the ionizing radiation response. *Proc Natl Acad Sci U S A* *98*, 5116-5121.
- Tyanova, S., Temu, T., Sinitcyn, P., Carlson, A., Hein, M.Y., Geiger, T., Mann, M., and Cox, J. (2016). The Perseus computational platform for comprehensive analysis of (prote)omics data. *Nature methods* *13*, 731-740.
- Udayar, V., Buggia-Prevot, V., Guerreiro, R.L., Siegel, G., Rambabu, N., Soohoo, A.L., Ponnusamy, M., Siegenthaler, B., Bali, J., Simons, M., *et al.* (2013). A paired RNAi and RabGAP overexpression screen identifies Rab11 as a regulator of beta-amyloid production. *Cell Rep* *5*, 1536-1551.
- Vanier, M.T. (2010). Niemann-Pick disease type C. *Orphanet journal of rare diseases* *5*, 16.
- Vassar, R., Bennett, B.D., Babu-Khan, S., Kahn, S., Mendiáz, E.A., Denis, P., Teplow, D.B., Ross, S., Amarante, P., Loeloff, R., *et al.* (1999). Beta-secretase cleavage of Alzheimer's amyloid precursor protein by the transmembrane aspartic protease BACE. *Science* *286*, 735-741.
- Vassar, R., Kovacs, D.M., Yan, R., and Wong, P.C. (2009). The beta-secretase enzyme BACE in health and Alzheimer's disease: regulation, cell biology, function, and therapeutic potential. *J Neurosci* *29*, 12787-12794.

- Vassar, R., Kuhn, P.H., Haass, C., Kennedy, M.E., Rajendran, L., Wong, P.C., and Lichtenthaler, S.F. (2014). Function, therapeutic potential and cell biology of BACE proteases: current status and future prospects. *J Neurochem* *130*, 4-28.
- Vetrivel, K.S., Meckler, X., Chen, Y., Nguyen, P.D., Seidah, N.G., Vassar, R., Wong, P.C., Fukata, M., Kounnas, M.Z., and Thinakaran, G. (2009). Alzheimer disease A β production in the absence of S-palmitoylation-dependent targeting of BACE1 to lipid rafts. *J Biol Chem* *284*, 3793-3803.
- von Arnim, C.A., Spoelgen, R., Peltan, I.D., Deng, M., Courchesne, S., Koker, M., Matsui, T., Kowa, H., Lichtenthaler, S.F., Irizarry, M.C., *et al.* (2006). GGA1 acts as a spatial switch altering amyloid precursor protein trafficking and processing. *J Neurosci* *26*, 9913-9922.
- Wakana, S., Sugaya, E., Naramoto, F., Yokote, N., Maruyama, C., Jin, W., Ohguchi, H., Tsuda, T., Sugaya, A., and Kajiwara, K. (2000). Gene mapping of SEZ group genes and determination of pentylentetrazol susceptible quantitative trait loci in the mouse chromosome. *Brain Res* *857*, 286-290.
- Walker, D.G., and McGeer, P.L. (1992). Complement gene expression in human brain: comparison between normal and Alzheimer disease cases. *Brain research Molecular brain research* *14*, 109-116.
- Wang, J.Z., Grundke-Iqbal, I., and Iqbal, K. (1996). Glycosylation of microtubule-associated protein tau: an abnormal posttranslational modification in Alzheimer's disease. *Nat Med* *2*, 871-875.
- Wang, P., Yang, G., Mosier, D.R., Chang, P., Zaidi, T., Gong, Y.D., Zhao, N.M., Dominguez, B., Lee, K.F., Gan, W.B., *et al.* (2005). Defective neuromuscular synapses in mice lacking amyloid precursor protein (APP) and APP-Like protein 2. *J Neurosci* *25*, 1219-1225.
- Wang, Q. (2017). CpG methylation patterns are associated with gene expression variation in osteosarcoma. *Molecular medicine reports* *16*, 901-907.
- Weidemann, A., Konig, G., Bunke, D., Fischer, P., Salbaum, J.M., Masters, C.L., and Beyreuther, K. (1989). Identification, biogenesis, and localization of precursors of Alzheimer's disease A4 amyloid protein. *Cell* *57*, 115-126.
- Wille, M., Schumann, A., Wree, A., Kreutzer, M., Glocker, M.O., Mutzbauer, G., and Schmitt, O. (2015). The Proteome Profiles of the Cerebellum of Juvenile, Adult and Aged Rats--An Ontogenetic Study. *International journal of molecular sciences* *16*, 21454-21485.
- Willem, M., Garratt, A.N., Novak, B., Citron, M., Kaufmann, S., Rittger, A., DeStrooper, B., Saftig, P., Birchmeier, C., and Haass, C. (2006). Control of peripheral nerve myelination by the beta-secretase BACE1. *Science* *314*, 664-666.
- Willem, M., Tahirovic, S., Busche, M.A., Ovsepian, S.V., Chafai, M., Kootar, S., Hornburg, D., Evans, L.D., Moore, S., Daria, A., *et al.* (2015). β -Secretase processing of APP inhibits neuronal activity in the hippocampus. *Nature* *526*, 443-447.
- Williams, J.M., Zurawski, J., Mikecz, K., and Glant, T.T. (1993). Functional assessment of joint use in experimental inflammatory murine arthritis. *Journal of orthopaedic research : official publication of the Orthopaedic Research Society* *11*, 172-180.
- Wisniewski, K.E., Wisniewski, H.M., and Wen, G.Y. (1985). Occurrence of neuropathological changes and dementia of Alzheimer's disease in Down's syndrome. *Annals of neurology* *17*, 278-282.
- Xie, B., Fan, X., Lei, Y., Chen, R., Wang, J., Fu, C., Yi, S., Luo, J., Zhang, S., Yang, Q., *et al.* (2016). A novel de novo microdeletion at 17q11.2 adjacent to NF1 gene associated with developmental delay, short stature, microcephaly and dysmorphic features. *Molecular cytogenetics* *9*, 41.
- Xu, C., Mullersman, J.E., Wang, L., Bin Su, B., Mao, C., Posada, Y., Camarillo, C., Mao, Y., Escamilla, M.A., and Wang, K.S. (2013). Polymorphisms in seizure 6-like gene are associated with bipolar disorder I: evidence of gene x gender interaction. *J Affect Disord* *145*, 95-99.
- Xu, J.Y., Xia, Q.Q., and Xia, J. (2012). A review on the current neuroigin mouse models. *Sheng li xue bao : [Acta physiologica Sinica]* *64*, 550-562.

- Yaguchi, H., Yabe, I., Takahashi, H., Watanabe, M., Nomura, T., Kano, T., Matsumoto, M., Nakayama, K.I., Watanabe, M., and Hatakeyama, S. (2017). Sez612 regulates phosphorylation of ADD and neuritogenesis. *Biochem Biophys Res Commun* 494, 234-241.
- Yan, R., Bienkowski, M.J., Shuck, M.E., Miao, H., Tory, M.C., Pauley, A.M., Brashier, J.R., Stratman, N.C., Mathews, W.R., Buhl, A.E., *et al.* (1999). Membrane-anchored aspartyl protease with Alzheimer's disease beta-secretase activity. *Nature* 402, 533-537.
- Yan, R., Munzner, J.B., Shuck, M.E., and Bienkowski, M.J. (2001). BACE2 functions as an alternative alpha-secretase in cells. *J Biol Chem* 276, 34019-34027.
- Yardan, T., Erenler, A.K., Baydin, A., Aydin, K., and Cokluk, C. (2011). Usefulness of S100B protein in neurological disorders. *JPMA The Journal of the Pakistan Medical Association* 61, 276-281.
- Yildirim, M.A., Goh, K.I., Cusick, M.E., Barabasi, A.L., and Vidal, M. (2007). Drug-target network. *Nat Biotechnol* 25, 1119-1126.
- Yu, J., Mu, J., Guo, Q., Yang, L., Zhang, J., Liu, Z., Yu, B., Zhang, T., and Xie, J. (2017). Transcriptomic profile analysis of mouse neural tube development by RNA-Seq. *IUBMB life* 69, 706-719.
- Zhang, Z., Song, M., Liu, X., Su Kang, S., Duong, D.M., Seyfried, N.T., Cao, X., Cheng, L., Sun, Y.E., Ping Yu, S., *et al.* (2015). Delta-secretase cleaves amyloid precursor protein and regulates the pathogenesis in Alzheimer's disease. *Nat Commun* 6, 8762.
- Zhou, L., Barao, S., Laga, M., Bockstael, K., Borgers, M., Gijssen, H., Annaert, W., Moechars, D., Mercken, M., Gevaert, K., *et al.* (2012). The neural cell adhesion molecules L1 and CHL1 are cleaved by BACE1 protease in vivo. *J Biol Chem* 287, 25927-25940.
- Zhu, K., Peters, F., Filser, S., and Herms, J. (2018a). Consequences of Pharmacological BACE Inhibition on Synaptic Structure and Function. *Biol Psychiatry*.
- Zhu, K., Xiang, X., Filser, S., Marinkovic, P., Dorostkar, M.M., Crux, S., Neumann, U., Shimshek, D.R., Rammes, G., Haass, C., *et al.* (2018b). Beta-Site Amyloid Precursor Protein Cleaving Enzyme 1 Inhibition Impairs Synaptic Plasticity via Seizure Protein 6. *Biol Psychiatry* 83, 428-437.
- Zundorf, G., and Reiser, G. (2011). Calcium dysregulation and homeostasis of neural calcium in the molecular mechanisms of neurodegenerative diseases provide multiple targets for neuroprotection. *Antioxidants & redox signaling* 14, 1275-1288.

8. ACKNOWLEDGMENT

I would like to thank my supervisor, Prof. Dr. Stefan Lichtenthaler, for giving me the opportunity to conduct the thesis in his lab, for the constant scientific and financial support in advancing my knowledge and skills by attending workshops, conferences and visiting labs abroad. I am as well grateful for many fruitful discussions throughout my PhD that yielded this thesis and a publication with additional ones in preparation.

This work would not have been possible without the generous financial support of the Bavarian Academic Center for Central, Eastern and Southeastern Europe through their scholarship program of the Free State of Bavaria for studies in Bavaria.

I wish to acknowledge Dr. Alessio Colombo, Dr. Johanna Wanngren and Dr. med. Peer-Hendrik Kuhn who helped me especially in the beginning with their mentorship and advices in the lab. My appreciation goes to Dr. Stephan Müller, for all the proteomic-related advices, inputs and assistance throughout my PhD. I am thankful for the discussions with Dr. Julia Herber that yielded the shared publication. Technical assistances provided by Katrin Moschke and Anna Berghofer were as well greatly appreciated.

My sincere gratitude goes to Dr. Jenny Gunnensen and her lab for the fruitful collaboration, including valuable discussions and the opportunity to conduct part of my dissertation work in her lab.

Advices given by the members of my Thesis Advisory Committee, Prof. Dr. Wolfgang Wurst and Dr. Silva Katusic Hecimovic have been of a great help in progressing with my thesis.

Many thanks to all my friends, colleagues and collaborators both in scientific, but also non-scientific environment that helped me grow as a scientist and as a person. I am particularly grateful for my lab partner and dear friend Martina Pigoni, with whom I shared endless private and scientific discussions during my PhD time.

Finally, I would like to express my deep appreciation to Roni and my family for being my constant source of encouragement, support and inspiration. This work is dedicated to my parents, Sonja and Milorad, for having a life-long unconditional love and guidance in following my personal and professional choices.

List of publications

Herber, J.* , **Njavro, J.***, Feederle, R., Schepers, U., Muller, U.C., Brase, S., Muller, S.A., and Lichtenthaler, S.F. (2018). Click Chemistry-mediated Biotinylation Reveals a Function for the Protease BACE1 in Modulating the Neuronal Surface Glycoproteome. *Molecular & Cellular Proteomics*.

* Shared first authors